CASL-U-2017-1280-000
ORNL/TM-2017/95

Development of the V4.2m5 and V5.0m0 Multigroup Cross Section Libraries for MPACT for PWR and BWR

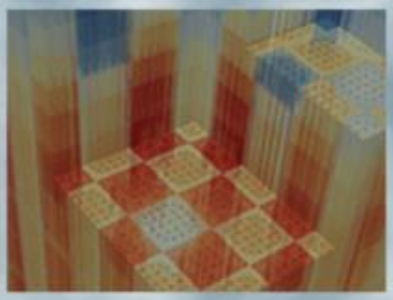
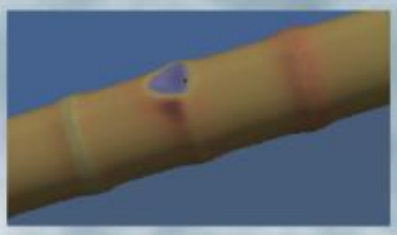
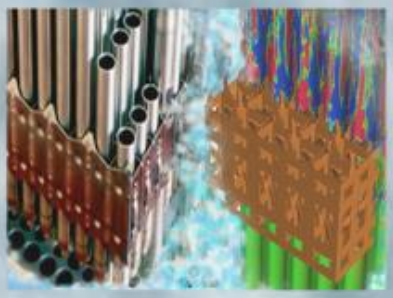

Revision 0

Kang Seog Kim
Kevin Clarno
Cole Gentry
Andrew Godfrey
Dorothea Wiarda
Mark Williams
Oak Ridge National Laboratory

Brendan Kochunas
Yuxuan Liu
University of Michigan

Scott Palmtag
Core Physics Inc.

February 28, 2017

U.S. DEPARTMENT OF ENERGY | Nuclear Energy

REVISION LOG

Revision	Date	Affected Pages	Revision Description
0	2/28/2017	All	Initial version

Export Controlled None

IP/Proprietary/NDA Controlled None

Sensitive Controlled None

Unlimited All Pages

Requested Distribution:

To: N/A

Copy: N/A

Reviewed by:

Date:

Reviewer:

EXECUTIVE SUMMARY

The MPACT neutronics module of the Consortium for Advanced Simulation of Light Water Reactors (CASL) core simulator is a 3-D whole core transport code being developed for the CASL toolset, Virtual Environment for Reactor Analysis (VERA). Key characteristics of the MPACT code include (1) a subgroup method for resonance self-shielding and (2) a whole-core transport solver with a 2-D/1-D synthesis method. The MPACT code requires a cross section library to support all the MPACT core simulation capabilities which would be the most influencing component for simulation accuracy.

Due to the limitation of computing capacity even in high performance computing the cross section library needs to be developed to enhance computational efficiency in memory and computing time without losing accuracy and generality, which requires very coarse energy group structure with about 50 groups. Multigroup (MG) neutron cross section libraries for the CASL VERA-CS neutronics simulator MPACT have been developed by using the AMPX/SCALE code package developed at Oak Ridge National Laboratory.

A new 51-group structure was developed for efficient simulation to be applicable for both pressurized water reactor (PWR) and boiling water reactor (BWR) simulations. New v4.2m5 MPACT 51-group libraries with the ENDF/B-VII.0 and VII.1 nuclear data were developed for MPACT. Since this MPACT library format has drawbacks limiting further improvement and generality, a new format of cross section library called Simplified AMPX (SAMPX) was developed. New v5.0m0 SAMPX 51- and 252-group libraries with the ENDF/B-VII.0 and VII.1 nuclear data were developed. This study focuses on the development of the MPACT and SAMPX libraries including verification and validation.

This document includes library generation methodology and procedure, accuracy requirements, verification procedure and benchmark results compared to continuous energy Monte Carlo results by using newly developed cross section libraries. Performances of the MPACT and SAMPX libraries in accuracy and computing time can be summarized as follows:

- The MPACT results with the v4.2m5 MPACT and v5.0m0 SAMPX 51-group libraries satisfy the accuracy goal (≤ 200 pcm) for multiplication factors for all PWR cases except for several severe cases regardless of ^{235}U enrichment, moderator density, temperature, burnup, burnable poison, and boron concentration.
- The MPACT results with the v4.2m5 MPACT and v5.0m0 SAMPX 51-group libraries satisfy the accuracy goal (≤ 3.0 % for 3D core) for pin power distributions for all PWR cases.
- While the computational performance with the MPACT 51-g library is good enough, the computational performance with the SAMPX 51-g library needs to be improved.
- Since the neutron spectrum variations are very wide for BWR, the 51-group library is not able to cover the whole range which requires to use the 252-group library.

TABLE OF CONTENTS

FIGURES

TABLES

ACRONYMS

1D	one-dimensional
2D	two-dimensional
AMPX	resonance processing code; the name is no longer an acronym
BWR	boiling water reactor
CASL	Consortium for Advanced Simulation of Light Water Reactors
CE	continuous energy (as in cross sections)
DBRC	Doppler-broadening rejection correction
ENDF	evaluated nuclear data file
ESSM	Embedded Self-Shielding Method
FP	fission product
IR	intermediate resonance
MG	multi-group (as in cross sections)
MOC	Method Of Characteristics
MWD	megawatt day
MPACT	radiation transport code; the name is no longer an acronym
NLC	neutron leakage conservation
NR	narrow resonance
ORNL	Oak Ridge National Laboratory
PW	pointwise
PWR	pressurized water reactor
RI	resonance integral
SAMPX	Simplified AMPX
SCALE	Standardized Computer Analyses for Licensing Evaluations
SG	subgroup
SPH	super homogenization
SQA	software quality assurance
VERA	Virtual Environment for Reactor Applications
VERA-CS	VERA Core Simulator
XS	cross section

1. INTRODUCTION

The MPACT [Mpa13] neutronics module of the Consortium for Advanced Simulation of Light Water Reactors (CASL) [CAS15] core simulator is a 3-D whole core transport code being developed for the CASL toolset, Virtual Environment for Reactor Analysis (VERA) [Tur16]. MPACT is under development for neutronics simulation coupled with the CTF code for thermal-hydraulics simulation for pressurized light water reactors. Key characteristics of the MPACT code include (1) a subgroup method for resonance self-shielding and (2) a whole-core transport solver with a 2-D/1-D synthesis method. Thus the MPACT code requires a cross-section library to support all the MPACT core simulation capabilities.

Multigroup (MG) neutron cross section libraries for the Consortium for the Advanced Simulation of Light-Water Reactors (CASL) MPACT neutronics code [Mpa13], which is part of the Virtual Environment for Reactor Applications (VERA) core simulator (VERA-CS), have been developed by using the AMPX code package [Wia16] and the XSTools software in VERA. The native MPACT cross section library format, which is based on the HELIOS [Sta98] and DeCART [Cho02] formats, is the primary structure available for CASL. While sufficient, this library format includes drawbacks that could restrict further improvement because it is not able to take advantage of the more general AMPX MG library developed for SCALE [Sca16] by Oak Ridge National Laboratory (ORNL). Therefore, a new intermediate format of cross section library, called Simplified AMPX (SAMPX) has been developed, that provides the generality of AMPX with the MPACT-specific requirements for subgroup processing, depletion, and transients. It is required to deliver verified and validated MPACT and SAMPX MG cross section libraries based upon the CASL Software Quality Assurance (SQA) procedure.

This document includes the following:

- Accuracy goals (Chapter 2),
- Library generation procedure including methodology and verification (Chapter 3),
- Generation of the v4.2m5 MPACT and v5.0m5 simplified AMPX 51- and 252-g libraries with ENDF/B-7.0 and 7.1 (Chapter 4),
- Benchmark calculations and results (Chapter 5),
- Performance of cross section processing in MPACT (Chapter 6).

This study is a part of verification and validation of the CASL VERA-CS focusing on MG cross section library.

2. ACCURACY GOALS

The completeness and quality of the cross section library will be evaluated through two primary metrics:

1. Comparison of the MPACT results with the continuous-energy Monte Carlo (MC) results at specific states to estimate the error associated with the multi-group nuclear data library and subgroup processing step. This eliminates the complexity associated with errors in the fundamental nuclear data and presumes that the spatial- and angular-discretization error is relatively small.
2. Comparison of the MPACT results during a depletion simulation with depletion-enabled continuous-energy MC codes. While MC with depletion introduces discretization error (in time and space) and includes approximations in heat generation, benchmarking MPACT's use of the nuclear data library would reveal potential issues related to the depletion data and MPACT's use of it.

Comparison of MPACT results with zero-power physics testing at reactor plants is a key metric of success to demonstrate the quality of the nuclear data library, but it is also a validation of the MPACT code; therefore, these results are presented in that report. Because the state of the reactor is well-known, differences between the continuous-energy MC solution and operational data will reveal errors in the fundamental nuclear data; differences between the MPACT solution and the continuous-energy MC solution provide a relative comparison between the fundamental data errors and those introduced through the multi-group library and processing step.

The following are accuracy targets for reactivity and pin power distribution due to approximations in the multi-group cross sections, presuming that the spatial, angular, and scattering-order discretization errors are insignificant.

- Eigenvalue (for pin, assembly, and core comparisons):
  - For all states evaluate the differences between CE-MC and MPACT, where pcm stands for "per cent mille" or 10^{-5}.
  - keff > 1.0 : ± 200 pcm $\Delta\rho$
  - keff ≤ 1.0 : ± 200 pcm Δk
  - Depletion : ± 200 pcm Δk

- Group-dependent reaction rate comparisons (for pincell comparisons)
  - Maximum : < 100 pcm
  - RMS : < 20 pcm

- Power distributions (for assembly and core comparisons)
  - Maximum: ±1.5 % (2D Fuel assembly),
±2.5 % (2D Core)
±3.0 % (3D Core)
  - RMS: 1.0% (2D Fuel assembly),
1.5 % (2D Core),

2.0 % (3D Core)

- Trends (for pincell and assembly comparisons)
  - No clear trends due to changes in particular aspects of the problem (fuel temperature, geometry, coolant density, etc.)

Note that these target accuracies are different from target accuracies in multi-physics simulations.

3. LIBRARY GENERATION PROCEDURE AND VERIFICATION

The VERA-CS neutronics simulator MPACT requires multi-group neutron cross section data to solve Boltzmann transport equation to obtain neutron flux distribution. The evaluated nuclear data such as ENDF/B are processed to generate multi-group (MG) cross sections by using the AMPX-6 [Wia14] and SCALE [Sca16] code packages developed at Oak Ridge National Laboratory. This chapter summarizes methodology and procedure to prepare the VERA-CS MPACT cross section library. The detailed procedure used is provided in Reference [Kim15].

3.1 LIBRARY GENERATION METHODOLOGY AND PROCEDURE

3.1.1 Multi-Group Cross Section Processing

AMPX-6 is a modular system of FORTRAN computer programs to generate the MG and continuous energy (CE) cross section libraries for modern deterministic and Monte Carlo transport codes by processing the ENDF/B libraries. Since the CASL neutronics simulator MPACT is a deterministic transport code, only the AMPX MG library generation procedure is discussed. Figure 3.1.1 illustrates the AMPX procedure to generate the AMPX MG library where the left side of flow chart is for the conventional procedure and the right side is for the new procedure to improve the Bondarenko resonance data.

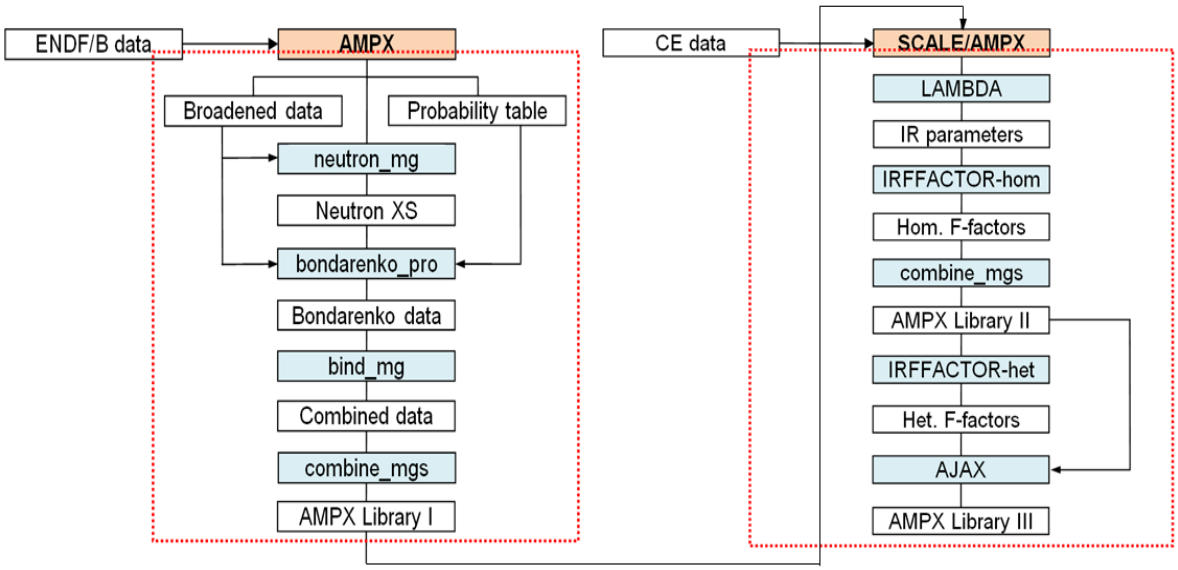

Figure 3.1.1 Flow chart of the AMPX procedure for generating the VERA MG library

The AMPX MG library includes Bondarenko F-factors for various reactions as a function of background cross section for resolved and unresolved resonance groups. The resolved resonance F-factors have been generated by the narrow resonance (NR) approximation and the unresolved ones by the J-function method [Lee11] based on the

NR approximation. The MG 1D and 2D data have been obtained by using a weighting function that consists of a Maxwellian spectrum at thermal energies, 1/E at epithermal energies and fission spectrum at fast energy ranges, or typical LWR spectrum. It should be noted that the 2D scattering data are temperature independent in the AMPX MG library. In the standard SCALE procedure, self-shielded MG 1D and 2D data for resolved resonance and thermal energy groups are determined by performing the CENTRM [Wil06] slowing down transport calculation with Equation (3.1.1), and thus the resolved resonance data in the AMPX MG library are insignificant.

$$\hat{\Omega}\cdot\nabla\psi+\Sigma_t(\vec{r},u)\psi(\vec{r},u,\hat{\Omega})=\int_{u-\ln(1/\alpha)}^{u}\frac{\Sigma_s(u')\phi(u')}{(1-\alpha)}e^{u'-u}du'\,, \tag{3.1.1}$$

where *u* denotes lethargy, and ϕ and ψ scalar and angular fluxes, respectively. In Equation (3.1.1) Σ_t and Σ_s are total and scattering cross sections, respectively, and α is defined as $(A\text{-}1)^2/(A+1)^2$ where *A* is atomic mass.

3.1.2 Intermediate Resonance (IR) Parameter

The IR parameter [Gol62] can be defined as a probability passing through resonance without any reaction which correlates the NR and wide resonance (WR) approximations. Since the atomic mass of hydrogen (^{1}H) is very close to unity, the lethargy gain of any neutron colliding with hydrogen is very large and the neutron can scatter beyond a resonance without any collision. This is essentially the same as the narrow resonance approximation. Therefore, for hydrogen, the intermediate resonance parameter is defined as unity. For other nuclides, the IR parameter is obtained by comparing results of various ^{238}U/^{1}H mixtures where the hydrogen is partly replaced by the other isotopes [Les87]. This is often referred to as a hydrogen-equivalence parameter.

At first a self-shielded cross section table, $\sigma_{g,a}^{238}$ vs. $\sigma_{g,b}^{238}$, must be prepared by performing slowing down calculations with various hydrogen atomic number densities (N^1) with a fixed ^{238}U atomic number density (N^{238}). The background cross sections can be obtained using the following equation assuming the ^{1}H (λ_g^1) and ^{238}U (λ_g^{238}) IR parameters to be unity.

$$\sigma_{g,b}^{238}=\frac{N^{238}\lambda_g^{238}\sigma_p^{238}+N^1\lambda_g^1\sigma_p^1}{N^{238}}=\frac{\sum_{i=all}N^i\lambda_g^i\sigma_p^i}{N^R}\,. \tag{3.1.2}$$

Then the slowing down calculation is performed for a mixture of ^{238}U, ^{1}H and a target nuclide *x*. A new $\sigma_{g,a}^{238}$ is calculated, and the corresponding $\sigma_{g,b}^{238}$ is read from the prepared $\sigma_{g,a}^{238}$ table. The IR parameter (λ_g^x) for a nuclide *x* can be obtained by using Equation (3.1.3)

$$\lambda_g^x = \frac{\sigma_{g,b}^{238} N^{238} - N^{238} \lambda_g^{238} \sigma_p^{238} - N^1 \lambda_g^1 \sigma_p^1}{N^x \sigma_p^x}, \quad (3.1.3)$$

where σ_p^x is the potential cross section. The IR parameter of ^{238}U should be determined first, and then the IR parameters of other nuclides should be evaluated. The LAMBDA program in Figure 3.1.1 computes all of the IR parameters for all nuclides by using this procedure.

3.1.3 Homogeneous Resonance Data

The Bondarenko F-factor (or resonance) tables are to be generated by performing homogeneous slowing down calculations with a mixture of ^{1}H and target nuclide. This process is identical to that used for preparing a self-shielded cross section table for the IR parameter as described in Section 3.1.2. The Bondarenko F-factor tables must be determined to cover all background cross sections, from zero to infinity. Figure 3.1.2 illustrates the procedure to generate the F-factors by using IRFFACTOR, which executes CENTRM and performs ESSM (Embedded Self-Shielding Method) [Wil12]. These homogenous F-factors are typically generated for nuclides with atomic mass numbers larger than 40. New Bondarenko F-factors are to be incorporated into the AMPX MG library.

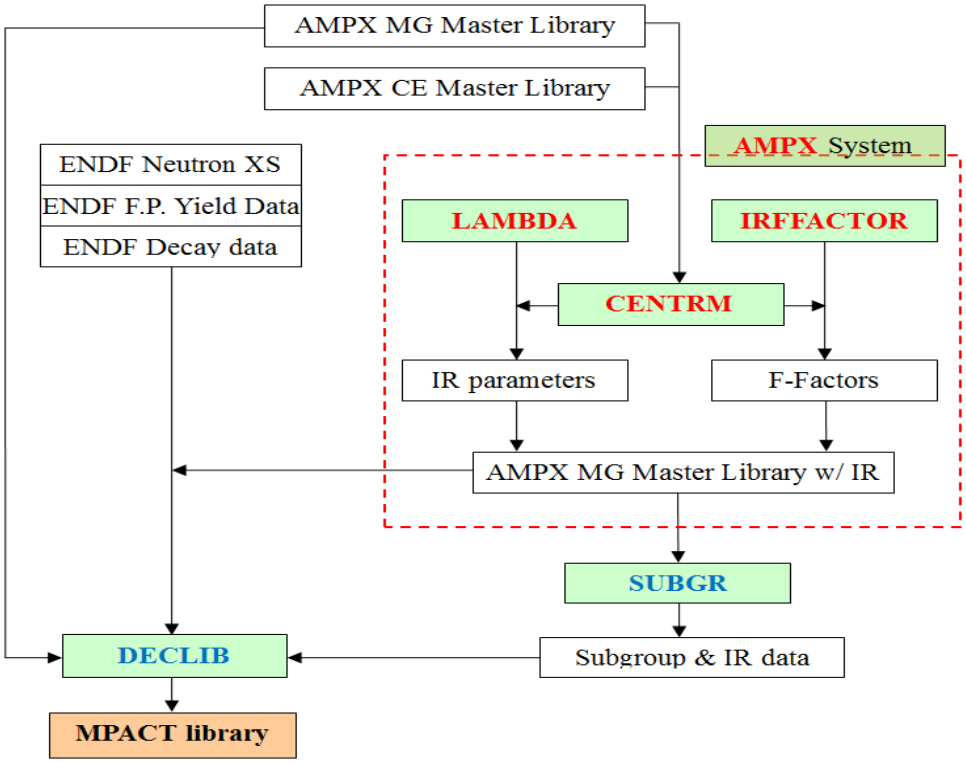

Figure 3.1.2 Flow chart of the MPACT library generation procedure

Table 3.1.1 Example of variations

Case		1	2	3	4	5	6	7	8	9	10	11	12	13	14	15	16
Volume	Fuel	1.0	1.0	1.0	1.0	1.0	1.0	1.0	1.0	1.0	1.0	1.0	1.0	1.0	1.0	1.0	1.0
	Clad	1.0	1.0	1.0	1.0	1.0	1.0	1.0	1.0	1.0	1.0	1.0	1.0	1.0	1.0	1.0	1.0
	Mod	1.0	1.0	1.0	1.0	1.0	2.0	5.0	5.0	5.0	5.0	5.0	5.0	5.0	5.0	5.0	5.0
Fuel	^{235}U	1.0	1.0	1.0	1.0	1.0	1.0	1.0	0.5	0.25	0.125	0.0625	0.03125	0.01	0.01	0.01	0.01
	^{238}U	1.0	1.0	1.0	1.0	1.0	1.0	1.0	0.5	0.25	0.125	0.0625	0.03125	0.01	0.001	1.0E-6	1.0E-7
	^{16}O	1.0	1.0	1.0	1.0	1.0	1.0	1.0	0.5	0.25	0.125	0.0625	0.03125	0.01	0.01	0.01	0.01
H_2O	^{1}H	2.5E-3	0.2	0.5	0.75	1.0	1.0	1.0	1.0	1.0	1.0	1.0	1.0	1.0	1.0	1.0	1.0
	^{16}O	2.5E-3	0.2	0.5	0.75	1.0	1.0	1.0	1.0	1.0	1.0	1.0	1.0	1.0	1.0	1.0	1.0

3.1.4 Heterogeneous Resonance Data

The Bondarenko F-factor tables are also generated by using heterogeneous slowing down models, which ensures more precise results compared to those obtained using homogeneous models. As shown in Figure 3.1.2, the IRFFACTOR module is responsible for this calculation. The pointwise (PW) slowing down calculations using Equation (3.1.1) are performed with CENTRM for the heterogeneous models, and then the MG self-shielded absorption ($\sigma_{g,a}$), fission ($\sigma_{g,f}$) and scattering ($\sigma_{g,s}$) cross sections are edited. The final step is to estimate the corresponding background cross section by solving the following MG fixed source transport problem using Equation (3.1.4) and converting the scalar flux (ϕ_g) into a background cross section using Equation (3.1.5) based on equivalence theory

$$\hat{\Omega}\cdot\nabla\psi_g + \sum_i (\Sigma_{i,g,a} + \lambda_{i,g}\Sigma_{i,p})\psi_{g,k}(\hat{\Omega}) = \sum_i \lambda_{i,g}\Sigma_{i,p}\,, \tag{3.1.4}$$

$$\sigma_{b,g}^{k} = \frac{\Sigma_{b,g}}{N_k} = \frac{\Sigma_{a,g}\phi_g}{1-\phi_g}\,, \tag{3.1.5}$$

where *k* denotes the resonant nuclide. Various background cross sections can be achieved by changing geometrical and compositional configurations as shown in Table 3.1.1. Appendix A.1 provides the IFFACTOR input including 16 variations.

3.1.5 Subgroup Resonance Data

The primary resonance self-shielding method in MPACT is the subgroup method [Kha71, Sta98] requiring subgroup data which can be transformed from the Bondarenko F-factor tables. The essential aspect of the subgroup method is that the effective resonance cross sections are approximated by quadratures in which the resonances are divided into the subgroup levels, and the corresponding subgroup weights are assigned as probabilities. Fixed source transport calculations are performed at each subgroup level, corresponding background cross sections are determined, and then self-shielded cross sections are estimated with a consideration of resonance interference effect between nuclides. As shown in Figure 3.1.2, the SUBGR code computes the subgroup data through a least square fitting by using the IR parameters

and F-factor tables in the AMPX MG library. The IR parameters and F-factor tables are computed using the IRFFACTOR and LAMBDA modules. Subgroup data are composed of the subgroup levels for the absorption, the ν*fission cross sections, and the corresponding temperature-dependent subgroup weights. The subgroup data can be generated by conserving either self-shielded resonance integrals [Sta98] or cross sections [Joo09]. Capabilities for these are included in SUBGR.

3.1.6 Transport Corrected Cross Sections

The method of characteristics (MOC) calculation with high order ($\geq P_2$) scattering source requires as much as twice the computational time as the P_0 MOC calculation. Most transport lattice codes typically perform transport corrected P_0 scattering calculations in which diagonal terms of P_0 scattering matrix are subtracted by the total P_1 scattering cross sections or adjusted by other transport correction methods. The P_1 corrected P_0 scattering matrix for ^{1}H may include negative value in the diagonal components. This can lead to negative fluxes, resulting in nonconvergence. This is still an open problem. The DECLIB code has been developed to consider various transport correction methods, such as typical out-scattering approximation, the nTRACER in-scattering approximation [Ryu14] and the neutron leakage conservation (NLC) method [Her13]. While transport cross sections and transport corrected P_0 scattering matrices with out- and in-scattering approximations can be easily generated, the NLC approximation requires transport correction factors to be generated independently. A new SCALE procedure called h1TransportXS based on 1D slab discrete ordinate transport calculation has been developed to generate transport correction factors by using the NLC method. [Kim16e] Figure 3.1.3 provides the 51-group transport correction factors for ^{1}H with various temperatures.

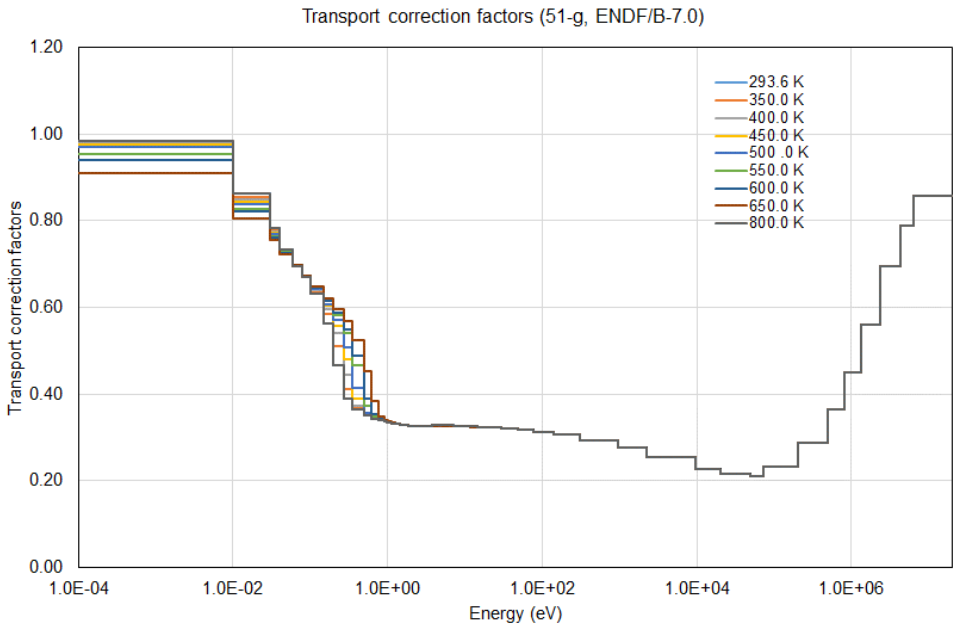

Figure 3.1.3 The NLC transport correction factors for ^{1}H

3.1.7 Monte Carlo Based Heterogeneous Resonance Data

No deterministic slowing down program is available that considers epithermal upscattering. Therefore, the Bondarenko f-factor tables must be generated by performing continuous energy Monte Carlo calculations and evaluating the corresponding background cross sections [Kim03]. The Bondarenko F-factor tables can be generated by using either homogeneous or heterogeneous models. The key feature of this procedure is to perform the Monte Carlo calculations to obtain MG self-shielded cross sections instead of solving deterministic PW slowing down calculations. In this study, the CE-KENO calculations were performed to edit effective microscopic cross sections rather than the CENTRM slowing down calculations. The corresponding background cross sections can be obtained by the same method described in Section 3.1.4. The Bondarenko F-factors have been obtained by performing the CE-KENO calculations without and with the Doppler Broadening Rejection Correction (DBRC) option to consider the resonance upscattering effect.

3.1.8 Transient Data

The ORNL AMPX code package [Wia14] does not provide transient data such as decay constants and delayed neutron fractions, but the capability is under development. The NJOY program [Mac94] developed at LANL has been used to generate the transient data. NJOY input files were generated for 21 heavy nuclides in the MPACT library. Tape 24 from the GROUPR module includes MG neutron data including transient data. A simple program has been developed to edit transient data such as decay constants and delayed neutron fractions. The total number of neutrons released per fission used in obtaining delayed neutron fraction can be obtained by using a typical PWR spectrum.

The ENDF/B-7.0 and 7.1 neutron data include transient data for 21 nuclides. Appendix A.2 provides transient data including nuclide identification, total number of neutrons released per fission, decay constants and delayed neutron fractions for each nuclide.

3.1.9 Effective Recoverable Energy Per Fission

The energy release per fission is required for burnup calculations, and is usually defined without the kinetic energy of the incident neutrons and the energy carried away by neutrinos. However, the energy release per fission includes the contributions from the kinetic energy of incident neutrons and from the decay of the capture products:

$$W_{fiss}^{i} = E_{r}^{i} + Q_{c}^{i} + W_{n}^{i}, \tag{3.1.6}$$

where W^{i}_{fiss} is the effective energy release in fission, E^{i}_{r} is the energy release in fission excluding the energy carried away by neutrinos and the kinetic energy of the incident neutrons, Q^{i}_{c} is the contribution from the decay of the capture products, and W^{i}_{n} is the kinetic energy of the incident neutrons. Index i refers to a fissionable nuclide in all cases.

E^i_r values are extracted from the MF=1/MT=458 section of an evaluated nuclear data file, while the kinetic energy of the incident neutron is obtained by approximately averaging the energy with the fission reaction rate. The averaging process involves the multi-group approximation and the cross sections obtained from the MCNP calculations based on ENDF/B cross section data:

$$W_n^i = \frac{\sum_g \bar{E}_g \sigma^i_{f,g} \phi_g}{\sum_g \sigma^i_{f,g} \phi_g}, \tag{3.1.7}$$

where $\sigma^i_{f,g}$ is the microscopic fission cross section of the fissionable nuclide i in the energy group g, ϕ_g is the neutron spectrum, and E_g is the average group energy. A typical PWR fuel pin was used in this calculation.

The average group energy was a simple mean of the group boundary values, except for the highest energy groups for which more accurate values were adopted to give the average energy in a Maxwellian fission spectrum at a temperature corresponding to 1.4 MeV:

$$E_g = \frac{\int_g E\sqrt{E} \cdot \exp(-E/T)dE}{\int_g \sqrt{E} \cdot \exp(-E/T)dE}. \tag{3.1.8}$$

The additional energy released due to gamma activation is calculated from

$$Q_c = (\bar{\nu} - 1)Q, \tag{3.1.9}$$

where ($\bar{\nu}$ -1) represents the average number of neutrons that are captured, and Q=6.1 MeV [Jam99]. Appendix A.3 provides recoverable energies per fission obtained by the above procedure.

3.1.10 Effective Background Cross Sections

While the AMPX MG library includes resonance data for all nuclides and energy groups, the MPACT MG library includes resonance data for the specified nuclides and energy groups. For example, 49 nuclides include subgroup data and resonance integral tables and 191 nuclides out of 295 include IR parameters for groups 10~31 in the 51-group structure. If infinitely dilute cross sections are provided in the MPACT MG library, the corresponding MPACT results would underestimate the multiplication factors at very high burnup points due to higher capture cross sections. Therefore, pre-self-shielded cross sections need to be included in the MPACT MG library.

At low burnup points heavy and fission product nuclides produced by decay and neutron reactions do not significantly contribute to the multiplication factor due to their small atomic number densities. It is reasonable to determine high burnup point at which background cross sections are estimated to be used in obtaining 1D self-shielded cross sections. This work can be done by the MPACT single pin depletion calculation to obtain atomic number density at high burnup point (45 MWD/kgU) and then effective microscopic background cross sections can be obtained from the MPACT subgroup or ESSM calculations.

3.1.11 Super Homogenization (SPH) Factor

Figure 3.1.4 provides a procedure to obtain the super homogenization (SPH) factor for ^{238}U to conserve reaction rates between the CE-KENO reference solutions and the MPACT subgroup results for which the CE-KENO models include the same variation cases as the heterogeneous IRFFACTOR cases. The SPH factors can be selectively applied to the specified energy groups indicating significant reaction rate differences.

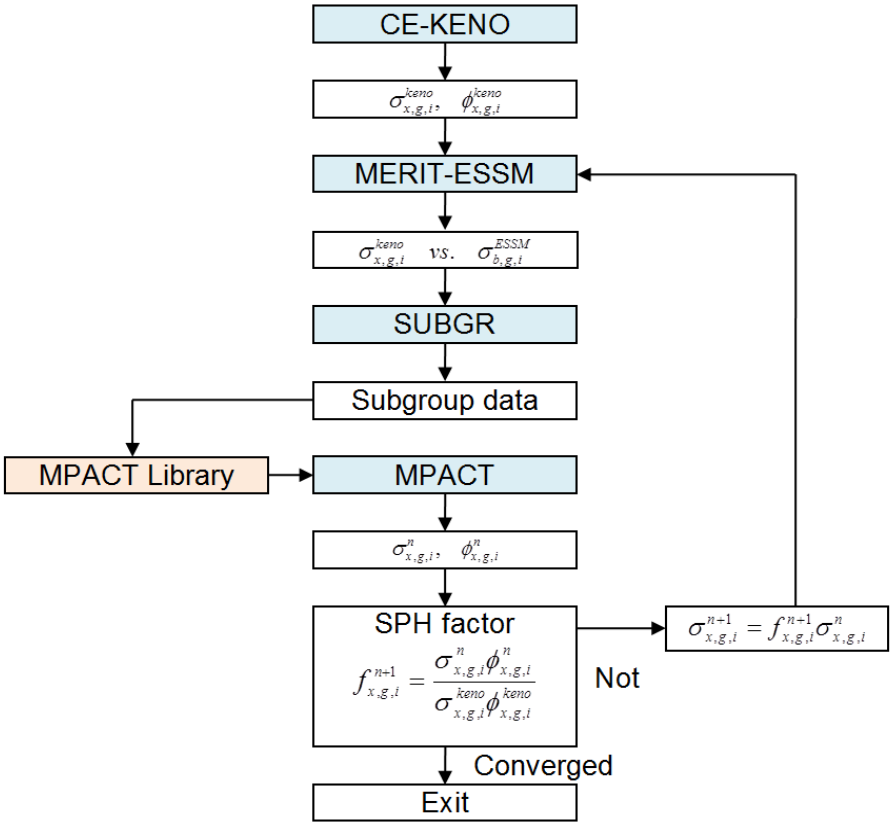

Figure 3.1.4 Procedure to generate the SPH Factors

3.2 VERIFICATION

3.2.1 AMPX and SCALE Code Package

All of subroutines and functionalities in the AMPX and SCALE code packages are under verification through CMAKE unit and regression tests based on the ORNL SCALE SQA procedure. Version control is provided by Mercurial.

Table 3.2.1 provides versions of the AMPX and SCALE code packages including constituent modules used in generating the AMPX MG library which have been developed at Oak Ridge National Laboratory.

Table 3.2.1 Programs to generate the AMPX MG library

Code Package	Version	Module	Version
AMPX	6.3	FILTER	6.3.pre-b1
		SIMONIZE	6.3.pre-b1
		AJAX	6.3
		RADE	6.3
		TGEL	6.3
		ZEST	6.3
		Y12	6.3.pre-b1
		FABULOUS	6.3.pre-b1
		PICKEZE	6.3.pre-b1
		PRELL	6.3
		X10	6.3.pre-b1
		LAMBDA	6.3.pre-b1
		CSAS25	6.3.pre-b1
		IRFFACTOR-HOM	6.3.pre-b1
		SUBGR	6.3.pre-b1
SCALE	6.3	IRFFACTOR-HET	6.3
		CSAS6	6.3.pre-b1
		KENO-VI	6.3.beta1
		ORIGEN	6.3

3.2.2 Programs to Generate MPACT and Simplified AMPX Libraries

All of subroutines and functionalities in the VERA-CS code package including XSTools to generate the MPACT and Simplified AMPX (SAMPX) libraries are under verification through CMAKE unit and regression tests based on the CASL VERA SQA procedure. Version control is provided by GIT.

Table 3.2.2 provides versions of the VERA-CS XSTools code package including constituent modules to generate the MPACT and SAMPX MG libraries. The transient data were generated by the NJOY program developed at Los Alamos National Laboratory.

Table 3.2.2 Programs to generate the MPACT and SAMPX MG library

Code Package	Version	Module	Version
VERA-CS XSTools	-	AMPXSLIB	1.1 mod 0
		DECLIB	1.2 mod 0
		FF2RI	1.1 mod 0
		MERIT	2.0 mod 0
NJOY	99.161	-	-

3.2.3 Assessment of the resonance data generation [Kim16c]

Currently, heterogeneous models are being used to generate resonance self-shielded cross section tables as a function of background cross sections by performing the CENTRM (Continuous Energy Transport Model) [Wil06] slowing down calculation with the MOC (Method of Characteristics) spatial discretization and ESSM (Embedded Self-Shielding Method) [Wil12] calculations to obtain background cross sections by using the SCALE IRFFACTOR. The resonance self-shielded cross section tables are then converted into subgroup data using the SUBGR program [Kim16f] which are to be used in estimating problem dependent self-shielded cross sections in MPACT. All of the programs and procedures include unit and regression tests for verification under the SCALE and AMPX [Wia16] SQA procedure. Although this procedure has been developed and thus resonance data have been generated, an assessment has never been performed to review if the resonance data are properly generated by the procedure and correctly utilized in MPACT. This study focuses on assessing the data generation procedure and subsequent use of the data in MPACT, including the following:

- Are the CENTRM slowing down calculations with MOC and Sn (Discrete Ordinate Method) working correctly?
- Are the corresponding background cross sections correctly obtained by performing the ESSM fixed source calculations?
- Are the self-shielded cross sections estimated by using subgroup method in MPACT acceptable?

There have been significant improvements in CENTRM since SCALE-6.1. The improvements are summarized as follows:

a. Figure 3.2.1 provides a comparison of reactivity analysis between the old SCALE-6.1 238-group and the new 252-group CENTRM-MOC only due to the cross section differences for the same problem. Even though there are some differences in cross sections of CENTRM-MOC at low resolved resonance groups, there are significant improvements on thermal, high epithermal and fast energy groups. Some cross section differences at low ^{238}U resonances need to be improved which may be achieved by improving group structures.
b. Figure 3.2.2 provides a comparison of cross-section difference between CENTRM-MOC and KENO-CE for the old SCALE-6.1 238-g and new SCALE-6.2

252-group CENTRM calculations. There are significant improvements in 1D self-shielded cross sections.

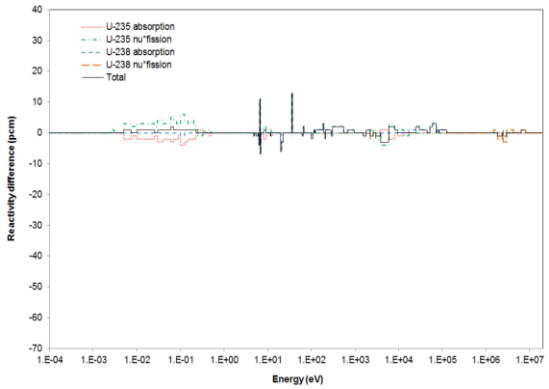

[Old MOC, 238-group]

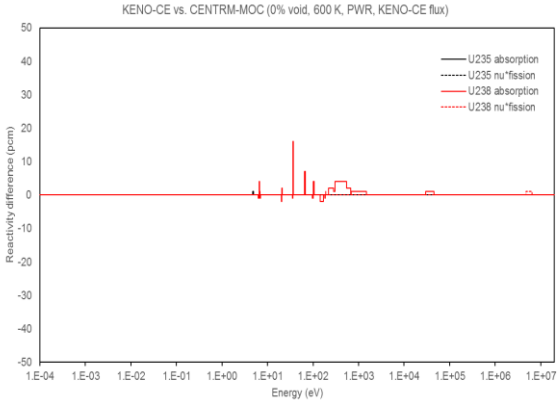

[New MOC, 252-group]

Figure 3.2.1 Comparison of reaction rate differences (Old vs. New, PWR, 600 K, ENDF/B-7.0)

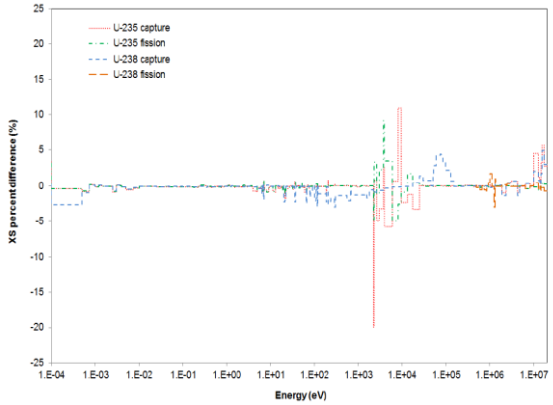

[Old MOC, 238-group]

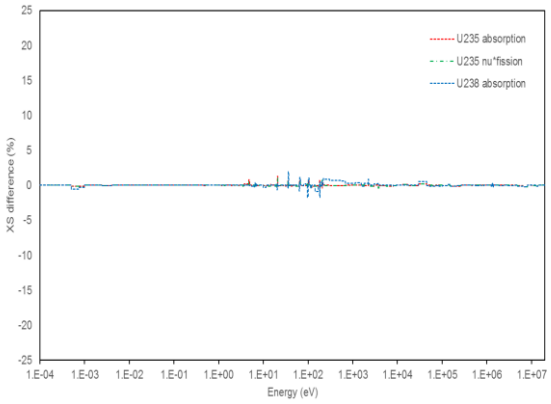

[New MOC, 252-group]

Figure 3.2.2 Comparison of cross section differences (Old vs. New, PWR, 600 K, ENDF/B-7.0)

Figure 3.2.3 provides comparisons of self-shielded absorption cross-section tables for important resonance group-23 (6.25~7.15 eV) of ^{235}U in the 51-group structure. This figure shows the data are very consistent with each other.

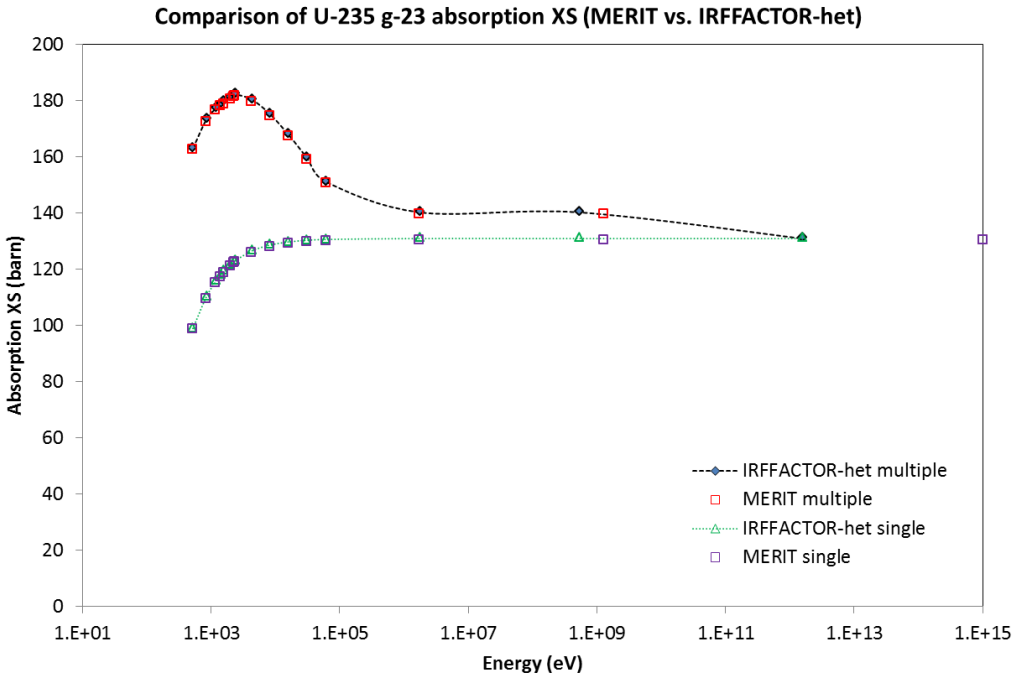

Figure 3.2.3 Comparison of self-shielded XS tables for ^{235}U group-23 absorption

The SUBGR program includes a verification procedure by comparing the reconstructed RIs or XSs from subgroup data to the original RIs or XSs. However, it is required to review if the MPACT subgroup module is able to correctly estimate self-shield cross sections to be consistent with the original resonance self-shielded cross-section data. The MPACT subgroup module includes a Bondarenko iteration to consider resonance interferences between resonance nuclides.

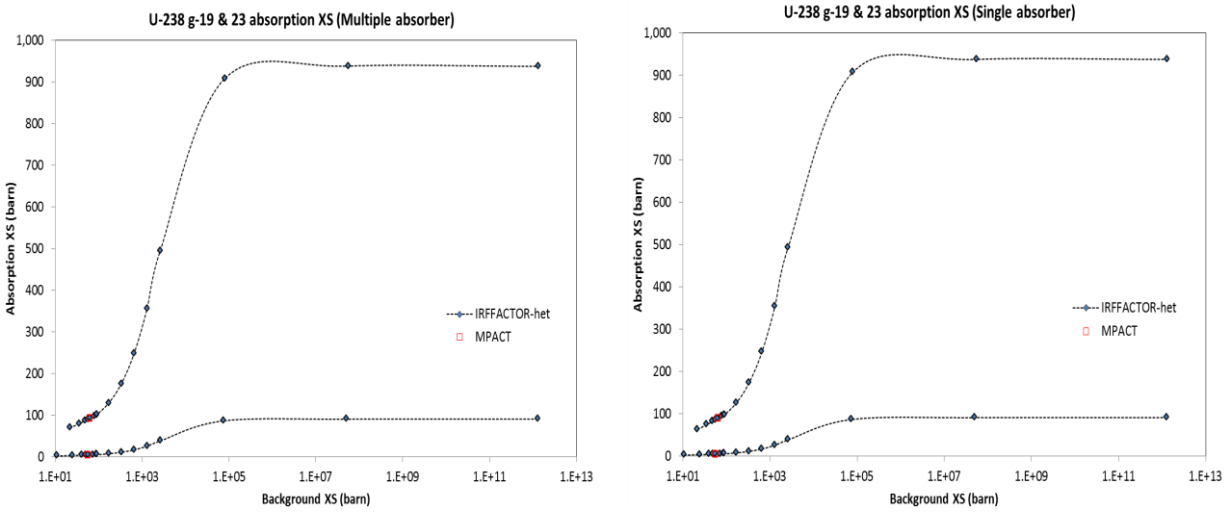

Figure 3.2.4 Reconstruction of the self-shielded cross sections by MPACT (^{238}U groups-19 and -23, absorption, single/multiple absorber models)

Since resonance self-shielded cross-section tables are typically generated without considering resonance interference, the Bondarenko iteration must be skipped for this assessment. Because MPACT does not include a user option to skip the Bondarenko iteration, MPACT was modified to skip the Bondarenko iteration for this verification process only. Self-shielded absorption and ν*fission cross sections for ^{235}U and ^{238}U have been estimated by the MPACT subgroup calculations without considering resonance interferences. Figure 3.2.4 provides comparisons of self-shielded cross sections between MPACT and IRFFACTOR which are very consistent with each other.

Investigation has demonstrated that the current CENTRM-MOC is working correctly. It is noted that the current CENTRM-MOC is working correctly. However, there remain non-negligible errors in predicting the self-shielded cross sections for some of the larger ^{238}U resonances which can contribute 10-20-pcm reactivity error for each resonance in the 252-group structure. The total reactivity by CENTRM-MOC is underestimated, on average, by about 100 pcm, which needs to be improved. The 51-group structure is not optimized resulting in temperature reactivity bias and larger reactivity differences compared to the 252-group results. Therefore, the 51-g structure needs to be improved to resolve the temperature reactivity bias and relatively large reactivity errors. Self-shielded cross section tables generated by IRFFACTOR with heterogeneous models are very consistent with those by another slowing down program called MERIT, that employs the same ESSM calculation to obtain background cross sections. Note that the AMPX self-shielded cross section tables are being correctly generated by the SCALE/AMPX IRFFACTOR. Note also that the self-shielded cross sections estimated by the MPACT subgroup module are very consistent with the original self-shielded cross-section tables prepared by IRFFACTOR, which indicates that the MPACT subgroup module is working correctly.

3.2.4 Programs used in the evaluation of the MPACT and SAMPX libraries

Table 3.2.3 provides list of programs used in the evaluation of the MPACT and SAMPX libraries. Reference solutions were obtained by various continuous energy Monte Carlo programs.

Table 3.2.3 Programs for library evaluation

Code	Version	Developer
VERA-CS MPACT	2.1.0	CASL
MCNP	6.1	Los Alamos National Laboratory
SERPENT	2.1.27	VTT Technical Research Center
McCARD	1.0.1.1	Seoul National University

4. CROSS SECTION LIBRARY GENERATION

Neutron cross section libraries were developed for the VERA-CS MPACT with the 51- and 252-group structures based on the ENDF/B-7.0 and 7.1 nuclear data as follows:

- The ENDF/B-7.0 v4.2m5 MPACT 51-g library
- The ENDF/B-7.1 v4.2m5 MPACT 51-g library (default)
- The ENDF/B-7.0 v4.2m0 MPACT 252g library
- The ENDF/B-7.1 v4.2m0 MPACT 252-g library
- The ENDF/B-7.0 v5.0m0 SAMPX 51-g library
- The ENDF/B-7.1 v5.0m0 SAMPX 51-g library
- The ENDF/B-7.0 v5.0m0 SAMPX 252g library
- The ENDF/B-7.1 v5.0m0 SAMPX 252-g library

4.1 AMPX MG LIBRARY

The AMPX MG library was generated by using the AMPX EXSITE utility to generate the AMPX input files for all nuclides by expanding a template. Figure 3.1.1 provides the AMPX procedure to generate the AMPX MG library where the left side of the flow chart is for the conventional procedure and the right side is for the new procedure that improves the Bondarenko resonance data. The following data are required in generating the AMPX MG library.

- ENDF/B-VII neutron cross section data
- ENDF/B-VII listing file
- ENDF/B-VII Doppler broadening data files
- ENDF/B-VII probability table files
- Pointwise weighting function

After completing the AMPX calculations for all nuclides, individual MG data files can be merged into an initial AMPX MG library by the AMPX AJAX module. We generated the AMPX 51- and 252-g libraries by using both ENDF/B-7.0 and 7.1.

The intermediate resonance (IR) parameters are generated for all nuclides by using the AMPX-LAMBDA module with a procedure introduced in Section 3.1.2 in which the IR parameters are estimated only for the specified energy groups and unity is assigned to other energy groups. In addition homogeneous F-factors are generated for the same energy groups for the IR parameters by the AMPX-IRFFACTOR-hom module with a procedure described in Section 3.1.3 which are substituted for the original F-factors. The following data are included in the AMPX MG master library.

- Intermediate resonance parameters : all nuclides, all energy groups
- Homogeneous F-factors : Nuclides Atomic number ≥ 40 (Zr)

Only selected resonance nuclides include heterogeneous F-factors; they have been determined to be important resonance nuclides because they can significantly impact

the neutronics result. The following 20 (22 for v5.0m0) nuclides have been selected to have heterogeneous F-factors. The option for level dependent background cross sections has been used for all nuclides except for Ag, In and Cd nuclides.

- ^{107}Ag, ^{109}Ag, ^{113}Cd, ^{113}In, ^{115}In, ^{155}Gd, ^{156}Gd, ^{157}Gd, ^{158}Gd, ^{232}Th, ^{233}U, ^{235}U, ^{236}U, ^{238}U, ^{238}Pu, ^{239}Pu, ^{240}Pu, ^{241}Pu, ^{242}Pu, ^{241}Am, (^{155}Eu and ^{237}Np for v5.0m0)

Since the Bondarenko approach is not typically able to consider resonance interference effects explicitly, heterogeneous F-factors can be generated in two different ways with or without consideration of explicit resonance interference. 'Single' and 'Multiple' indicate without and with resonance interference, respectively. The single absorber model has been applied only to 6 nuclides including ^{107}Ag, ^{109}Ag, ^{113}Cd, ^{113}In, ^{115}In and ^{238}U.

The heterogeneous IRFFACTOR results in two F-factor tables of which the first one can be incorporated by AMPX-AJAX and the second one (subgrpdata) is for SUBGR to generate subgroup data. The first one (or the AMPX MG master library) can also be utilized in the subgroup data generation. However, in order to generate subgroup data to conserve cross sections, subgroup level dependent background cross sections should be added to the F-factor tables (self-shielded cross section table). The AMPX MG library does not include the subgroup level dependent background cross sections, but the 'subgrpdata' file includes them.

4.2 MPACT MG LIBRARY

The Bondarenko F-factors in the AMPX MG library should be converted into resonance integral tables to be used in the subgroup data generation. Then the subgroup data are generated by using SUBGR. Subgroup data including weights and levels have been generated for 49 important resonance nuclides as shown in Table 4.2.1 for all energy groups.

Table 4.2.1 List of nuclides that include subgroup data

No	Nuclide	No	Nuclide	No	Nuclide	No	Nuclide	No	Nuclide
1	^{91}Zr	11	^{131}Xe	21	^{157}Gd	31	^{177}Hf	41	^{235}U
2	^{96}Zr	12	^{133}Cs	22	^{158}Gd	32	^{178}Hf	42	^{236}U
3	^{95}Mo	13	^{152}Sm	23	^{160}Dy	33	^{179}Hf	43	^{238}U
4	^{99}Tc	14	^{151}Eu	24	^{161}Dy	34	^{180}Hf	44	^{238}Pu
5	^{103}Rh	15	^{152}Eu	25	^{162}Dy	35	^{182}W	45	^{239}Pu
6	^{108}Pd	16	^{153}Eu	26	^{163}Dy	36	^{183}W	46	^{240}Pu
7	^{107}Ag	17	^{154}Eu	27	^{164}Dy	37	^{184}W	47	^{241}Pu
8	^{109}Ag	18	^{155}Eu	28	^{166}Er	38	^{186}W	48	^{242}Pu
9	^{113}In	19	^{155}Gd	29	^{167}Er	39	^{232}Th	49	^{241}Am
10	^{115}In	20	^{156}Gd	30	^{176}Hf	40	^{233}U		

Appendix B.1 provides the nuclide list of the MPACT 51- and 252-g libraries. The following data files are required for DECLIB to generate the MPACT MG library.

- The AMPX MG library
- ENDF/B files: Neutron data, decay constants, fission product yields
- Subgroup data and resonance integral table (49 nuclides, groups 10-31 in 51-g)
- Transport correction factors (^{1}H)
- Pre-determined background cross sections (105 nuclides)
- Transient data (21 nuclides)
- Subgroup data with epithermal upscattering (^{238}U)

Figure 4.2.1 provides a flow diagram of DECLIB to generate the MPACT MG library of which data structure is shown in Appendix B.2.

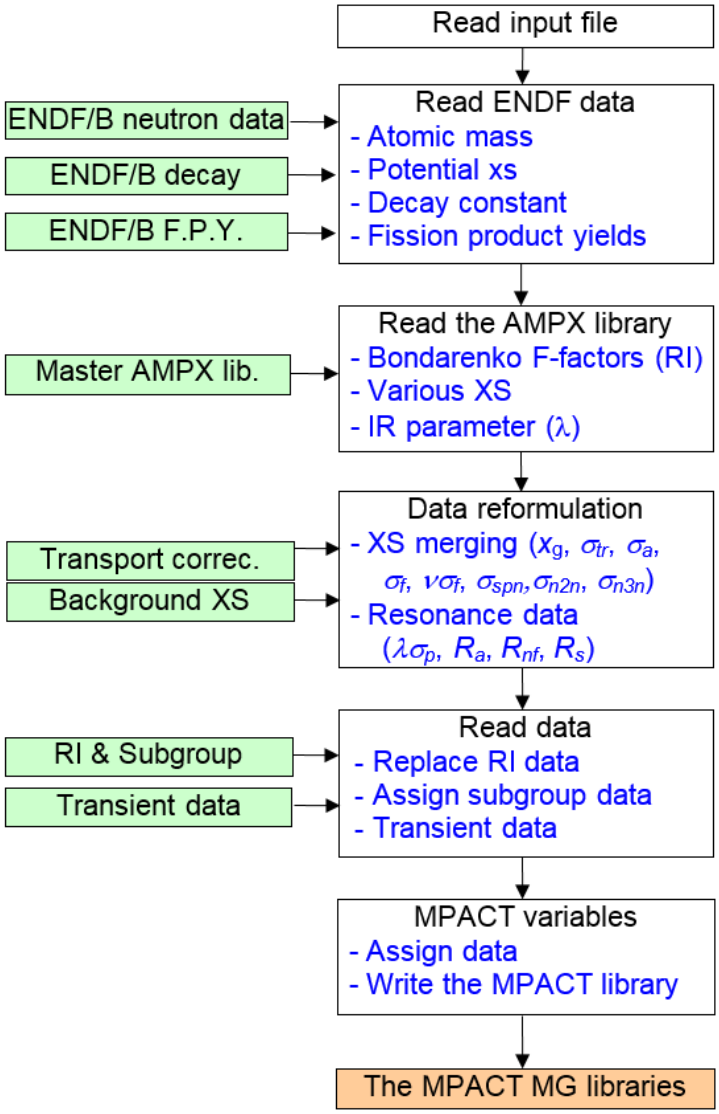

Figure 4.2.1 DECLIB calculation flow

The required data for the steady-state transport calculation are the transport cross section, fission cross section, the average number of neutrons released from a fission reaction, and fission spectrum for each nuclide. Since the absorption and fission cross sections are modified through the resonance treatment and are needed for the depletion calculation, those cross sections should be included. The (n,2n) and (n,3n) cross sections are required for the depletion calculation. High order (P_1~ P_3) scattering matrices are also included. Therefore, the multigroup data required in the library are as follows:

a. Transport cross section (σ_{tr})
b. Absorption cross section ($\sigma_{a}= \sigma_{c}+\sigma_{f}$)
c. Fission cross section (σ_{f})
d. Neutrons released from a fission (ν)
e. Scattering cross sections ($\sigma_{s0\sim3}$)
f. (n,2n) cross section ($\sigma_{n,2n}$)
g. (n,3n) cross section ($\sigma_{n,3n}$)
h. $P_{0\sim3}$ scattering matrix ($\sigma_{sngg'}$)
i. Fission spectrum (χ_g)

Since the AMPX MG master library includes cross section data for various reactions, it is required to merge cross sections to generate the above underlined data. Table 4.2.2 provides which MT numbers are to be merged for the required data.

Table 4.2.2 MT numbers to be merged

Cross section	MT numbers in the AMPX master library		
	F-factors	1D cross section	2D cross section
σ_t	1	-	-
σ_c	102	103~117	-
σ_f	18	-	-
ν	-	452	-
σ_{s0}	2	4	-
$\sigma_{n,2n}$	-	11, 16	11, 16
$\sigma_{n,3n}$	-	17	17
$\sigma_{sngg'}$	-	-	2, 50~91, 1007, 1008
χ_g*	-	18, 452, 455, 1055, 1056, 1099	-
λ	-	2000	-
$\sigma_{s,g}^{within}$	2022	-	-

*Since MT=1018 is just for prompt neutron, χ_g is internally recalculated.

4.3 SIMPLIFIED AMPX MG LIBRARY

The MPACT MG library includes the following drawbacks:

- Only 49 nuclides include the full resonance data such as subgroup data, RI table and IR parameters.
- Only groups 10 through 31 in the 51-group structure include resonance data.
- Pre-self-shielded cross sections are utilized for non-resonance nuclides and non-resonance energy groups.
- Temperature dependent elastic scattering matrices are not available. (This is a drawback of the AMPX MG library.)
- Although the ENDF/B-7.0 AMPX MG library includes 419 nuclides, the MPACT MG library includes 298 nuclides.
- Many of fission product nuclides include only absorption cross sections.
- There are many duplicated nuclides at activation and fission product nuclides.
- High order scattering matrices (≥P_2) are available only for important nuclides.

The simplified AMPX (SAMPX) MG library is based entirely on the AMPX MG library for which most of reactions are simplified to be quickly utilized in deterministic transport calculations. All of the ENDF/B nuclides are included in the simplified AMPX library. Therefore, the following data are included in the SAMPX library.

- Resonance self-shielded cross sections as a function of background cross sections: total (σ_t), transport (σ_{tr}), absorption (σ_a), fission (σ_f), elastic scattering ($\sigma_{el,l}$), within-group elastic scattering (σ_{wel})
- Non-resonance cross sections: non-elastic scattering (σ_{ne}), neutrons released from a fission (ν), (n,2n) ($\sigma_{n,2n}$), (n,3n) ($\sigma_{n,3n}$), total fission spectrum (χ_g), delayed fission spectrum ($\chi_{g,d}$), delayed neutrons released from a fission (ν_d),
- Scattering matrix: elastic P_n scattering matrix ($\sigma_{elngg'}$), non-elastic P_n scattering matrix ($\sigma_{nengg'}$), P_n thermal scattering matrix ($\sigma_{nengg'}$),
- Subgroup data: 49 nuclides
- Miscellaneous data: decay constants for delayed neutron, delayed neutron yield, fission and capture kappas

The data format of the SAMPX MG library is shown in Appendix B.3. Appendix B.4 provides lists of nuclides included in the ENDF/B-7.0 and 7.0 SAMPX 51 and 252-g libraries which have 425 and 455 nuclides, respectively.

5. VALIDATION BY CODE-TO-CODE COMPARISON

Given a nuclear data library and fully-specified problem, CE Monte Carlo calculations provide the correct answer, to within statistical uncertainty; MG deterministic transport calculations also include error associated with various approximations in spatial, angular, and energy discretizations. Therefore, comparison of CE Monte Carlo and MG deterministic results for a given statepoint will quantify errors in the nuclear data processing, when the spatial and angular meshes are fully-refined, to verify the correct implementation. While CE Monte Carlo with depletion introduces discretization error (in time and space) and includes approximations in heat generation, benchmarking MPACT's use of the nuclear data library will reveal potential issues related to the depletion data and MPACT's use of it.

Nine sets of benchmark problems have been developed to verify and validate the cross section libraries for the VERA neutronics simulator MPACT as follows:

A. VERA Progression Problems
B. Extended VERA Progression Problems
C. VERA Depletion Benchmark Problems
D. AP1000 Depletion Benchmark Problems
E. Reaction Rate Analysis Problems
F. Extensive PWR Pin and Assembly Benchmark Problems
G. BWR Assembly Benchmark Problems
H. Non-Uniform Fuel Temperature Problems
I. WBN-1 Power Plant Depletion Problems

Table 5.0.1 provides current status of benchmark calculations by using the ENDF/B-7.0 and 7.1 MPACT and SAMPX 51 and 252-g libraries. Reference solutions have been obtained by using continuous energy Monte Carlo codes such as CE-KENO and SHIFT developed by ORNL, MCNP by LANL, SERPENT by VTT and McCARD by SNU.

Table 5.0.1 Status for benchmark calculations

Contents	ENDF/B		Epithermal Up		MPACT		Simplified AMPX	
	7.0	7.1	No	Yes	51-g	252-g	51-g	252-g
VERA progression problems	X	X	X	X	X	X	X	X
Extended VERA progression problems	X	X	X	O	X	X	X	X
VERA depletion benchmark problems	X	O	X	O	X	O	Δ	O
AP1000 & KRSKO depletion benchmark problems	X	O	X	O	X	O	Δ	O
Reaction rate analysis problems	X	X	X	O	X	X	X	X
Extensive PWR pin & assembly benchmark problems	X	X	X	O	X	O	X	O
BWR pin and assembly benchmark problems	X	O	X	O	X	X	X	X
Non-uniform fuel temperature problems	X	O	X	O	X	O	X	O
WBN-1 Power Plant Depletion Problems	X	O	X	O	X	O	O	O

X: Yes; O: No; Δ: Partly

Because many of the original benchmark CE Monte Carlo solutions were produced with ENDF/B-7.0 using many core-hour simulations, we continue to benchmark MPACT with these libraries because there has not been sufficient justification for updating all of these cases. Similarly, the group-by-group reaction rate analyses required significantly more computational resources for new 252-group structure, so these have not been run for every benchmark problem below. Finally, some of the CE Monte Carlo codes are incapable of modeling resonance upscattering (Epithermal Up), therefore this option was removed for some comparisons.

5.1 VERA CORE PHYSICS BENCHMARK PROGRESSION PROBLEMS

5.1.1 Characteristics of Problems

The VERA Core Physics Benchmark Progression Problems were developed to provide a method for developing and demonstrating increasing capabilities for reactor physics methods and software. [God14] The progression problems range from a simple 2D pin cell to the full cycle depletion and refueling of a 3D reactor core configuration with control rods and burnable poisons consistent with actual nuclear power plant designs.

Table 5.1.1 Description of the VERA progression problems

Problem		Description	^{235}U w/o	Temperature (K)			Moderator	
				Mod.	Clad	Fuel	g/cm^3	PPM
1	1A	PWR pin	3.1	565	565	565	0.743	1300
	1B	PWR pin	3.1	600	600	600	0.661	1300
	1C	PWR pin	3.1	600	600	900	0.661	1300
	1D	PWR pin	3.1	600	600	1200	0.661	1300
	1E	PWR pin + IFBA	3.1	600	600	600	0.743	1300
2	2A	PWR FA, no BP	3.1	565	565	565	0.743	1300
	2B	PWR FA, no BP	3.1	600	600	600	0.661	1300
	2C	PWR FA, no BP	3.1	600	600	900	0.661	1300
	2D	PWR FA, no BP	3.1	600	600	1200	0.661	1300
	2E	PWR FA + 12 Pyrex	3.1	600	600	600	0.743	1300
	2F	PWR FA + 24 Pyrex	3.1	600	600	600	0.743	1300
	2G	PWR FA + 24 AIC CR	3.1	600	600	600	0.743	1300
	2H	PWR FA + 24 B_4C CR	3.1	600	600	600	0.743	1300
	2I	PWR FA + Instrument Thimble	3.1	600	600	600	0.743	1300
	2J	PWR FA + Instrument Thimble + 24 Pyrex	3.1	600	600	600	0.743	1300
	2K	PWR FA + Zoned enrichment + 24 Pyrex	3.1/3.6	600	600	600	0.743	1300
	2L	PWR FA + 80 IFBA	3.1	600	600	600	0.743	1300
	2M	PWR FA + 128 IFBA	3.1	600	600	600	0.743	1300
	2N	PWR FA + 104 IFBA + 20 WABA	3.1	600	600	600	0.743	1300
	2O	PWR FA + 12 Gadolinia	1.8/3.1	600	600	600	0.743	1300
	2P	PWR FA + 24 Gadolinia	1.8/3.1	600	600	600	0.743	1300
	2Q	PWR FA + Zircaloy Spacer grid	3.1	565	565	565	0.743	1300
5	5A-2D	PWR 2D core	2.1/2.6/3.1	565	565	565	0.743	1285
	5A-3D	PWR 3D core	2.1/2.6/3.1	565	565	565	0.743	1285

Most of the data are based on fuel and plant data from the initial core loading of Watts Bar Nuclear 1, a Westinghouse-designed 17x17 Pressurized Water Reactor (PWR) of the common vintage built in the U.S. in the 1980's and 1990's. We have selected the single-physics 2D benchmark problems to evaluate the neutron cross section library for the VERA neutronics simulator MPACT. Table 5.1.1 lists the selected VERA progression problems used for this benchmarking exercise. Figure 5.1.1 provides layouts of the pins and assemblies. Appendix C.1 provides specifications of geometry and composition.

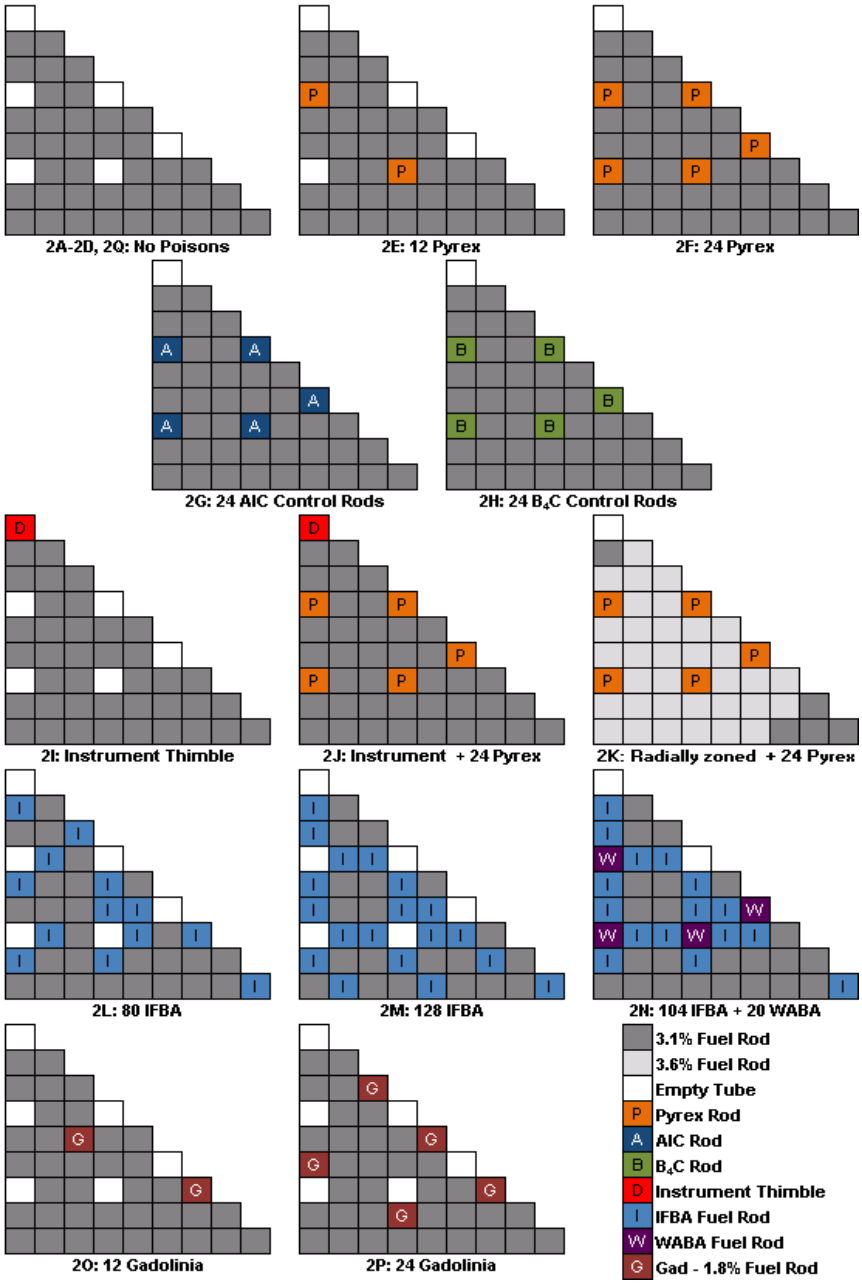

Figure 5.1.1 Problem 2 lattice layouts (Octant symmetry)

5.1.2 Benchmark Results

Benchmark calculations have been performed by using the following MPACT and SAMPX 51- and 252-g libraries.

- V4.2m5 ENDF/B-7.0 MPACT 51-g Library
- V4.2m5 ENDF/B-7.0 MPACT 51-g Library with ^{238}U epithermal upscattering data
- V4.2m5 ENDF/B-7.1 MPACT 51-g Library
- V4.2m5 ENDF/B-7.1 MPACT 51-g Library with ^{238}U epithermal upscattering data
- V4.2m0 ENDF/B-7.0 MPACT 252-g Library
- V4.2m0 ENDF/B-7.1 MPACT 252-g Library
- V5.0m0 ENDF/B-7.0 SAMPX 51-g Library
- V5.0m0 ENDF/B-7.0 SAMPX 51-g Library with ^{238}U epithermal upscattering data
- V5.0m0 ENDF/B-7.1 SAMPX 51-g Library
- V5.0m0 ENDF/B-7.1 SAMPX 51-g Library with ^{238}U epithermal upscattering data
- V5.0m0 ENDF/B-7.0 SAMPX 252-g Library
- V5.0m0 ENDF/B-7.0 SAMPX 252-g Library with ^{238}U epithermal upscattering data
- V5.0m0 ENDF/B-7.1 SAMPX 252-g Library
- V5.0m0 ENDF/B-7.1 SAMPX 252-g Library with ^{238}U epithermal upscattering data

Presently the default cross section library for MPACT is the v4.2m5 ENDF/B-7.1 MPACT 51-g library. Recently new SAMPX 51 and 252-g libraries have been developed which will be primary cross section libraries for MPACT in the near future after intensive testing and optimization of computational efficiency. Tables 5.1.1~5.1.3 provide benchmark results using the ENDF/B-7.1 MPACT 51-g and SAMPX 51 and 252-g libraries. The benchmark results are summarized as follows:

- All of the MPACT and SAMPX P_2 results satisfy the accuracy goals for prediction of multiplication factors (< 200 pcm $\Delta\rho$ or Δk) and pin power distributions.
- ^{238}U epithermal upscattering resonance data (DBRC option in Monte Carlo) have been generated correctly.
- A temperature reactivity bias shown in the MPACT library has been almost resolved in the SAMPX library.
- Since the transport cross sections of ^{1}H have been generated to conserve neutron leakage for the whole core problems, there are some reactivity differences for single pin and assembly problems when performing transport corrected P_0 (TCP0) calculations. When using the 252-g library, the difference is much more significant.
- Cases 2G and 2H are control rod insertion cases which show significant k_{eff} differences when performing TCP0 calculations. The TCP0 calculation is not able to correctly simulate highly anisotropic neutron angular fluxes in and around control rods in single-lattice rodded problems, but these errors dissipate in full-core calculations.
- Prediction of the power distribution is good for all cases regardless of the number of energy groups.

Table 5.1.1 Results with the ENDF/B-7.1 MPACT 51-g library

	Case	CE-KENO		MPACT P2[b]				MPACT TCP0[c]			
		k_{eff}	S.D.[a]	k_{eff}	Δk pcm	Pin power %		k_{eff}	Δk pcm	Pin power %	
						S.D.	Max.			S.D.	Max.
No DBRC	1A	1.18698	0.00011	1.18751	-53	-	-	1.18790	-92	-	-
	1B	1.18209	0.00009	1.18258	-49	-	-	1.18319	-111	-	-
	1C	1.17152	0.00008	1.17156	-4	-	-	1.17225	-73	-	-
	1D	1.16246	0.00009	1.16225	21	-	-	1.16302	-56	-	-
	1E	0.77158	0.00010	0.77311	-153	-	-	0.77289	-131	-	-
	2A	1.18191	0.00008	1.18256	-65	0.12	0.24	1.18232	-41	0.12	-0.26
	2B	1.18307	0.00009	1.18343	-37	0.12	-0.27	1.18342	-35	0.13	-0.31
	2C	1.17358	0.00010	1.17336	22	0.11	0.28	1.17340	17	0.13	0.33
	2D	1.16531	0.00010	1.16484	47	0.12	0.39	1.16495	36	0.12	0.35
	2E	1.06933	0.00009	1.06992	-59	0.13	-0.37	1.07044	-111	0.12	-0.36
	2F	0.97598	0.00009	0.97635	-38	0.15	0.40	0.97717	-119	0.15	0.39
	2G	0.84799	0.00008	0.84990	-192	0.26	0.61	0.85226	-427	0.29	0.71
	2H	0.78810	0.00012	0.78882	-72	0.22	-0.61	0.79232	-422	0.29	-0.83
	2I	1.17969	0.00008	1.18029	-60	0.13	0.31	1.18008	-39	0.14	0.29
	2J	0.97503	0.00010	0.97560	-57	0.17	-0.39	0.97641	-139	0.16	-0.39
	2K	1.01961	0.00010	1.02062	-101	0.14	0.36	1.02138	-177	0.13	0.32
	2L	1.01856	0.00010	1.01905	-49	0.12	0.33	1.01883	-27	0.13	0.34
	2M	0.93861	0.00009	0.93910	-50	0.15	-0.32	0.93881	-20	0.17	-0.43
	2N	0.86962	0.00008	0.86974	-12	0.20	0.59	0.87011	-49	0.15	0.47
	2O	1.04726	0.00010	1.04676	50	0.15	-0.37	1.04771	-45	0.16	0.37
	2P	0.92668	0.00010	0.92558	110	0.16	-0.40	0.92726	-58	0.18	-0.41
DBRC	1A	1.18603	0.00010	1.18602	1	-	-	1.18640	-37	-	-
	1B	1.18094	0.00009	1.18094	0	-	-	1.18153	-59	-	-
	1C	1.16946	0.00009	1.16900	46	-	-	1.16967	-22	-	-
	1D	1.15925	0.00009	1.15857	68	-	-	1.15932	-7	-	-
	1E	0.77099	0.00010	0.77220	-121	-	-	0.77197	-99	-	-
	2A	1.18099	0.00009	1.18122	-23	0.10	-0.28	1.18097	2	0.11	-0.29
	2B	1.18225	0.00009	1.18194	31	0.11	-0.23	1.18191	34	0.11	-0.22
	2C	1.17169	0.00008	1.17105	64	0.12	-0.27	1.17108	61	0.11	0.27
	2D	1.16252	0.00009	1.16152	100	0.10	0.31	1.16162	89	0.11	0.33
	2E	1.06840	0.00008	1.06866	-26	0.12	-0.26	1.06916	-76	0.10	-0.22
	2F	0.97501	0.00010	0.97518	-17	0.17	-0.38	0.97599	-98	0.17	-0.43
	2G	0.84716	0.00009	0.84892	-176	0.25	0.51	0.85127	-411	0.28	0.61
	2H	0.78768	0.00010	0.78793	-24	0.22	0.55	0.79142	-374	0.25	0.66
	2I	1.17858	0.00008	1.17891	-33	0.11	0.25	1.17868	-11	0.12	-0.29
	2J	0.97424	0.00009	0.97443	-19	0.13	-0.29	0.97524	-100	0.13	0.32
	2K	1.01901	0.00010	1.01941	-40	0.17	0.33	1.02016	-115	0.17	0.41
	2L	1.01774	0.00009	1.01788	-15	0.14	0.34	1.01766	8	0.16	0.38
	2M	0.93803	0.00011	0.93804	-1	0.11	-0.23	0.93774	29	0.15	-0.37
	2N	0.86882	0.00009	0.86875	8	0.17	0.42	0.86911	-29	0.13	-0.29
	2O	1.04643	0.00010	1.04555	88	0.13	-0.30	1.04649	-6	0.15	-0.39
	2P	0.92611	0.00010	0.92452	159	0.17	-0.44	0.92619	-8	0.18	-0.42

[a] S.D.: Standard Deviation
[b] P2: P_2 scattering
[c] TCP0: Transport correct P_0 scattering

Table 5.1.2 Results with the ENDF/B-7.1 SAMPX 51-g library

	Case	CE-KENO		SAMPX P2				SAMPX TCP0			
		k_{eff}	S.D.	k_{eff}	Δk pcm	Pin power %		k_{eff}	Δk pcm	Pin power %	
						S.D.	Max.			S.D.	Max.
No DBRC	1A	1.18698	0.00011	1.18727	-29	-	-	1.18771	-73	-	-
	1B	1.18209	0.00009	1.18242	-33	-	-	1.18308	-99	-	-
	1C	1.17152	0.00008	1.17165	-13	-	-	1.17240	-88	-	-
	1D	1.16246	0.00009	1.16231	15	-	-	1.16314	-68	-	-
	1E	0.77158	0.00010	0.77248	-90	-	-	0.77241	-83	-	-
	2A	1.18191	0.00008	1.18216	-26	0.12	0.24	1.18208	-17	0.12	-0.28
	2B	1.18307	0.00009	1.18312	-5	0.12	0.27	1.18326	-20	0.13	-0.32
	2C	1.17358	0.00010	1.17330	28	0.11	0.27	1.17351	7	0.13	0.32
	2D	1.16531	0.00010	1.16473	58	0.12	0.40	1.16500	31	0.12	0.34
	2E	1.06933	0.00009	1.06942	-9	0.13	-0.37	1.07019	-86	0.12	-0.34
	2F	0.97598	0.00009	0.97579	18	0.15	0.38	0.97694	-96	0.15	0.48
	2G	0.84799	0.00008	0.84983	-184	0.26	0.56	0.85275	-476	0.25	-0.61
	2H	0.78810	0.00012	0.78843	-33	0.20	-0.58	0.79268	-458	0.25	-0.73
	2I	1.17969	0.00008	1.17991	-22	0.14	0.32	1.17985	-16	0.14	0.30
	2J	0.97503	0.00010	0.97504	-1	0.16	-0.38	0.97618	-116	0.16	0.45
	2K	1.01961	0.00010	1.01992	-31	0.13	0.35	1.02099	-138	0.14	-0.32
	2L	1.01856	0.00010	1.01927	-71	0.13	0.36	1.01923	-67	0.14	-0.37
	2M	0.93861	0.00009	0.93931	-70	0.15	0.32	0.93920	-59	0.17	0.43
	2N	0.86962	0.00008	0.86975	-13	0.21	0.64	0.87042	-80	0.20	0.49
	2O	1.04726	0.00010	1.04675	51	0.16	0.37	1.04795	-69	0.15	0.39
	2P	0.92668	0.00010	0.92588	80	0.18	-0.39	0.92785	-117	0.18	-0.44
DBRC	1A	1.18603	0.00010	1.18584	19	-	-	1.18629	-26	-	-
	1B	1.18094	0.00009	1.18085	8	-	-	1.18152	-59	-	-
	1C	1.16946	0.00009	1.16889	57	-	-	1.16965	-19	-	-
	1D	1.15925	0.00009	1.15885	40	-	-	1.15969	-44	-	-
	1E	0.77099	0.00010	0.77161	-62	-	-	0.77155	-56	-	-
	2A	1.18099	0.00009	1.18087	12	0.11	-0.27	1.18079	20	0.11	-0.30
	2B	1.18225	0.00009	1.18169	56	0.11	-0.22	1.18184	40	0.11	-0.25
	2C	1.17169	0.00008	1.17077	92	0.12	-0.27	1.17100	70	0.11	0.27
	2D	1.16252	0.00009	1.16159	92	0.10	0.31	1.16188	64	0.11	0.33
	2E	1.06840	0.00008	1.06820	20	0.12	-0.26	1.06899	-58	0.11	-0.26
	2F	0.97501	0.00010	0.97467	34	0.17	-0.37	0.97582	-81	0.17	0.50
	2G	0.84716	0.00009	0.84889	-173	0.24	0.49	0.85182	-466	0.24	-0.60
	2H	0.78768	0.00010	0.78760	8	0.19	0.55	0.79185	-417	0.23	0.47
	2I	1.17858	0.00008	1.17857	0	0.11	0.25	1.17852	5	0.13	-0.31
	2J	0.97424	0.00009	0.97392	32	0.13	0.28	0.97507	-83	0.15	0.34
	2K	1.01901	0.00010	1.01875	26	0.17	0.35	1.01983	-82	0.17	0.51
	2L	1.01774	0.00009	1.01814	-41	0.15	-0.35	1.01812	-38	0.16	0.40
	2M	0.93803	0.00011	0.93829	-26	0.12	-0.24	0.93819	-16	0.16	-0.42
	2N	0.86882	0.00009	0.86879	3	0.18	0.41	0.86947	-65	0.19	-0.52
	2O	1.04643	0.00010	1.04558	85	0.14	-0.3	1.04679	-36	0.15	-0.37
	2P	0.92611	0.00010	0.92486	125	0.19	-0.45	0.92684	-73	0.20	0.43

Table 5.1.3 Results with the ENDF/B-7.1 SAMPX 252-g library

	Case	CE-KENO		SAMPX P2				SAMPX TCP0			
		k_{eff}	S.D.	k_{eff}	Δk pcm	Pin power %		k_{eff}	Δk pcm	Pin power %	
						S.D.	Max.			S.D.	Max.
No DBRC	1A	1.18698	0.00011	1.18666	32	-	-	1.18834	-136	-	-
	1B	1.18209	0.00009	1.18175	34	-	-	1.18376	-168	-	-
	1C	1.17152	0.00008	1.17119	33	-	-	1.17336	-184	-	-
	1D	1.16246	0.00009	1.16208	38	-	-	1.16439	-193	-	-
	1E	0.77158	0.00010	0.77163	-5	-	-	0.77231	-73	-	-
	2A	1.18191	0.00008	1.18171	20	0.12	0.24	1.18246	-56	0.12	-0.28
	2B	1.18307	0.00009	1.18262	45	0.12	0.27	1.18372	-66	0.13	-0.32
	2C	1.17358	0.00010	1.17301	57	0.11	0.27	1.17422	-64	0.13	0.32
	2D	1.16531	0.00010	1.16467	64	0.12	0.4	1.16598	-67	0.12	0.34
	2E	1.06933	0.00009	1.06888	45	0.13	-0.37	1.07047	-114	0.12	-0.34
	2F	0.97598	0.00009	0.97510	88	0.15	0.38	0.97703	-105	0.15	0.48
	2G	0.84799	0.00008	0.84721	78	0.26	0.56	0.85065	-266	0.25	-0.61
	2H	0.78810	0.00012	0.78761	49	0.2	-0.58	0.79245	-435	0.25	-0.73
	2I	1.17969	0.00008	1.17951	18	0.14	0.32	1.18030	-61	0.14	0.3
	2J	0.97503	0.00010	0.97434	68	0.16	-0.38	0.97627	-125	0.16	0.45
	2K	1.01961	0.00010	1.01919	42	0.13	0.35	1.02108	-147	0.14	-0.32
	2L	1.01856	0.00010	1.01879	-23	0.13	0.36	1.01947	-91	0.14	-0.37
	2M	0.93861	0.00009	0.93878	-17	0.15	0.32	0.93933	-72	0.17	0.43
	2N	0.86962	0.00008	0.86908	54	0.21	0.64	0.87040	-78	0.2	0.49
	2O	1.04726	0.00010	1.04662	64	0.16	0.37	1.04855	-129	0.15	0.39
	2P	0.92668	0.00010	0.92597	71	0.18	-0.39	0.92856	-188	0.18	-0.44
DBRC	1A	1.18603	0.00010	1.18585	18	-	-	1.18754	-151	-	-
	1B	1.18094	0.00009	1.18085	9	-	-	1.18288	-194	-	-
	1C	1.16946	0.00009	1.16981	-35	-	-	1.17200	-254	-	-
	1D	1.15925	0.00009	1.16015	-90	-	-	1.16250	-325	-	-
	1E	0.77099	0.00010	0.77113	-14	-	-	0.77181	-82	-	-
	2A	1.18099	0.00009	1.18099	0	0.10	-0.28	1.18176	-77	0.11	-0.29
	2B	1.18225	0.00009	1.18181	44	0.11	-0.23	1.18293	-68	0.11	-0.24
	2C	1.17169	0.00008	1.17177	-8	0.12	-0.26	1.17300	-131	0.11	0.27
	2D	1.16252	0.00009	1.16294	-43	0.10	0.31	1.16428	-177	0.11	0.32
	2E	1.06840	0.00008	1.06820	20	0.12	-0.25	1.06980	-140	0.11	-0.26
	2F	0.97501	0.00010	0.97447	54	0.16	0.36	0.97641	-139	0.17	0.49
	2G	0.84716	0.00009	0.84667	49	0.20	-0.42	0.85012	-296	0.24	-0.64
	2H	0.78768	0.00010	0.78714	54	0.19	0.53	0.79198	-430	0.22	0.45
	2I	1.17858	0.00008	1.17877	-19	0.11	0.25	1.17957	-99	0.13	-0.30
	2J	0.97424	0.00009	0.97371	53	0.12	0.27	0.97565	-141	0.14	0.33
	2K	1.01901	0.00010	1.01854	47	0.16	0.34	1.02043	-142	0.17	0.49
	2L	1.01774	0.00009	1.01816	-42	0.15	-0.37	1.01886	-112	0.16	0.40
	2M	0.93803	0.00011	0.93821	-18	0.12	-0.23	0.93876	-73	0.16	-0.42
	2N	0.86882	0.00009	0.86854	28	0.17	0.40	0.86987	-105	0.18	-0.47
	2O	1.04643	0.00010	1.04598	45	0.14	-0.30	1.04791	-148	0.15	-0.38
	2P	0.92611	0.00010	0.92541	70	0.19	-0.44	0.92801	-190	0.19	0.42

Table 5.1.4 and Figures 5.1.2~5.2.4 provides benchmark results for the VERA progression problem 5A 2D and 3D quarter core problems by using the v4.2m5 MPACT and v5.0m0 SAMPX 51-g libraries. The reference solutions were obtained by using CE-KENO with the ENDF/B-7.0 nuclear data. The benchmark results with the v4.2m5 MPACT and v5.0m0 SAMPX 51-g libraries with ENDF/B-7.0 are very consistent with the reference CE-KENO result for both multiplication factor and pin power distributions. The SAMPX library result for multiplication factor is better than the MPACT library results. However, The MPACT library results for radial and axial pin and assembly power distributions are slightly better than the SAMPX library results.

Table 5.1.4 Results for 5A with the ENDF/B-7.0 library

Problem	Parameter	MPACT	SAMPX
5A-2D	Δk diff. (pcm)	44	11
	Radial power, RMS (%)	0.262	0.552
	Radial power, Max. (%)	0.762	1.249
5A-3D	Δk diff. (pcm)	45	15
	3D pin power, RMS (%)	0.468	0.644
	3D pin power, Max. (%)	2.688	2.777
	Axial power, RMS (%)	0.276	0.286
	Axial power, Max. (%)	0.459	0.460
	Axial power, Axial Offset (%)	0.242	0.243
	Radial power, RMS (%)	0.270	0.486
	Radial power, Max. (%)	0.818	1.112
	3D Assembly power, RMS (%)	0.391	0.585
	3D Assembly power, Max. (%)	1.157	1.367
	2D Assembly power, RMS (%)	0.237	0.463
	2D Assembly power, Max. (%)	0.531	0.750

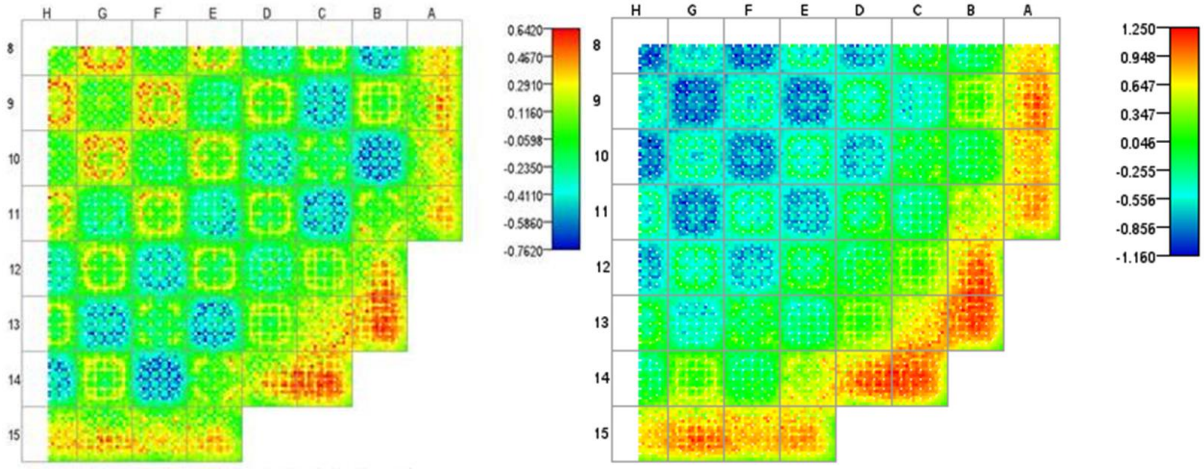

(a) MPACT library (b) SAMPX library

Figure 5.1.2 Pin power comparisons for Problem 5A-2D

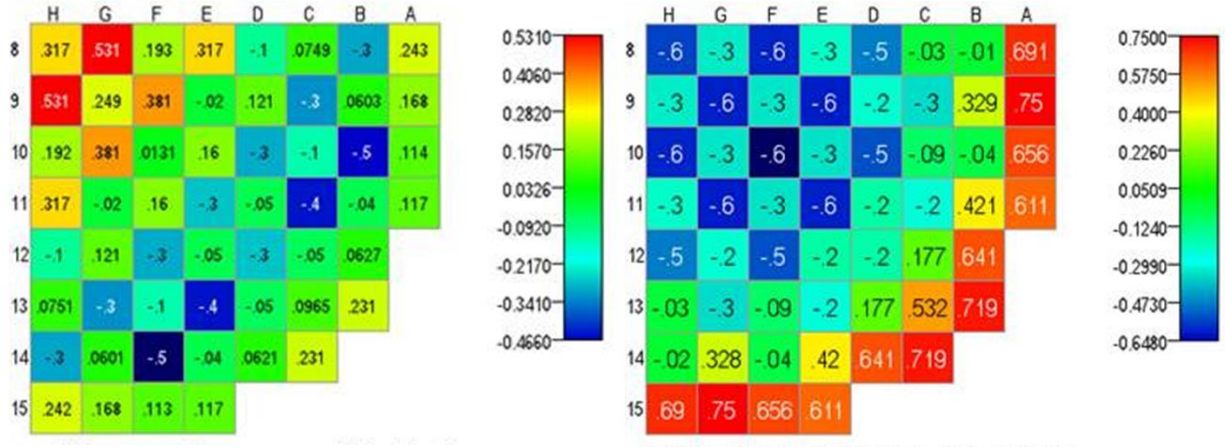

(a) MPACT library (b) SAMPX library

Figure 5.1.3 Assembly power comparisons for Problem 5A-3D

(a) MPACT library (b) SAMPX library

Figure 5.1.4 Axial power comparisons for Problem 5A-3D

5.2 EXTENDED VERA BENCHMARK PROGRESSION PROBLEMS

5.2.1 Characteristics of Problems

Since the VERA Core Physics benchmark progression problems do not include various ^{235}U enrichment and burnup compositions, additional benchmark problems have been developed to see the sensitivities of the libraries to ^{235}U enrichment, burnup and the number of radial fuel rings. These benchmark problems are based on the VERA progression problems 1B and 1C. Table 5.2.1 provides list of new extended VERA benchmark problems. Cases 1C-10-1h ~ 1C-60-1h include only heavy nuclides excluding fission product isotopes. Appendix C.2 provides geometry and atomic number densities at 0, 10, 20, 40 and 60 MWD/kgU burnup points.

Table 5.2.1 Extended VERA benchmark problems

Case	Description	^{235}U w/o	Burnup (MWD/kgU)	Temperature (K)			Moderator	
				Mod.	Clad	Fuel	g/cm^3	PPM
1B-21	PWR pin ^{235}U 2.1 w/o	2.1	0	600	600	600	0.661	1300
1B-26	PWR pin ^{235}U 2.6 w/o	2.6	0	600	600	600	0.661	1300
1B-31	PWR pin ^{235}U 3.1 w/o	3.1	0	600	600	600	0.661	1300
1B-36	PWR pin ^{235}U 3.6 w/o	3.6	0	600	600	600	0.661	1300
1B-41	PWR pin ^{235}U 4.1 w/o	4.1	0	600	600	600	0.661	1300
1B-46	PWR pin ^{235}U 4.6 w/o	4.6	0	600	600	600	0.661	1300
1C-00-3a	PWR pin 3-ring, full isotopes	3.1	0	600	600	900	0.661	1300
1C-10-3a	PWR pin 3-ring, full isotopes	3.1	10	600	600	900	0.661	1300
1C-20-3a	PWR pin 3-ring, full isotopes	3.1	20	600	600	900	0.661	1300
1C-40-3a	PWR pin 3-ring, full isotopes	3.1	40	600	600	900	0.661	1300
1C-60-3a	PWR pin 3-ring, full isotopes	3.1	60	600	600	900	0.661	1300
1C-10-1h	PWR pin 1-ring, heavy isotopes	3.1	10	600	600	900	0.661	1300
1C-20-1h	PWR pin 1-ring, heavy isotopes	3.1	20	600	600	900	0.661	1300
1C-40-1h	PWR pin 1-ring, heavy isotopes	3.1	40	600	600	900	0.661	1300
1C-60-1h	PWR pin 1-ring, heavy isotopes	3.1	60	600	600	900	0.661	1300

5.2.2 Benchmark Results

Benchmark calculations have been performed using the ENDF/B-7.0 and 7.1 MPACT and SAMPX 51-g libraries. The benchmark results can be summarized as follows:

- As shown in the benchmark results in Section 5.1, there is about 60 pcm difference between P2 and TCP0. The P2 results should be more reliable at single pin level simulations.
- When using the MPACT 51-g libraries, only 1C-60-1h does not meet the accuracy goals.
- When using the SAMPX 51-g libraries, all cases meet the accuracy goals.

Table 5.2.1 Benchmark result with the ENDF/B-7.0 MPACT 51-g library

Case	No Epithermal Upscatt			Epithermal Upscatt		
	KENO	P2, pcm	TCP0, pcm	KENO	P2, pcm	TCP0,pcm
1C-21	1.07024	-38	-78	1.06908	-72	-110
1C-26	1.13537	-45	-89	1.13423	-73	-116
1C-31	1.18226	-38	-86	1.18114	-62	-108
1C-36	1.22099	-60	-112	1.21999	-71	-121
1C-41	1.25275	-39	-94	1.25159	-66	-118
1C-46	1.27880	-48	-106	1.27767	-72	-127
1C-00-3a	1.24716	-8	-79	1.24507	-10	-78
1C-10-3a	1.08701	-150	-231	1.08542	-153	-233
1C-20-3a	1.00195	-71	-189	1.00022	-102	-219
1C-40-3a	0.88108	4	-140	0.87993	9	-133
1C-60-3a	0.80657	41	-107	0.80529	20	-127
1C-10-1h	1.17459	-88	-175	1.17256	-119	-205
1C-20-1h	1.11707	28	-101	1.11492	-24	-152
1C-40-1h	1.03606	165	2	1.03434	143	-17
1C-60-1h	0.98776	238	68	0.98611	215	47

Table 5.2.2 Benchmark result with the ENDF/B-7.1 MPACT 51-g library

Case	No Epithermal Upscatt			Epithermal Upscatt		
	KENO	P2, pcm	TCP0, pcm	KENO	P2, pcm	TCP0,pcm
1C-21	1.07008	-46	-86	1.06908	7	-32
1C-26	1.13506	-69	-114	1.13402	-13	-57
1C-31	1.18199	-59	-109	1.18087	-7	-54
1C-36	1.22098	-58	-111	1.21992	4	-47
1C-41	1.25239	-75	-131	1.25153	9	-45
1C-46	1.27881	-51	-109	1.27764	4	-53
1C-00-3a	1.24699	48	-25	1.24496	111	40
1C-10-3a	1.08728	-86	-169	1.08541	-65	-147
1C-20-3a	1.00259	-45	-164	1.00111	-6	-125
1C-40-3a	0.88304	34	-111	0.88157	47	-97
1C-60-3a	0.80899	22	-127	0.80736	2	-147
1C-10-1h	1.17408	-11	-101	1.17176	-14	-103
1C-20-1h	1.11658	81	-50	1.11468	106	-25
1C-40-1h	1.03617	186	21	1.03419	186	23
1C-60-1h	0.98862	228	56	0.98682	236	65

Table 5.2.3 Benchmark result with the v5.0m0 ENDF/B-7.0 SAMPX 51-g library

Case	No Epithermal Upscatt			Epithermal Upscatt		
	KENO	P2, pcm	TCP0, pcm	KENO	P2, pcm	TCP0,pcm
1C-21	1.07024	-26	-81	1.06908	-40	-100
1C-26	1.13537	-28	-87	1.13423	-36	-100
1C-31	1.18226	-17	-80	1.18114	-21	-89
1C-36	1.22099	-35	-101	1.21999	-26	-96
1C-41	1.25275	-11	-80	1.25159	-17	-91
1C-46	1.27880	-20	-92	1.27767	-22	-99
1C-00-3a	1.24716	-8	-92	1.24507	40	-51
1C-10-3a	1.08701	-98	-195	1.08542	-94	-195
1C-20-3a	1.00195	-100	-234	1.00022	-122	-260
1C-40-3a	0.88108	-69	-230	0.87993	-51	-216
1C-60-3a	0.80657	-62	-229	0.80529	-71	-242
1C-10-1h	1.17459	-82	-185	1.17256	-105	-214
1C-20-1h	1.11707	-60	-204	1.11492	-101	-250
1C-40-1h	1.03606	30	-146	1.03434	22	-158
1C-60-1h	0.98776	95	-88	0.98611	86	-101

Table 5.2.4 Benchmark result with the v5.0m0 ENDF/B-7.1 SAMPX 51-g library

Case	No Epithermal Upscatt			Epithermal Upscatt		
	KENO	P2, pcm	TCP0, pcm	KENO	P2, pcm	TCP0,pcm
1C-21	1.07008	-35	-93	1.06908	10	-50
1C-26	1.13506	-54	-117	1.13402	-6	-70
1C-31	1.18199	-43	-109	1.18087	2	-65
1C-36	1.22098	-38	-107	1.21992	16	-55
1C-41	1.25239	-53	-125	1.25153	24	-50
1C-46	1.27881	-27	-102	1.27764	20	-57
1C-00-3a	1.24699	16	-73	1.24496	101	10
1C-10-3a	1.08728	-114	-215	1.08541	-56	-158
1C-20-3a	1.00259	-143	-280	1.00111	-67	-205
1C-40-3a	0.88304	-95	-259	0.88157	-48	-212
1C-60-3a	0.80899	-133	-302	0.80736	-120	-290
1C-10-1h	1.17408	-93	-201	1.17176	-55	-164
1C-20-1h	1.11658	-86	-234	1.11468	-19	-168
1C-40-1h	1.03617	-19	-198	1.03419	23	-158
1C-60-1h	0.98862	21	-165	0.98682	70	-117

5.3 VERA DEPLETION BENCHMARK PROBLEMS

5.3.1 Characteristics of Problems

The VERA depletion benchmark problems [Kim16a] have been developed based on the VERA progression problems [God14]. Appendix C.1 provides the geometrical and material data for the benchmark problems which come from the VERA progression problems #1 and #2.

The depletion benchmark suite includes 9 single pin and 16 fuel assembly problems with various fuel temperatures, ^{235}U enrichments, control rods and burnable poisons as shown in Table 5.3.1. The pin configurations of fuel rods, guide/instrument tubes and burnable poisons are shown in Figure 5.1.1.

Table 5.3.1 Single pin and assembly depletion benchmark problems

Case	Description	Temperature (K)			Moderator Density (g/cc)	^{235}U w/o	Power density (w/gU)
		Moderator	Clad	Fuel			
1A	Pin 3.1w/o T_F=565K	565	565	565	0.743	3.1	40.0
1B	Pin 3.1w/o T_F=600K	600	600	600	0.700	3.1	40.0
1C	Pin 3.1w/o T_F=900K	600	600	900	0.700	3.1	40.0
1D	Pin 3.1w/o T_F=1200K	600	600	1200	0.700	3.1	40.0
1E	Pin IFBA 3.1w/o T_F=600K	600	600	900	0.700	3.1	40.0
1F	Pin 2.1w/o T_F=900K	600	600	900	0.700	2.1	40.0
1G	Pin 3.6w/o T_F=900K	600	600	900	0.700	3.6	40.0
1H	Pin 4.6w/o T_F=900K	600	600	900	0.700	4.6	40.0
1I	Pin Gadolinia rod (5% Gd_2O_3)	600	600	900	0.700	1.8	40.0
1J	Pin 3.1w/o T_F=600/900/1200K	600	600	600/900/1200	0.700	3.1	40.0
2A	FA No Poisons T_F=565K	565	565	565	0.743	3.1	40.0
2B	FA No Poisons T_F=600K	600	600	600	0.700	3.1	40.0
2C	FA No Poisons T_F=900K	600	600	900	0.700	3.1	40.0
2D	FA No Poisons T_F=1200K	600	600	1200	0.700	3.1	40.0
2E	FA 12 Pyrex	600	600	900	0.700	3.1	40.0
2F	FA 24 Pyrex	600	600	900	0.700	3.1	40.0
2G	FA 24 AIC	600	600	900	0.700	3.1	40.0
2H	FA 24 B4C	600	600	900	0.700	3.1	40.0
2I	FA Instrument Thimble	600	600	900	0.700	3.1	40.0
2J	FA Instrument + 24 Pyrex	600	600	900	0.700	3.1	40.0
2K	FA Zoned + 24 Pyrex	600	600	900	0.700	3.1/3.6	40.0
2L	FA 80 IFBA	600	600	900	0.700	3.1	40.0
2M	FA 128 IFBA	600	600	900	0.700	3.1	40.0
2N	FA 104 IFBA + 20 WABA	600	600	900	0.700	3.1	40.0
2O	FA 12 Gadolinia	600	600	900	0.700	3.1/1.8	40.0
2P	FA 24 Gadolinia	600	600	900	0.700	3.1/1.8	40.0

The computational results of the depletion calculations would be dependent upon user options and libraries. Therefore, to minimize differences due to the user options and library the following user options and library should be utilized in the calculations.

- Xenon option
  - Non-equilibrium for all cases
- Power density
  - Table 5.3.1 provides the specific power density for each case (40.0 w/gU).
- Burnup points
  - Table 5.3.2 provides the editing burnup points.
- Library
  - ENDF/B-7.0 or ENDF/B-7.1 (7.0 is recommended since SERPENT carries only the ENDF/B-7.0 cross sections.)
- The number of depletion zones
  - UO_2 pellet: 3 equi-volumetric zones
  - UO_2+Gd_2O_3 Gadolinia rod: 5 equi-volumetric zones
  - WABA & PYREX: 3 equi-volumetric zones

Table 5.3.2 Burnup points and editing options

Step	Burnup		Edit			Step	Burnup		Edit		
	MWD/kgU	EFPD	P.D.	R.R.	Flux		MWD/kgU	EFPD	P.D.	R.R.	Flux
1	0.00	0.00	O	O	O	21	17.00	425.00			
2	0.01	0.25				22	18.00	450.00			
3	0.25	6.25				23	19.00	475.00			
4	0.50	12.50				24	20.00	500.00	O	O	O
5	1.00	25.00				25	22.50	562.50			
6	2.00	50.00				26	25.00	625.00			
7	3.00	75.00				27	27.50	687.50			
8	4.00	100.00				28	30.00	750.00	O	O	O
9	5.00	125.00	O	O	O	29	32.50	812.50			
10	6.00	150.00				30	35.00	875.00			
11	7.00	175.00				31	37.50	937.50			
12	8.00	200.00				32	40.00	1000.00	O	O	O
13	9.00	225.00				33	42.50	1062.50			
14	10.00	250.00	O	O	O	34	45.00	1125.00			
15	11.00	275.00				35	47.50	1187.50			
16	12.00	300.00				36	50.00	1250.00	O	O	O
17	13.00	325.00				37	52.50	1312.50			
18	14.00	350.00				38	55.00	1375.00			
19	15.00	375.00	O	O	O	39	57.50	1437.50			
20	16.00	400.00				40	60.00	1500.00			

P.D. : Power Distribution
R.R. : Reaction Rate

5.3.2 Benchmark Results

The benchmark calculations have been performed by using VERA-CS (MPACT+ORIGEN) with the ENDF/B-7.0 MPACT and SAMPX 51-g libraries with simplified and full burnup chains. Reference solutions have been obtained by using two continuous energy Monte Carlo codes, SERPENT and McCARD, using ENDF/B-7.0 data. Since multiplication factors as a function of burnup are sensitive to neutron flux levels, same values of recoverable energies per fission have been used for all three codes which are provided in Reference [Kim16a]. Table 5.3.3 provides a list of codes engaged in benchmark calculations.

Table 5.3.3 Transport depletion codes

Code	Solver			Developer	Group
	Transport	Depletion	Resonance		
MPACT	MOC	ORIGEN	Subgroup	CASL	51
McCARD	Monte Carlo	ORIGEN	CE	SNU	CE
SERPENT	Monte Carlo	CRAM	CE	VTT	CE

*ORIGEN: Exponential matrix + Bateman

In order to verify the input data prepared for the participating codes, the multiplication factors at 0.0 MWD/kgU have been compared as shown in Table 5.3.4.

Since there is additional computational burden when using the full ORIGEN burnup chain tracking over 2200 isotopes, a simplified burnup chain with 255 isotopes was developed to minimize errors in multiplication factors [Kim16a]. Sensitivity calculations have been performed by using full and simplified burnup chains for all of the VERA depletion problems. Figure 5.3.1 provides differences of the multiplication factors in pcm for representative cases. All of the results with simplified burnup chains except, for gadolinia rods, are very consistent with those with the full burnup chains within 50 pcm at all burnup points. Even though the gadolinia rods are the most severe case showing largest difference, fuel assemblies with gadolinia rods also does show good consistency.

Figures 5.3.2~5.3.5 provide comparisons of multiplication factors as a function of burnup for representative cases including single pin and fuel assemblies with UO_2 fuels, Pyrex burnable poisons and gadolinia rods. The VERA-CS results with the MPACT and SAMPX 51-g libraries are very consistent with the SERPENT results within 100 pcm at all burnup points. Figure 5.3.2 includes a comparison with another Monte Carlo code McCARD developed by Seoul National University to identify any differences between Monte Carlo codes. In this comparison, there are large differences observed at high burnup points between the CE Monte Carlo codes.

To see a difference between the ENDF/B-7.0 and 7.1 libraries for burnup, a sensitivity calculation has been performed by using the ENDF/B-7.0 and 7.1 MPACT 51-g

libraries. As shown in Figure 5.3.6, even though there is almost no difference at 0 MWD/kgU, the ENDF/B-7.1 library is overestimating the multiplication factors at high burnup points. This result is very consistent with that of the extended VERA progress benchmark result which is included in Figure 5.1.6.

Table 5.3.4 Multiplication factors at 0.0 MWD/kgU burnup

Case	Description	KENO	McCARD	SERPENT	MPACT	SAMPX
1A	Pin 3.1w/o T_F=565K	1.18704	-3	210	8	47
1B	Pin 3.1w/o T_F=600K	1.18428	-32	72	18	59
1C	Pin 3.1w/o T_F=900K	1.17393	-72	-40	4	48
1D	Pin 3.1w/o T_F=1200K	1.16516	-116	-21	66	81
1E	Pin IFBA 3.1w/o T_F=600K	0.76521	3	35	-401	-320
1F	Pin 2.1w/o T_F=900K	1.05835	-69	-40	-11	21
1G	Pin 3.6w/o T_F=900K	1.21335	-47	24	27	76
1H	Pin 4.6w/o T_F=900K	1.27094	-69	15	-1	51
1I	Pin Gadolinia rod (5% Gd_2O_3)	0.21820	-45	-22	266	192
1J	Pin 3.1w/o T_F=600/900/1200K	1.17451	-59	-8	-	-
2A	FA No Poisons T_F=565K	1.18218	-14	195	-33	21
2B	FA No Poisons T_F=600K	1.1824	-62	-7	-52	3
2C	FA No Poisons T_F=900K	1.17354	-32	29	-13	43
2D	FA No Poisons T_F=1200K	1.16543	-121	-13	29	60
2E	FA 12 Pyrex	1.06072	-10	81	-6	60
2F	FA 24 Pyrex	0.96541	-33	49	-103	-32
2G	FA 24 AIC	0.83443	36	136	-312	-172
2H	FA 24 B4C	0.77337	9	33	-133	-74
2I	FA Instrument Thimble	1.17256	-41	16	-23	34
2J	FA Instrument + 24 Pyrex	0.96476	-131	58	-90	-19
2K	FA Zoned + 24 Pyrex	1.00886	-43	53	-97	-18
2L	FA 80 IFBA	1.01133	-83	1	-98	-23
2M	FA 128 IFBA	0.93205	-59	34	-105	-24
2N	FA 104 IFBA + 20 WABA	0.86123	-	52	-10	64
2O	FA 12 Gadolinia	1.04004	-29	50	89	106
2P	FA 24 Gadolinia	0.91993	2	22	164	146

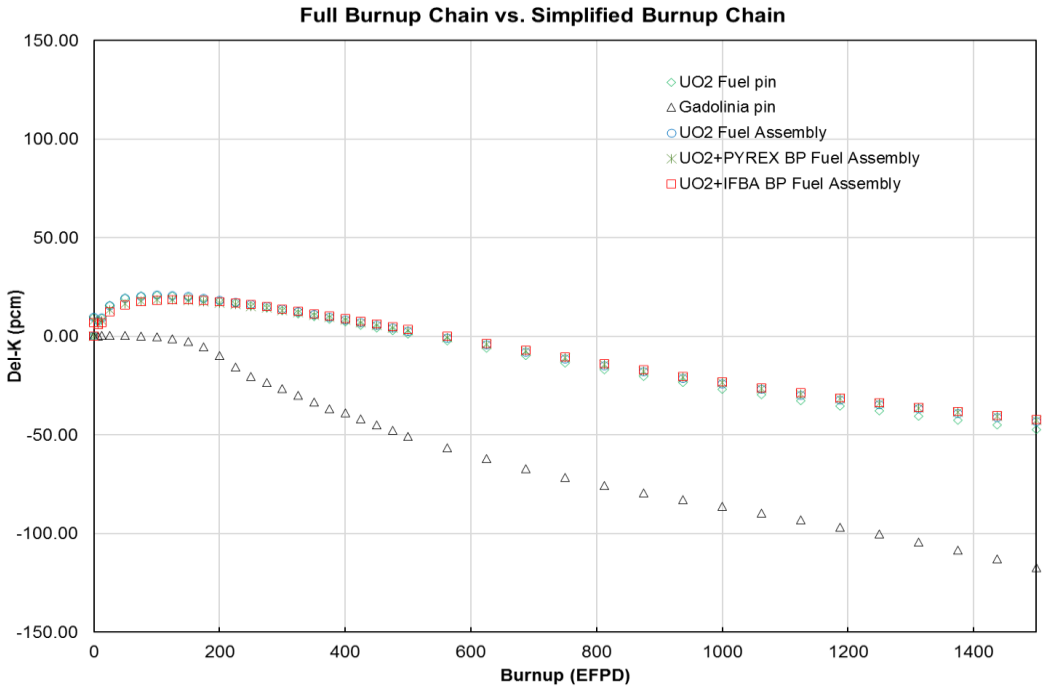

Figure 5.3.1 Comparison of simplified burnup chain with full burnup chain

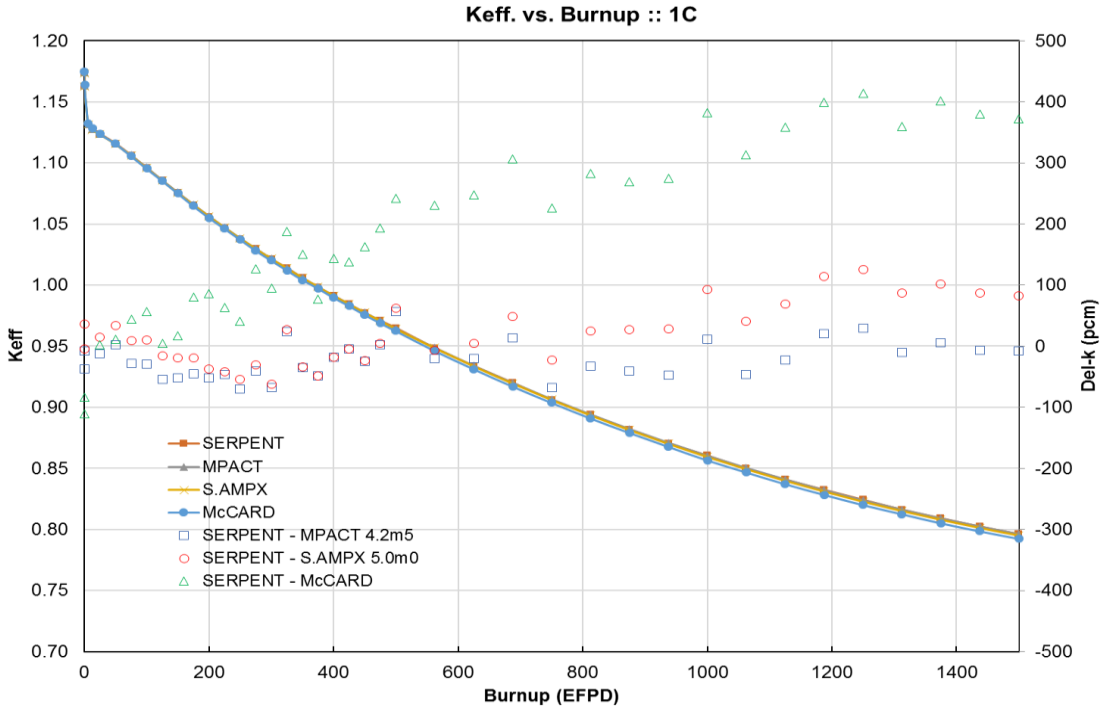

Figure 5.3.2 Comparison of multiplication factors for case 1C

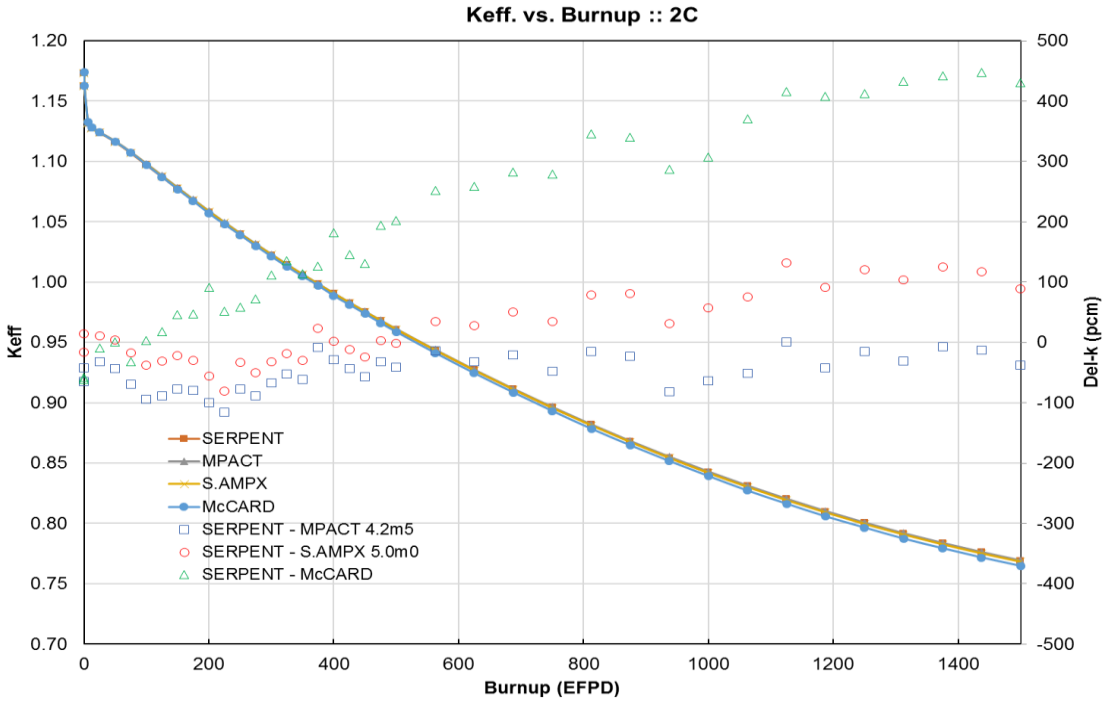

Figure 5.3.3 Comparison of multiplication factors for case 2C

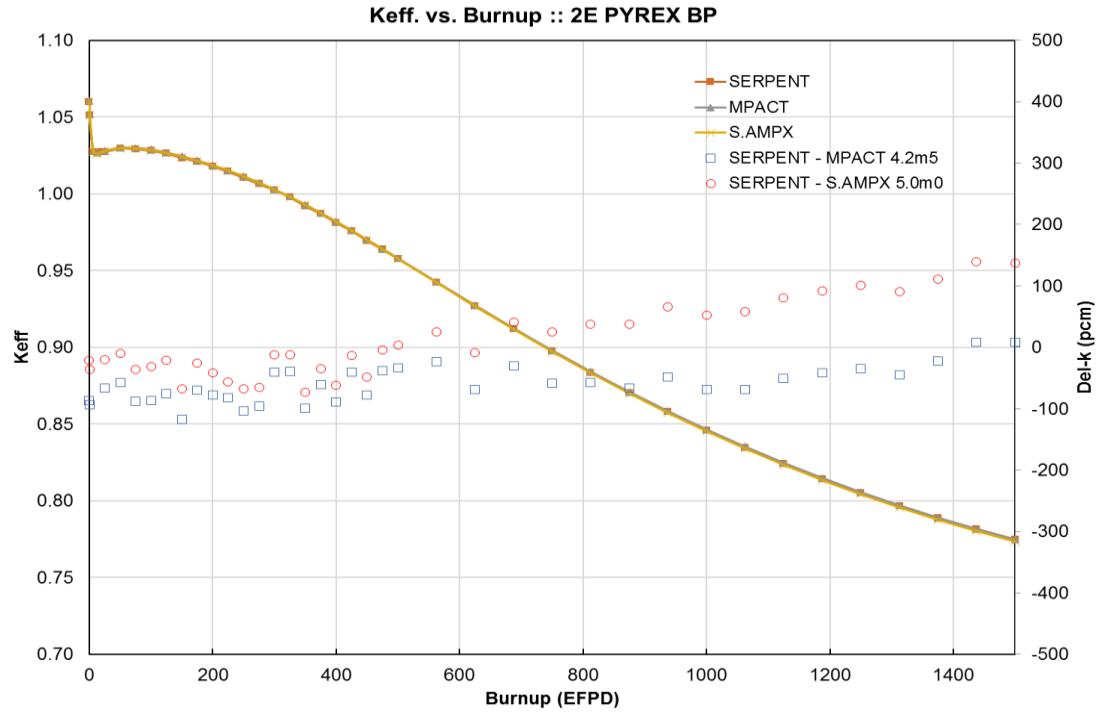

Figure 5.3.4 Comparison of multiplication factors for case 2E

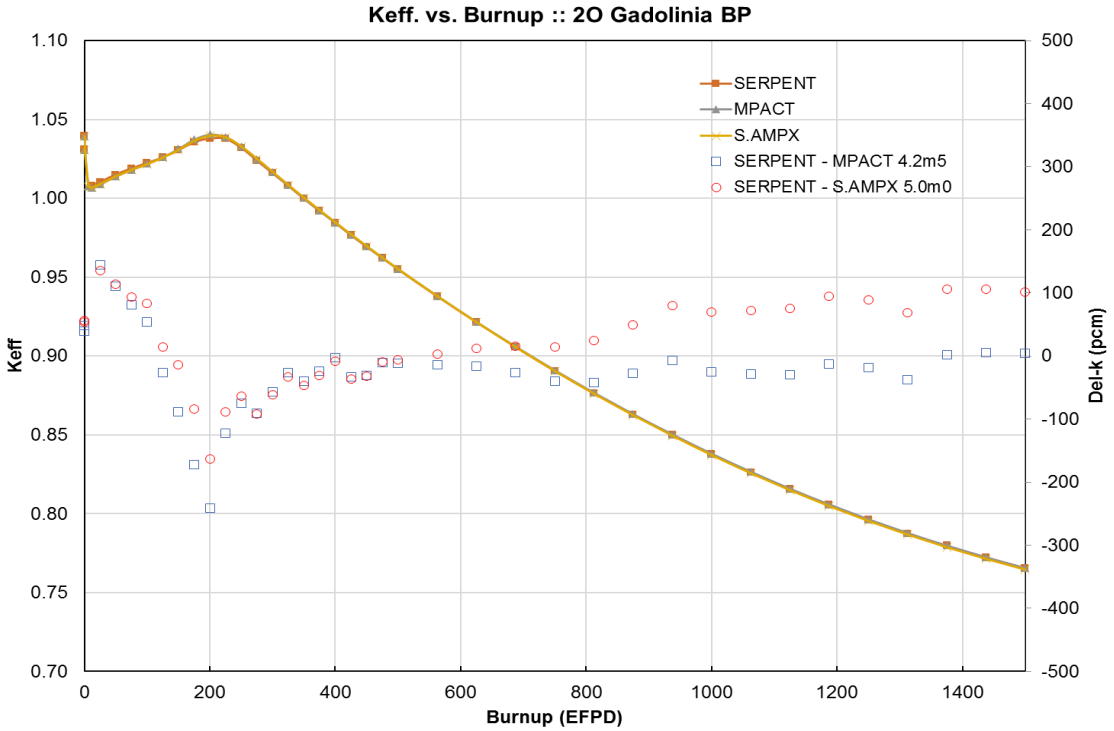

Figure 5.3.5 Comparison of multiplication factors for case 2O

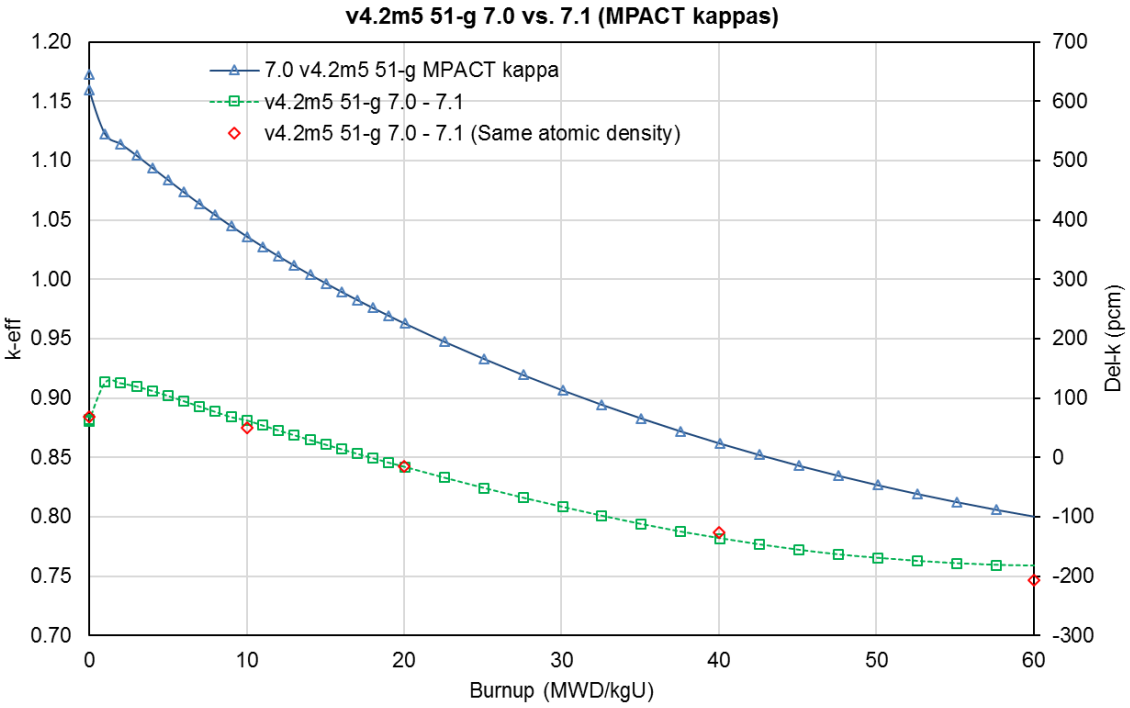

Figure 5.3.6 Comparison of multiplication factors between ENDF/B-7.0 and 7.1

5.4 AP1000 DEPLETION BENCHMARK PROBLEMS

5.4.1 Characteristics of Problems

Some additional depletion benchmark problems include the various fuel assemblies that comprise the AP1000 design. [Gen17] These problems include assembly regions A, B, C with uniform radial ^{235}U enrichment of 0.74%, 1.58%, and 3.2% respectively, regions D and E with heterogeneous fuel and IFBA loadings and average enrichments of 3.8% and 4.4% respectively, as well as the 3.2% enriched annular axial blanket region. Additionally, the Region B lattice was modeled with a “grey” Tungsten control rod inserted. A detailed depiction of benchmark problems is described in Appendix C.3. Figure 5.4.1 provides benchmark cases for AP1000 fuel assemblies.

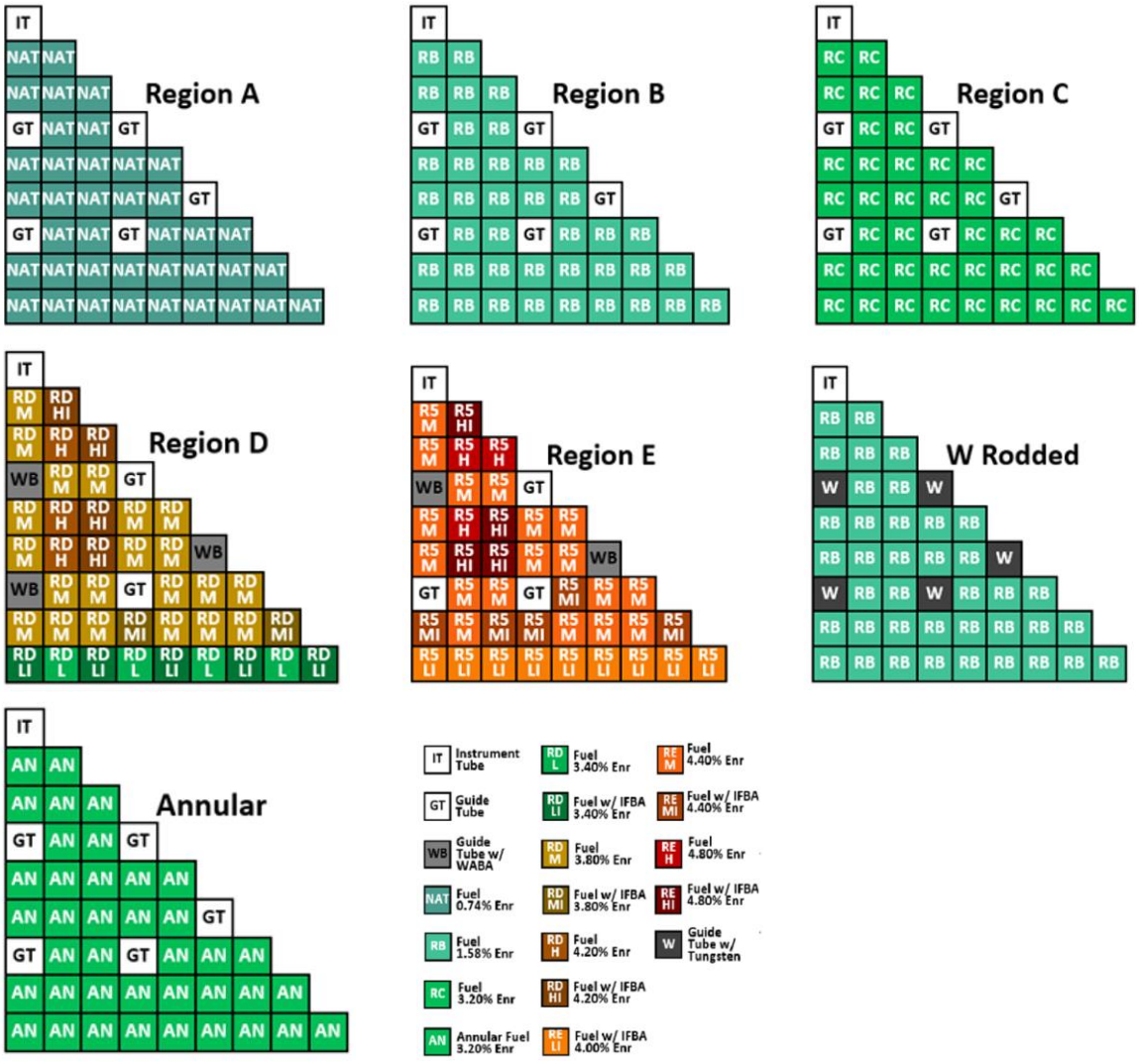

Figure 5.4.1 AP1000 2D lattice model pin maps

5.4.2 Benchmark Results

The lattice depletion simulations were performed with VERA-CS with the v4.2m5 ENDF/B-7.0 MPACT 51-g library and SHIFT, as well as the Monte Carlo code SERPENT, with SERPENT serving as the high-fidelity reference solution. Fixed temperatures of 900K for the fuel and 600K for the moderator and other non-fuel materials were assumed so as to ensure better model consistency between codes. The ENDF/B-7.0 library was utilized and "kappa" heating values were made consistent to SERPENT. It should be noted that the kappa-value consistency was not employed in the previous SERPENT-MPACT comparison, and as will be shown later did provide significant improvements in results. 73 depletion steps were used to simulate these models for a target burnup of 70 GWD/MTHM (~1 GWD/MTHM per time step).

As can be seen in Figures 5.4.2 and 5.4.3, and Table 5.4.1, the agreement between MPACT and SERPENT, both in terms of eigenvalue and power distribution, is good. Eigenvalue agreement remains within 115 pcm of the SERPENT reference for all models. Generally, the differences are fairly small, within 50 pcm, near zero exposure and increases in magnitude, with an MPACT under prediction within ~50 pcm to ~100 pcm and then gradually decreases with burnup to a 0 pcm to ~75 pcm MPACT over prediction. With regards to power distribution it can be seen that the maximum pin power differences are within 0.5% and RMS differences are within 0.15%. The general trend is that errors increase with burnup with most lattice models reaching plateau at some point over the course of the burnup, with the exception of the annular fuel pellet model. Also, the lower enriched assemblies tend to exhibit the greatest disagreement with SERPENT.

The exact cause for the observable variations between SERPENT and MPACT has yet to be determined, though the results hint at differences in isotopic depletion / production brought about possibly by difference in reaction rates (i.e. cross-sections) and / or depletion chains. These MPACT results employed the simplified burnup chain to minimize runtime, whereas SERPENT depletes with a much fuller chain.

Figures 5.4.4 and 5.4.5 illustrate the differences observed between SERPENT and SHIFT. The differences are considerably less than those observed between MPACT and SERPENT. Generally, eigenvalue disagreement begins within ~50 pcm and gradually increases with burnup to within a ~100 pcm under prediction by SHIFT for all cases. Pin power agreement is substantially better with the maximum difference observed to be within 0.3% and the RMS differences within ~0.05%. These levels of agreement are generally constant, with some slightly upward trend with burnup, and nearly the same for all lattice models. This agreement between SHIFT and SERPENT help to assuage concerns regarding the differences in Predictor-Corrector models and substep flux renormalization between the depletion time step methods. This indicates that the time discretization is sufficiently fine as to prevent substantial accumulation of errors brought about by differences in Predictor-Corrector / substepping treatments.

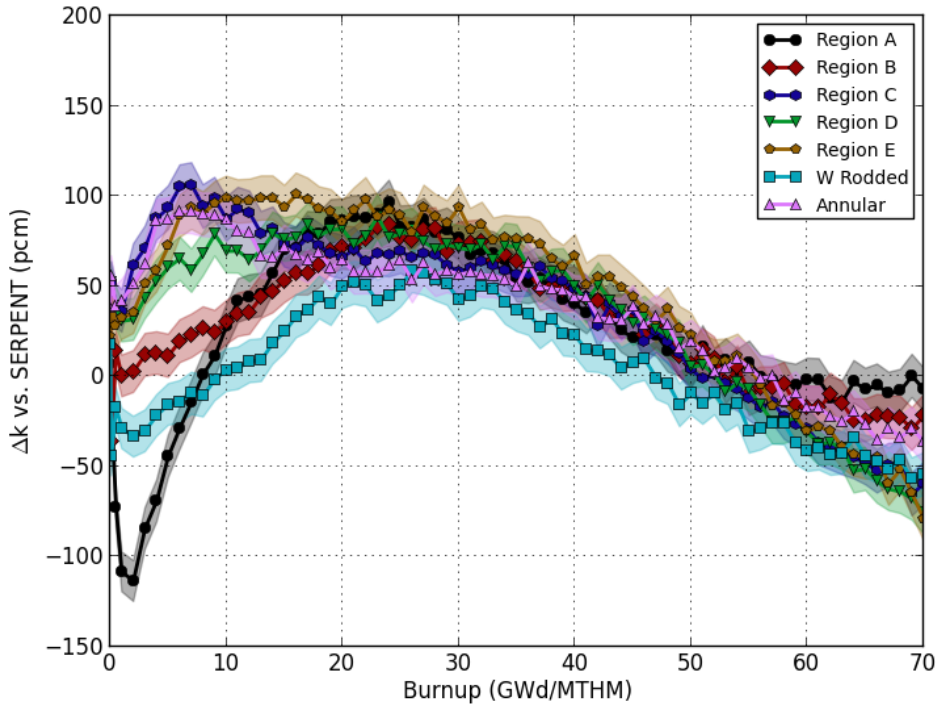

Figure 5.4.2 SERPENT-MPACT k-eff comparison with 3σ uncertainty bands

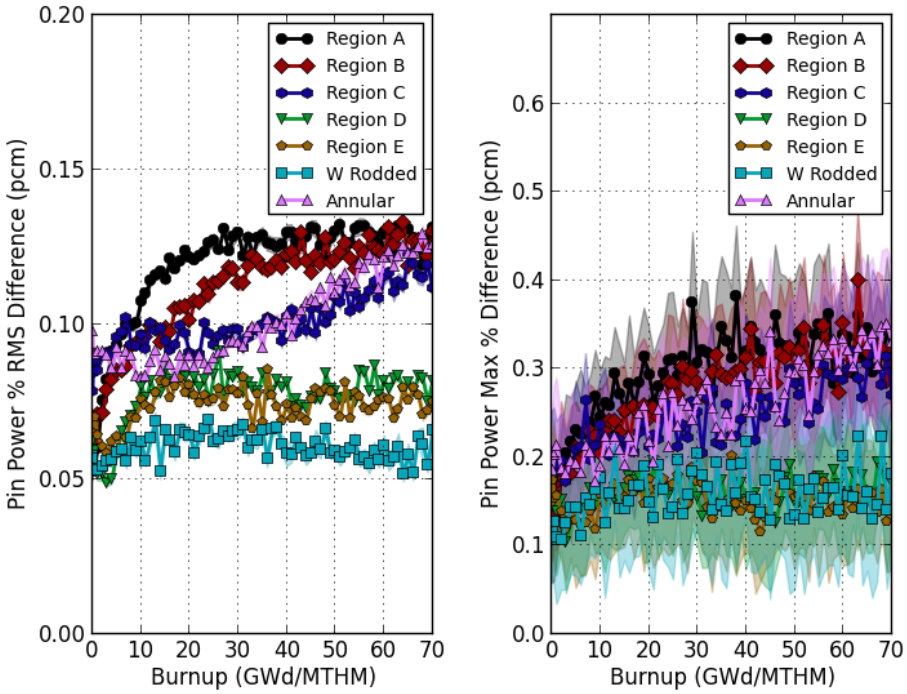

Figure 5.4.3 SERPENT-MPACT power distribution comparison with 3σ uncertainty bands

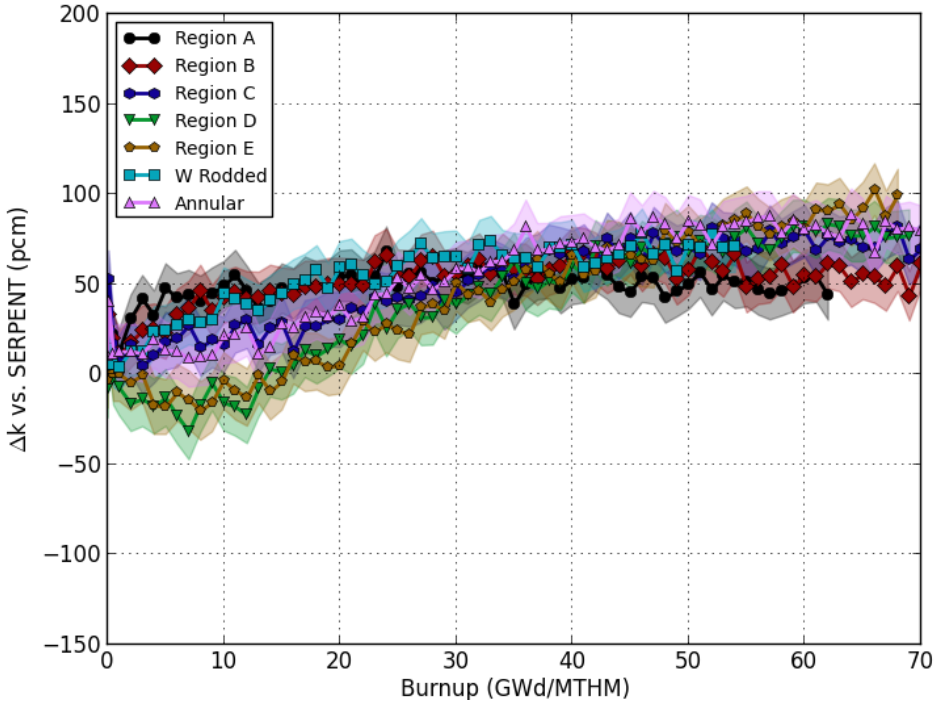

Figure 5.4.4 SERPENT-SHIFT k-eff comparison with 3σ uncertainty bands

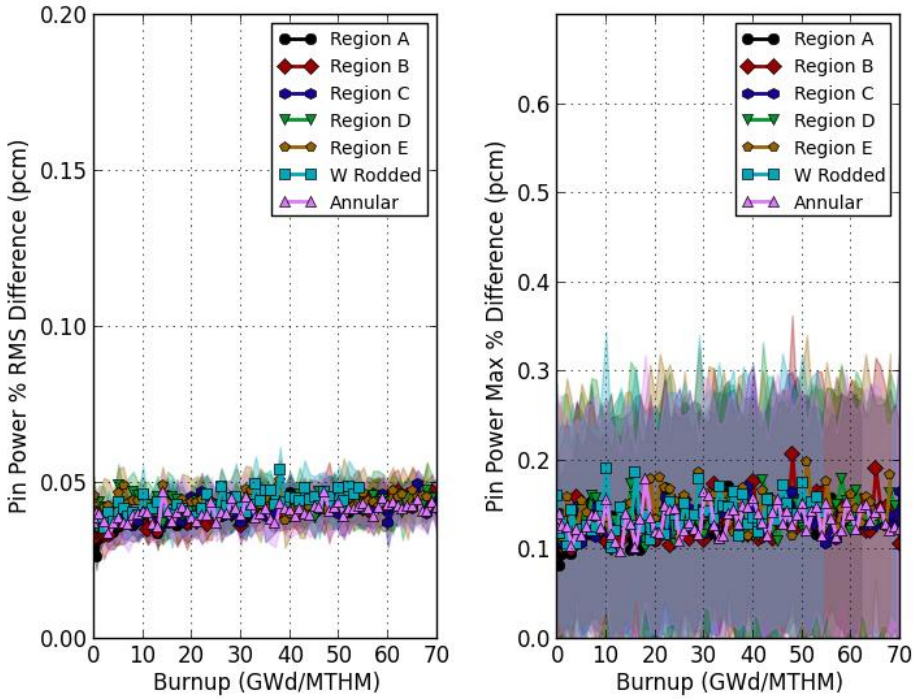

Figure 5.4.5 SERPENT-SHIFT power distribution comparison with 3σ uncertainty bands

Table 5.4.1 Summary of Eigenvalue and pin power differences

Model ID		SERPENT - SHIFT		SERPENT – MPACT	
		Δk (pcm)	Pin Power (%)	Δk (pcm)	Pin Power (%)
Reg A	Max ABS[a]	68	0.171	-114	0.382
	Max RMS[b]	48	0.047	24	0.132
	Max RMS Unc (1σ)	10	0.003	47	0.001
	Max Unc (1σ)	5	0.053	4	0.029
Reg B	Max ABS	70	0.206	84	0.399
	Max RMS	51	0.047	29	0.133
	Max RMS Unc (1σ)	14	0.004	34	0.001
	Max Unc (1σ)	5	0.054	4	0.029
Reg C	Max ABS	82	0.171	106	0.330
	Max RMS	50	0.050	36	0.123
	Max RMS Unc (1σ)	23	0.003	47	0.001
	Max Unc (1σ)	5	0.054	4	0.030
Reg D	Max ABS	83	0.180	89	0.196
	Max RMS	39	0.049	34	0.091
	Max RMS Unc (1σ)	35	0.004	47	0.001
	Max Unc (1σ)	5	0.054	4	0.029
Reg E	Max ABS	103	0.198	101	0.201
	Max RMS	42	0.051	45	0.085
	Max RMS Unc (1σ)	37	0.004	51	0.001
	Max Unc (1σ)	5	0.054	4	0.029
W Rod	Max ABS	78	0.192	58	0.224
	Max RMS	52	0.054	3	0.069
	Max RMS Unc (1σ)	20	0.004	34	0.002
	Max Unc (1σ)	5	0.056	4	0.031
Ann	Max ABS	89	0.179	91	0.350
	Max RMS	55	0.047	37	0.129
	Max RMS Unc (1σ)	27	0.003	36	0.001
	Max Unc (1σ)	5	0.049	4	0.030

[a]ABS: Absolute difference
[b]RMS: Root mean square

5.5 REACTION RATE ANALYSIS PROBLEMS

5.5.1 Characteristics of Problems

The previous analysis was comparing eigenvalues and pin power distributions, which are integral terms that can mask errors in individual multigroup cross sections. Therefore, a more in-depth analysis is performed in this section to evaluate the quality of the nuclear data library for individual isotope-group reaction rates to discern errors in cross sections.

By doing a reaction rate analysis, one can quickly identify the dominating error sources of a cross section library specific to an isotope, a reaction channel, and an energy group/range, which is not easily detected by only comparing the overall multiplication factor of a system. Reaction rate analysis aims at converting the error of MG reaction rate into the error of eigenvalue between the Monte Carlo results and MPACT results.

We developed 18 representative cases for reaction rate analysis with various ^{235}U enrichments, fuel and moderator temperatures, soluble boron concentrations, burnup and void fractions for both PWR and BWR. Table 5.5.1 provides 18 representative cases for reaction rate analysis. Currently reference solutions have been obtained by MCNP with ENDF/B-7.0 and 7.1. A more detailed description can be found on Reference [Liu16].

Table 5.5.1 Representative cases for reaction rate analysis

Fuel	No	^{235}U w/o	Burnup	PPM	Temperature (K)			Void %	BP
					Fuel	Clad	Moderator		
PWR	1	3.1	0	0	900	600	600	0	-
	2	2.1	0	0	600	600	600	0	-
	3	4.1	0	0	900	600	600	0	-
	4	3.1	0	0	293.6	293.6	293.6	0	-
	5	3.1	0	0	600	600	600	0	-
	6	3.1	0	0	1200	600	600	0	-
	7	3.1	0	600	900	600	600	0	-
	8	3.1	0	1300	900	600	600	0	-
BWR	9	3.5	0	0	600	600	600	0	-
	10	3.5	0	0	900	600	600	50	-
	11	3.5	0	0	1200	600	600	70	-
	12	3.5	0	0	900	600	600	90	-
PWR	13	3.1	0	0	900	600	600	0	-
	14	3.1	0.1	0	900	600	600	0	-
	15	3.1	20	0	900	600	600	0	-
	16	3.1	40	0	900	600	600	0	-
	17	3.1	60	0	900	600	600	0	-
	18	3.1	0	0	900	600	600	0	1% Er_2O_3

5.5.2 Analysis Results

Reactivity (reaction rate) analysis between reference (MCNP) and target codes can be carried out by using the following procedure.

a. Perform Monte Carlo calculation to edit 51-g/252-g scalar fluxes, microscopic capture and fission cross sections, the number of neutrons (ν) released from a fission, and the multiplication factors.
b. Perform MPACT calculation to edit 51-g/252-g scalar fluxes, microscopic capture and fission cross sections.
c. Compare multiplication factors and convert the differences of cross sections of each nuclide and scalar fluxes into reactivity differences.
   As an example, absorption and ν*fission reaction rate differences between MCNP and MPACT for U^{235} are converted into the reactivity differences in *pcm* for each group by using the following equations.

$$\Delta\rho_{a,g'}^{235} = \left[\frac{1}{k_\infty} - \frac{\sum_{g,k} N_k \sigma_{a,g,k}\phi_g - N^{235}\left(\sigma_{a,g'}^{235}\phi_{g'} - \hat{\sigma}_{a,g'}^{235}\hat{\phi}_{g'}\right)}{\sum_{g,k} N_k \nu\sigma_{f,g,k}\phi_g}\right]\cdot 10^5, \qquad (5.5.1)$$

and

$$\Delta\rho_{\nu f,g'}^{235} = \left[\frac{1}{k_\infty} - \frac{\sum_{g,k} N_k \sigma_{a,g,k}\phi_g}{\sum_{g,k} N_k \nu\sigma_{f,g,k}\phi_g - N^{235}(\nu\sigma_{f,g'}^{235}\phi_{g'} - \nu\hat{\sigma}_{f,g'}^{235}\hat{\phi}_{g'}}\right]\cdot 10^5, \qquad (5.5.2)$$

where

$$k_\infty = \frac{\sum_{g,k} N_k \nu\sigma_{f,g,k}\phi_g}{\sum_{g,k} N_k \sigma_{a,g,k}\,\phi_g},$$

and the cap(^) indicates data from the MPACT calculations, *k* denotes fissionable nuclide and *g* energy group. These differences will show the difference between MCNP and MPACT reaction rates solutions, which are composed of differences in individual cross sections as well as differences in the neutron flux, which is effected by differences in all cross sections including the two-dimensional scattering matrices. To isolate the effect of cross section differences, the MPACT scalar flux is replaced with the MCNP scalar flux.

Reaction rate analysis has been performed while developing or improving the MPACT and SAMPX MG libraries to determine error sources resulting in bias in multiplication factors. Representatively Tables 5.5.2~5.5.4 provide analysis results for the ENDF/B-7.1 MPACT 51-g, the ENDF/B-7.1 SAMPX 51-g and the ENDF/B-7.0 SAMPX 252-g libraries. The followings are summary for reaction rate analysis.

- Large reaction rate difference at the largest 6.7 eV ^{238}U resonance has been partly resolved by adopting SPH factors when performing P_2 scattering calculation. This issue has been completely resolved by performing TCP0 calculation.

- There are error cancellations between absorption and ν*fission reactions in ^{235}U at thermal energy groups. This may be an intrinsic issue shown in coarse group approximation due to poor thermal scattering matrices.
- BWR cases show relatively large reaction rate differences compared to PWR cases since resonance data have been generated and optimized for PWR fuel configuration. The issue can be partly resolved by generating ^{238}U resonance data based on the BWR geometry.
- Errors in the 51-group structure for high-void BWR cases are larger than the target; the energy group structure may need to be refined to capture the harder spectra compared to the typical PWR. At this time, the 252-group structure should be used for BWR simulations.
- There is fuel temperature reactivity bias seen when comparing Cases 5(600K), 1(900K) and 6(1200K). The MPACT and SAMPX MG libraries have been generated by using the SCALE/AMPX code packages by which SCALE-KENO shows intrinsic difference in fuel temperature coefficients compared to MCNP.

Table 5.5.2 Analysis result for the ENDF/B-7.1 MPACT 51-g library

No	Case	k_{eff}		Δk, pcm		Absorption, pcm			ν*Fission, pcm		
		MCNP[a]	MPACT[b]	[a-b]	RR	Nuclide	Δk	Δk (grp)	Nuclide	Δk	Δk (grp)
1	rr_1_3.1%	1.29874	1.29762	-112	-113	922380	-112	-142.0(23)	922380	-13	-6.3(2)
2	rr_2_2.1%	1.21266	1.21155	-111	-121	922380	-126	-146.0(23)	922350	-35	127.4(45)
3	rr_3_4.1%	1.34863	1.34771	-92	-88	922380	-80	-132.6(23)	922380	-15	-6.3(2)
4	rr_4_293.6K	1.39603	1.39556	-47	-49	10010	112	62.1(50)	922380	-38	-17.5(4)
5	rr_5_600K	1.31010	1.31015	5	9	922350	-71	104.6(43)	922350	88	-155.0(43)
6	rr_6_1200K	1.28892	1.28706	-187	-184	922380	-165	-153.3(23)	922350	-76	-161.7(43)
7	rr_7_B600	1.23711	1.23678	-33	-47	922380	-94	-125.8(23)	922350	50	-157.8(43)
8	rr_8_B1300	1.17364	1.17372	8	14	922380	-95	-119.5(23)	922350	136	-152.3(43)
9	rr_9_bwr_0	1.37369	1.37121	-248	-246	922380	-287	-146.1(23)	922350	-17	-178.8(43)
10	rr_10_bwr_50	1.22621	1.22407	-215	-212	922350	239	145.4(43)	922350	-399	-229.8(43)
11	rr_11_bwr_70	1.10150	1.10064	-86	-89	922350	321	131.6(43)	922350	-546	-231.2(43)
12	rr_12_bwr_90	0.88894	0.89091	197	188	922380	432	190.5(14)	922350	-775	-135.9(43)
13	rr_13_burn_0	1.24743	1.24690	-53	-36	922380	-111	-133.0(23)	922350	97	-144.1(43)
14	rr_14_burn_001	1.20383	1.20367	-16	-14	922380	-97	-120.5(23)	922350	99	-146.8(43)
15	rr_15_burn_20	1.00246	1.00286	40	35	942390	206	85.8(43)	942390	-309	-143.3(43)
16	rr_16_burn_40	0.88270	0.88265	-5	-17	942390	144	62.8(43)	942390	-244	-119.0(43)
17	rr_17_burn_60	0.80859	0.80880	21	15	942390	125	52.1(43)	942390	-236	-107.8(43)
18	rr_18_erbium	1.01241	1.01100	-141	-147	922380	-87	-100.9(23)	922350	-56	-126.8(43)

Table 5.5.3 Analysis result for the ENDF/B-7.1 SAMPX 51-g library

Case	k_{eff}		Δk, pcm		Absorption, pcm			ν*Fission, pcm		
	MCNP[a]	MPACT[b]	[a-b]	RR	Nuclide	Δk	Δk (grp)	Nuclide	Δk	Δk (grp)
rr_1_3.1%	1.29874	1.29775	-99	-100	922380	-57	-116.3(23)	922380	-18	-14.6(3)
rr_2_2.1%	1.21266	1.21167	-99	-110	922380	-80	-121.7(23)	922350	-32	-137.1(50)
rr_3_4.1%	1.34863	1.34785	-78	-74	922350	-29	96.2(43)	922380	-20	-14.2(3)
rr_4_293.6K	1.39603	1.39531	-72	-75	10010	76	51.9(50)	922380	-42	-19.8(3)
rr_5_600K	1.31010	1.31000	-10	-6	922350	-78	78.6(43)	922350	72	-120.0(43)
rr_6_1200K	1.28892	1.28716	-176	-174	922380	-112	-131.6(23)	922350	-73	-125.7(43)
rr_7_B600	1.23711	1.23675	-36	-50	922350	-59	76.8(43)	922350	45	-123.6(43)
rr_8_B1300	1.17364	1.17355	-10	-3	922350	-99	71.1(43)	922350	123	-120.4(43)
rr_9_bwr_0	1.37369	1.37081	-288	-287	922380	-263	-124.1(23)	922350	-83	-139.4(43)
rr_10_bwr_50	1.22621	1.22400	-221	-218	922350	210	115.9(43)	922350	-381	-187.3(43)
rr_11_bwr_70	1.10150	1.10080	-70	-74	922350	272	105.3(43)	922350	-485	-189.2(43)
rr_12_bwr_90	0.88894	0.89180	286	276	922380	338	163.8(14)	922350	-617	-104.4(43)
rr_13_burn_0	1.24743	1.24695	-48	-31	922350	-85	69.6(43)	922350	90	-111.3(43)
rr_14_burn_001	1.20383	1.20377	-6	-4	922350	-68	70.1(43)	922350	69	-115.9(43)
rr_15_burn_20	1.00246	1.00360	114	110	942390	169	80.5(43)	922350	328	89.7(45)
rr_16_burn_40	0.88270	0.88362	92	80	922350	-70	-18.9(45)	922350	166	46.4(45)
rr_17_burn_60	0.80859	0.80998	139	134	922380	83	-67.2(23)	922350	67	21.5(45)
rr_18_erbium	1.01241	1.01066	-175	-181	681670	-95	-81.0(41)	922350	-80	-102.8(43)

Table 5.5.4 Analysis result for the ENDF/B-7.0 SAMPX 252-g library

Case	k_{eff}		Δk, pcm		Absorption, pcm			ν*Fission, pcm		
	MCNP[a]	MPACT[b]	[a-b]	RR	Nuclide	Δk	Δk (grp)	Nuclide	Δk	Δk (grp)
rr_p2_1_3.1%	1.29875	1.298201	-55	-45	922350	-76.6	-43.3(240)	922350	118	68.5(240)
rr_p2_2_2.1%	1.21284	1.212346	-49	-36	922350	-93.9	-40.8(240)	922350	153	69.1(240)
rr_p2_3_4.1%	1.34866	1.348076	-58	-48	922350	-75.6	-42.7(240)	922350	122	65.2(240)
rr_p2_4_293.6K	1.39633	1.395496	-83	-79	922380	-104.2	-76.6(121)	922350	46	-158.3(239)
rr_p2_9_bwr_0	1.37399	1.372688	-130	-143	922380	-175.1	-74.0(121)	922350	101	84.5(239)
rr_p2_10_bwr_50	1.22609	1.22506	-103	-92	922380	-88.9	-65.7(121)	922350	59	47.8(240)
rr_p2_11_bwr_70	1.10088	1.100982	10	-5	922350	-39.1	-22.9(239)	922350	72	42.8(239)
rr_p2_12_bwr_90	0.88787	0.890131	226	217	922380	164.2	-57.4(75)	922350	162	42.3(146)

5.6 EXTENSIVE PWR PIN AND ASSEMBLY BENCHMARK PROBLEMS

5.6.1 Characteristics of Problems

Extensive benchmark problems for PWR fuel pins and fuel assemblies have been developed to determine how well the MPACT MG library agrees with continuous-energy Monte Carlo results. [Pal17a, Pal17b] The PWR fuel pin cases consist of:

- Three ^{235}U enrichments (2.1%, 3.1%, and 4.1%)
- Four rod sizes corresponding to Watts Bar (WB) Unit 1 Cycle 1 (17x17), BEAVRS Cycle 1 (17x17), Surry Cycle 1 (15x15), and Krsko (16x16)
- Three hot coolant densities corresponding to typical inlet, average, and outlet conditions
- Three hot fuel temperatures (600, 900, and 1200K)
- Cold cases at room temperature
- Three boron concentrations (0, 600, and 1300 ppm)

There are a total of 360 cases, 324 (3x4x3x3x3) hot cases and 36 (3x4x3) cold cases. The PWR pincells were modeled as three concentric rings of fuel, helium gap, and zirconium, surrounded by a square region of coolant. The moderator densities correspond to typical PWR conditions at core inlet, core average, and core outlet. The hot densities are calculated from subcooled steam tables at 2250 psia. The cold density is at room conditions. Table 5.6.1 provides moderator temperatures and densities according to various reactor conditions. Table 5.6.2 provides pin cell dimensions and fuel-to-coolant volume ratios for fuel types. All fuel had a stack density of 10.257 g/cc and the ^{235}U enrichments are 2.1, 3.1, and 4.1%. The same number densities are used in all the rod geometries. In terms of fuel to moderator ratios, the BEAVRS rod is the "wettest" configuration and Krsko is the "driest" configuration.

Table 5.6.1 Moderator temperatures and densities

Reactor Condition	Nomenclature	Temperature (K)	Density (g/cc)
Cold	den0	293.6	1.000000
Hot Inlet	den1	566.0	0.740816
Hot Average	den2	583.9	0.703158
Hot Outlet	den3	601.7	0.655986

Table 5.6.2 Pincell dimensions

Fuel Type	WB 17x17	BEAVRS 17x17	Surry 15x15	Krsko 16x16
Pin Pitch (cm)	1.2600	1.2600	1.4300	1.2319
Fuel outer radius (cm)	0.4096	0.39218	0.4647	0.4096
Clad inner radius (cm)	0.4180	0.40005	0.4742	0.4180
Clad outer radius (cm)	0.4750	0.4572	0.5359	0.4750
Fuel-to-Coolant ratio	0.6000	0.5190	0.5940	0.6520

Additional benchmark problems have been developed for fourteen different PWR assembly types including 15x15, 16x16, and 17x17 designs by different fuel vendors with many different state point conditions encountered in a reactor. The complete set of assembly geometries is listed in Table 5.6.3. Each assembly type includes 90 different state points as follows:

- Three ^{235}U enrichments (2.1%, 3.1%, and 4.1%)
- Three hot coolant densities corresponding to typical inlet, average, and outlet conditions
- Three hot fuel temperatures (600, 900, and 1200K)
- One cold case at standard room temperature and density
- Three boron concentrations (0, 600, and 1300 ppm)

There are a total of 81 hot cases (3x3x3x3) and 9 cold cases (3x3) per assembly, for a total of 1260 cases. The Watts Bar assemblies are slightly modified. The modifications include:

- The cladding material is natural zirconium to reduce the number of isotopes in the MCNP model,
- The enrichment, boron, fuel temperatures, and moderator densities are set by the case matrix (described below), and
- The moderator density inside the guide tubes (GT) and instrument tube (IT) are set to the core inlet conditions.

The assembly geometry descriptions are given in Table 5.6.4.

Table 5.6.3 Assembly geometry descriptions

Geometry	Description
ce16	CE 16x16 Assembly with large water rods
krsko	Krško Westinghouse 16x16
surry	Surry Westinghouse 15x15
tmi1	TMI B&W 15x15 with 4 gad rods
tmi2	TMI B&W 15x15 with no gad
wb2a	Watts Bar 2A 17x17
wb2e	Watts Bar 2E 17x17 12 Pyrex
wb2f	Watts Bar 2F 17x17 24 Pyrex
wb2l	Watts Bar 2L 17x17 80 IFBA rods
wb2m	Watts Bar 2M 17x17 128 IFBA rods
wb2o	Watts Bar 2O 17x17 12 gad rods
wb2p	Watts Bar 2P 17x17 24 gad rods
wb2w	Watts Bar 2W 17x17 thermally expanded
wb2x	Watts Bar 2X 17x17 thermally expanded + zone enrichment

Table 5.6.4 Assembly dimensions

Type	Fuel Rod			Guide Tube			Instrument Tube		
	Pinpitch	FA pitch	Rfuel	Rgap	Rclad	Rin	Rout	Rin	Rout
ce16	1.28524	20.64	0.41339	0.42164	0.48514	1.143	1.2446	1.143	1.2446
krsko	1.232	19.718	0.40960	0.41800	0.47500	0.55250	0.59800	0.55250	0.59800
surry	1.43	21.5036	0.46469	0.47422	0.53594	0.61392	0.69012	0.61392	0.69012
tmi1	1.4427	21.811	0.46950	0.47880	0.54610	0.63245	0.6731	0.56005	0.6261
tmi2	1.4427	21.811	0.46950	0.47880	0.54610	0.63245	0.6731	0.56005	0.6261
wb2a	1.26	21.5	0.40960	0.41800	0.47500	0.561	0.602	0.559	0.605
wb2e	1.26	21.5	0.40960	0.41800	0.47500	0.561	0.602	0.559	0.605
wb2f	1.26	21.5	0.40960	0.41800	0.47500	0.561	0.602	0.559	0.605
wb2l	1.26	21.5	0.40960	0.41800	0.47500	0.561	0.602	0.559	0.605
wb2m	1.26	21.5	0.40960	0.41800	0.47500	0.561	0.602	0.559	0.605
wb2o	1.26	21.5	0.40960	0.41800	0.47500	0.561	0.602	0.559	0.605
wb2p	1.26	21.5	0.40960	0.41800	0.47500	0.561	0.602	0.559	0.605
wb2w	1.2626	21.605	0.41208	0.41894	0.47607	0.56226	0.60335	0.56226	0.60335
wb2x	1.2626	21.605	0.41208	0.41894	0.47607	0.56226	0.60335	0.56226	0.60335

5.6.2 Benchmark Results

Benchmark calculations by the ENDF/B-7.0 MPACT 51-g and ENDF/B-7.1 SAMPX 51-g libraries are summarized. [Pal17a, Pal17b]

ENDF/B-7.0 v4.2m5 MPACT 51-g library

Table 5.6.5 provides a summary of the PWR pin-cell eigenvalue results for MPACT with the ENDF/B-7.0 v4.2m5 MPACT 51-g library and MCNP with ENDF/B VII.0. All results show the differences between the MCNP and MPACT eigenvalues in pcm. Overall, the PWR pin results are acceptable. The average of all 324 hot cases was 50 pcm with a standard deviation of 67 pcm. All of the hot cases were between -132 and +167 pcm. The cold cases had an approximately -58 pcm bias compared with the hot cases. The PWR pin-cell results are shown as a histogram in Figure 5.6.1. The small peak on the left side of the graph corresponds to the cold results. The histogram shows that the results closely match a normal distribution.

Table 5.6.5 also shows the hot and cold results averaged over individual parameter subgroups (type, enrichment, boron, moderator density, and fuel temperature). A “subgroup" is defined as all the cases that have a particular parameter. Looking at the averages over subgroups allowed us to identify “trends" in parameters. Using a criterion of 100 pcm between subgroup differences to define a trend, no trends were observed in geometry, enrichment, boron concentration, or moderator density. A trend was observed in the fuel temperature (a 126 pcm difference from 600 to 1200 K). There is a -58 pcm bias between hot and cold cases and a 156 pcm trend observed in cold boron cases.

Table 5.6.6 provides a summary of PWR assembly benchmark results. Overall, the eigenvalue results are acceptable. The average of all 1134 hot cases is -72 pcm with a standard deviation of 94 pcm. All of the hot cases are between -277 and +184 pcm. A reasonable goal is to have all eigenvalue differences between +/- 200 pcm. The cold cases have an approximately +60 pcm bias compared to the hot cases, and a larger standard deviation. The hot pin power results look very good. All of the hot assemblies have a maximum pin power less than 0.5%. The cold pin power results are not as good, and the maximum error is almost 1%. It is suspected that we need to include additional coolant rings in the cold cases to reduce the maximum pin power errors.

Table 5.6.6 also shows the hot and cold results averaged over individual parameter subgroups (type, enrichment, boron, moderator density, and fuel temperature). Looking at the averages over subgroups allows us to identify “trends" in parameters. Using a criteria of 100 pcm between subgroup differences to define a trend, there are no trends in enrichment, boron, or moderator density. There is an observable trend in the fuel temperature (140 pcm). There are also trends in geometry type, and it appears that PYREX (wb2e and wb2f) and IFBA assemblies (wb2l and wb2m) have more positive eigenvalue differences.

None of the hot assemblies have a maximum pin power difference over 0.5%.
There is an approximate +60 pcm bias between hot and cold cases.
There are some cases with very large cold eigenvalue differences. For example, the high gad case (wb2p) at low enrichments has a maximum eigenvalue difference of -510 pcm. This large maximum is not observable in the hot cases. The largest cold pin power differences are in the “ce16" assemblies, which have the large water rods.
One possible cause for the larger pin power differences in cold cases is that we are not modeling enough rings (at source regions) in the coolant. This is more important for cold cases which have a higher moderator density than the hot cases. The eigenvalue results over all cases is shown as a histogram in Figure 5.6.2.

ENDF/B-7.1 v5.0m0 SAMPX 51-g library

Table 5.6.7 provides a summary of the PWR pin-cell eigenvalue results for MPACT with the ENDF/B-7.1 v5.0m0 SAMPX 51-g library and MCNP with ENDF/B VII.1.
All results show the differences between the MCNP and MPACT eigenvalues in pcm. The average of all 324 hot cases was 15 pcm with a standard deviation of 85 pcm. Compared to the MPACT 51-g library, the average has been decreased to 15 pcm from 44, but the standard deviation has been increased by 16 pcm. Even though some of eigenvalue differences are over 200 pcm, still reactivity differences are less than 200 pcm. Cold cases show much better agreement between MCNP and MPACT.

Table 5.6.8 provides a summary of PWR assembly benchmark results. Overall, the trend of fuel assembly eigenvalue results is similar with that of the MPACT 51-g library. The average of all 1134 hot cases is -59 pcm with a standard deviation of 90 pcm. All of the hot cases are between -262 and +164 pcm. A reasonable goal is to have all

eigenvalue differences between +/- 200 pcm. The cold cases have an approximately +20 pcm bias compared to the hot cases, and a larger standard deviation.

Discussion on reference solution and scattering order

The reference solutions for this benchmark suite were obtained by MCNP. However, the MPACT and SAMPX MG libraries have been developed to be consistent with the CE-KENO results for which the SPH factors were obtained by performing the CE-KENO calculations. There is an intrinsic difference between MCNP and CE-KENO in treating cutoff energy of thermal scattering data which results in significant difference in fuel temperature reactivity coefficient. To investigate the impact of the CE-KENO reference solutions, additional reference solutions were obtained for all single pin cases by using CE-KENO with the ENDF/B-7.0 nuclear data.

Table 5.6.9 provides a comparison of k_{eff} differences in pcm between MCNP and CE-KENO which shows a significant difference only for fuel temperature reactivity coefficient indicating about 90 pcm change from 600 K to 1200 K.

In this benchmark calculations, the MPACT calculations have been performed by the TCP0 option which is a default option for power plant simulation. The ^{1}H transport cross sections were developed to correctly consider neutron leakage for large size problem. Therefore, when developing cross section library and performing small size problem, high order scattering ($\geq P_2$) calculation should be more reasonable. The TCP0 results are getting closer to the P_2 results as the problem size increases. The MPACT results for all the single pin problems were obtained by using the P_2 option with the ENDF/B-7.0 v4.2m5 MPACT and v5.0m0 SAMPX 51-group libraries and compared to the MCNP and CE-KENO reference solutions. In addition differences of the multiplication factors between Monte Carlo and MPACT have been converted into reactivity differences which would be more reasonable in power plant simulation. Table 5.6.10 provides comparisons of k_{eff} and reactivity differences between MPACT and Monte Carlo codes. It is noted that the MPACT results with the MPACT and SAMPX 51-group libraries are very consistent with the CE-KENO results and satisfy the accuracy goals for all cases. Similar discussion can be made for assembly benchmark problems.

Table 5.6.5 Pin benchmark result with the v4.2m5 ENDF/B-7.0 MPACT 51-g library

	Category		Δk_{eff} Difference (pcm)				Count
			Average	S. Dev.	Min.	Max.	
Sum	All		44.4	69.4	-131.7	166.5	360
	Hot		50.3	67.2	-131.7	166.5	324
	Cold		-8.0	68.0	-119.6	108.6	36
Hot	Type	beav	51.8	60.6	-91.1	139.7	81
	Type	krsko	79.2	63.4	-65.0	166.5	81
	Type	WB	9.4	63.0	-131.7	107.4	81
	Type	surry	60.7	62.5	-79.9	155.1	81
	Enrich	21	36.4	65.9	-131.7	145.3	108
	Enrich	31	50.3	67.0	-121.4	161.5	108
	Enrich	41	64.1	66.3	-100.6	166.5	108
	Boron	0	21.9	68.9	-131.7	156.6	108
	Boron	600	50.3	62.5	-74.9	162.6	108
	Boron	1300	78.6	57.7	-45.6	166.5	108
	Density	den1	40.6	66.0	-131.7	147.5	108
	Density	den2	49.2	67.2	-126.2	166.5	108
	Density	den3	61.0	67.3	-111.1	162.6	108
	Tfuel	600	99.7	36.2	1.3	166.5	108
	Tfuel	900	77.3	39.6	-22.1	151.8	108
	Tfuel	1200	-26.2	40.3	-131.7	54.5	108
Cold	Type	Beav	8.2	73.3	-100.0	108.6	9
	Type	Krsko	-22.4	61.6	-116.8	60.3	9
	Type	WB	-6.1	78.5	-119.6	89.4	9
	Type	Surry	-11.9	66.0	-114.6	70.1	9
	Enrich	21	-27.7	70.6	-119.6	64.5	12
	Enrich	31	-4.9	68.4	-94.3	89.3	12
	Enrich	41	8.5	65.7	-83.3	108.6	12
	Boron	0	-89.0	21.2	-119.6	-54.5	12
	Boron	600	-2.4	19.3	-40.2	31.8	12

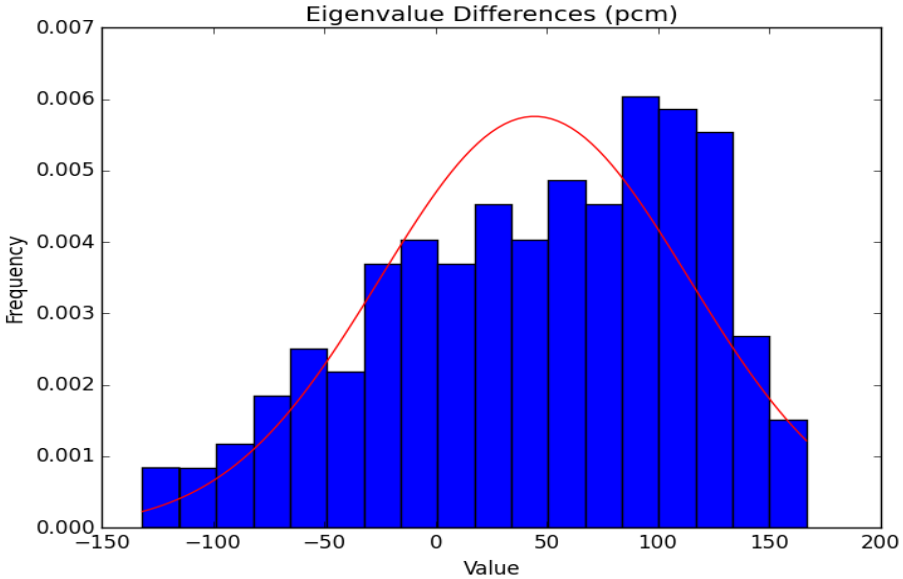

Figure 5.6.1 Pin k_{eff} difference distribution with the v4.2m5 ENDF/B-7.0 MPACT 51-g library

Table 5.6.6 Assembly benchmark result with the v4.2m5 ENDF/B-7.0 MPACT 51-g library

	Category		Δk_{eff} Difference (pcm)				Pin power diff. %		Count
			Average	S. Dev.	Min.	Max.	Ave. RMS	Max. Pin	
Sum	Total All		-65.6	100.5	-509.9	233.0	0.11	0.93	1260
	Total Hot		-71.5	93.7	-276.7	183.9	0.10	0.47	1134
	Total Cold		-12.9	138.0	-509.9	233.0	0.23	0.93	126
Hot	Type	ce16	-109.5	78.0	-257.6	21.5	0.09	0.26	81
	Type	krsko	-110.9	79.0	-263.3	20.0	0.09	0.37	81
	Type	surry	-127.3	77.6	-276.7	-0.2	0.07	0.24	81
	Type	tmi1	-138.6	72.2	-275.0	-16.9	0.10	0.47	81
	Type	tmi2	-127.1	76.6	-269.9	7.0	0.09	0.25	81
	Type	wb2a	-102.8	78.0	-247.9	26.1	0.09	0.30	81
	Type	wb2e	15.4	62.5	-103.1	120.6	0.07	0.24	81
	Type	wb2f	90.8	53.1	-9.8	183.9	0.11	0.32	81
	Type	wb2l	-32.1	56.8	-132.2	67.0	0.09	0.29	81
	Type	wb2m	-6.6	48.6	-93.5	83.7	0.10	0.27	81
	Type	wb2o	-68.3	65.4	-200.5	37.1	0.14	0.45	81
	Type	wb2p	-78.5	55.9	-192.3	10.8	0.16	0.42	81
	Type	wb2w	-101.8	78.3	-246.9	28.0	0.08	0.28	81
	Type	wb2x	-103.5	77.6	-251.0	26.5	0.08	0.27	81
	Enrich	21	-70.8	91.6	-276.7	164.8	0.09	0.45	378
	Enrich	31	-71.6	95.5	-275.0	183.9	0.10	0.41	378
	Enrich	41	-72.1	94.3	-267.2	181.1	0.10	0.47	378
	Boron	0	-113.2	99.8	-276.7	160.9	0.10	0.45	378
	Boron	600	-69.3	86.2	-216.6	176.8	0.10	0.46	378
	Boron	1300	-32.0	75.4	-177.4	183.9	0.09	0.47	378
	Density	den1	-74.3	91.6	-271.6	160.1	0.10	0.46	378
	Density	den2	-72.0	93.6	-275.0	170.4	0.10	0.46	378
	Density	den3	-68.2	96.2	-276.7	183.9	0.10	0.47	378
	Tfuel	600	0.8	66.2	-128.9	183.9	0.10	0.45	378
	Tfuel	900	-74.2	73.6	-202.7	120.4	0.10	0.46	378
	Tfuel	1200	-141.0	80.7	-276.7	66.4	0.10	0.47	378
Cold	Type	ce16	106.2	100.8	-41.4	233	0.28	0.93	9
	Type	krsko	12.9	87.8	-112.8	119.7	0.21	0.66	9
	Type	surry	80.5	107	-68.5	208.2	0.23	0.46	9
	Type	tmi1	1.9	115.7	-179	147.1	0.27	0.62	9
	Type	tmi2	71.1	105.1	-69.4	202.5	0.23	0.51	9
	Type	wb2a	44	93	-89.3	161.2	0.21	0.47	9
	Type	wb2e	-63.7	103	-243.8	75.1	0.21	0.58	9
	Type	wb2f	-105.7	103.7	-296.2	38.2	0.21	0.76	9
	Type	wb2l	-4.8	87.2	-154	116.9	0.2	0.65	9
	Type	wb2m	-3.7	79	-140.2	110.7	0.14	0.5	9
	Type	wb2o	-138.8	122.5	-354.6	22.2	0.26	0.65	9
	Type	wb2p	-269.7	132.4	-509.9	-90.9	0.3	0.8	9
	Type	wb2w	46	92.1	-84.9	161.5	0.21	0.47	9
	Type	wb2x	43.8	91.7	-83.9	157.1	0.21	0.47	9
	Enrich	21	-53.7	151.4	-509.9	174.3	0.22	0.77	42
	Enrich	31	-4.6	133.7	-392.3	218.5	0.23	0.84	42
	Enrich	41	19.8	120.1	-318.1	233	0.23	0.93	42
	Boron	0	-128.2	111.5	-509.9	5.2	0.26	0.93	42
	Boron	600	1.2	106.4	-336.6	145.7	0.23	0.76	42
	Boron	1300	88.4	100	-207.7	233	0.2	0.66	42

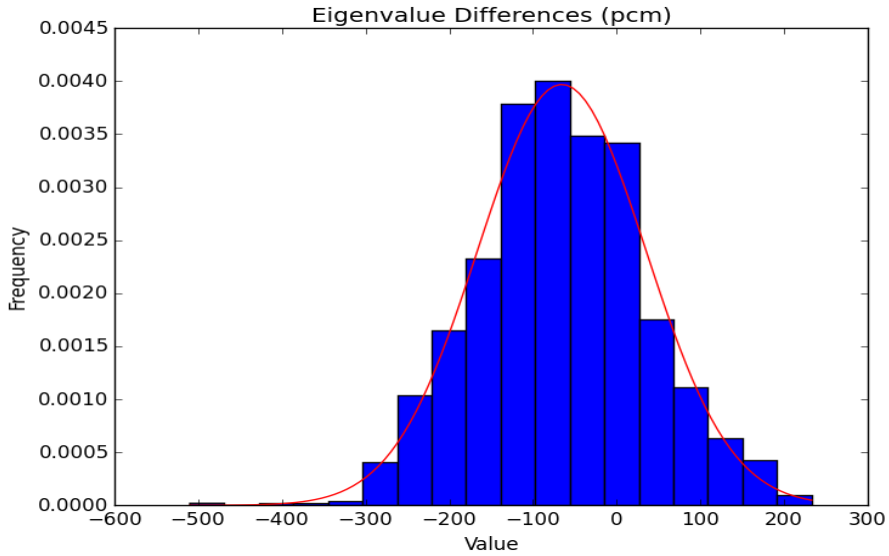

Figure 5.6.2 Assembly k_{eff} difference distribution with the v4.2m5 ENDF/B-7.0 MPACT 51-g library

Table 5.6.7 Pin benchmark result with the ENDF/B-7.0 v5.0m0 SAMPX 51-g library

	Category		Δk_{eff} Difference (pcm)				Count
			Average	S. Dev.	Min.	Max.	
Sum	All		15.4	84.6	-187.8	219.3	360
	Hot		13.7	86.3	-187.8	219.3	324
	Cold		30.8	66.4	-113.3	139.8	36
Hot	Type	beav	0.3	60.3	-123.1	91.6	81
	Type	krsko	109.9	61.3	-18.6	219.3	81
	Type	WB	-59.1	60.7	-187.8	37.9	81
	Type	surry	3.5	63.2	-128.3	107.1	81
	Enrich	21	4.0	81.7	-187.8	178.8	108
	Enrich	31	11.5	87.1	-184.8	202.1	108
	Enrich	41	25.5	89.5	-166.8	219.3	108
	Boron	0	-6.5	92.6	-187.8	219.3	108
	Boron	600	14.6	84.5	-139.5	215.4	108
	Boron	1300	33.0	77.4	-118.0	212.1	108
	Density	den1	1.5	84.8	-187.8	176.9	108
	Density	den2	12.3	86.0	-176.4	197.0	108
	Density	den3	27.3	87.0	-162.3	219.3	108
	Tfuel	600	76.9	65.4	-51.4	219.3	108
	Tfuel	900	23.1	66.0	-106.8	157.6	108
	Tfuel	1200	-58.9	66.4	-187.8	76.3	108
Cold	Type	Beav	34.4	61.8	-74.4	114.8	9
	Type	Krsko	85.2	48.5	-2.5	139.8	9
	Type	WB	-4.5	69.1	-113.3	77.3	9
	Type	Surry	8.3	54.9	-91.1	77.6	9
	Enrich	21	4.7	70.1	-113.3	112.7	12
	Enrich	31	33.8	65.1	-85.6	136.9	12
	Enrich	41	54.0	59.4	-51.6	139.8	12
	Boron	0	-34.0	55.0	-113.3	76.5	12
	Boron	600	37.4	41.0	-15.7	118.9	12

Table 5.6.8 Assembly benchmark result with the v5.0m0 ENDF/B-7.0 SAMPX 51-g library

	Category		Δk_{eff} Difference (pcm)				Count
			Average	S. Dev.	Min.	Max.	
Sum	Total All		-59.4	90.3	-465.3	178.7	1260
	Total Hot		-61.4	86.6	-262.1	164.6	1134
	Total Cold		-41.4	117.8	-465.3	178.7	126
Hot	Type	ce16	-105.9	63.7	-227.0	2.4	81
	Type	krsko	-95.5	64.7	-223.0	8.0	81
	Type	surry	-137.5	63.9	-262.1	-28.6	81
	Type	tmi1	-107.6	59.2	-222.8	-2.4	81
	Type	tmi2	-138.2	63.3	-258.8	-20.4	81
	Type	wb2a	-94.8	64.4	-218.1	12.6	81
	Type	wb2e	18.0	53.5	-95.7	111.9	81
	Type	wb2f	91.6	46.5	-10.1	164.6	81
	Type	wb2l	-52.7	49.1	-151.6	30.1	81
	Type	wb2m	-38.0	43.0	-130.2	34.4	81
	Type	wb2o	-15.0	58.3	-136.7	82.0	81
	Type	wb2p	7.2	55.1	-110.0	100.3	81
	Type	wb2w	-95.1	64.2	-220.6	11.2	81
	Type	wb2x	-96.0	63.4	-222.8	11.9	81
	Enrich	21	-49.9	89.5	-258.1	164.6	378
	Enrich	31	-62.5	87.3	-262.1	164.1	378
	Enrich	41	-71.8	81.5	-251.5	146.4	378
	Boron	0	-88.9	94.1	-262.1	154.2	378
	Boron	600	-60.1	82.8	-221.7	155.7	378
	Boron	1300	-35.2	73.4	-192.3	164.6	378
	Density	den1	-66.2	84.6	-262.1	140.2	378
	Density	den2	-62.0	86.3	-256.7	154.0	378
	Density	den3	-55.9	88.7	-258.1	164.6	378
	Tfuel	600	-3.8	64.5	-125.4	164.6	378
	Tfuel	900	-54.4	69.9	-179.0	136.0	378
	Tfuel	1200	-126.0	77.0	-262.1	80.7	378
Cold	Type	ce16	71.8	88.3	-65.4	178.7	9
	Type	krsko	-8.9	73.3	-122.8	79.2	9
	Type	surry	30.9	92.9	-107.7	136.4	9
	Type	tmi1	-22.0	99.5	-184.8	95.9	9
	Type	tmi2	21.5	89.6	-107.7	127.9	9
	Type	wb2a	13.9	77.7	-107.2	107.6	9
	Type	wb2e	-87.1	89.0	-249.1	28.2	9
	Type	wb2f	-123.1	89.8	-292.0	-4.2	9
	Type	wb2l	-53.3	77.7	-186.1	46.2	9
	Type	wb2m	-61.4	70.7	-179.1	32.5	9
	Type	wb2o	-140.9	107.3	-335.3	-5.2	9
	Type	wb2p	-249.4	117.4	-465.3	-97.7	9
	Type	wb2w	14.5	77.0	-103.1	107.0	9
	Type	wb2x	13.3	76.5	-104.3	103.8	9
	Enrich	21	-53.7	151.4	-509.9	174.3	42
	Enrich	31	-4.6	133.7	-392.3	218.5	42
	Enrich	41	19.8	120.1	-318.1	233	42
	Boron	0	-128.2	111.5	-509.9	5.2	42
	Boron	600	1.2	106.4	-336.6	145.7	42
	Boron	1300	88.4	100	-207.7	233	42

Table 5.6.9 Comparison between MCNP and CE-KENO with ENDF/B-7.0

	Category		Δk_{eff} Difference (pcm)				Count
			Average	S. Dev.	Min.	Max.	
Sum	All		-11	37.2	-99	70	360
	Hot		-11.9	38.8	-99	70	324
	Cold		-2.9	13	-28	22	36
Hot	Type	beav	-13.7	39.3	-99	64	81
	Type	krsko	-10.3	40.1	-93	70	81
	Type	WB	-12.1	38.4	-78	56	81
	Type	surry	-11.6	38.1	-79	57	81
	Enrich	21	-10.8	37.0	-99	68	108
	Enrich	31	-13.9	39.7	-93	64	108
	Enrich	41	-11.1	40.0	-95	70	108
	Boron	0	-16.6	41.7	-99	70	108
	Boron	600	-12.2	38.5	-95	54	108
	Boron	1300	-7.0	35.9	-78	64	108
	Density	den1	-13.6	37.4	-95	54	108
	Density	den2	-10.6	38.7	-99	58	108
	Density	den3	-11.6	40.6	-93	70	108
	Tfuel	600	30.6	13.8	-2	70	108
	Tfuel	900	-8.5	13.2	-46	23	108
	Tfuel	1200	-57.9	14.5	-99	-16	108
Cold	Type	Beav	-4.9	15.7	-19	22	9
	Type	Krsko	-5.0	11.7	-19	12	9
	Type	WB	-4.7	9.5	-28	3	9
	Type	Surry	3.1	14.6	-28	22	9
	Enrich	21	-2.1	13.7	-28	16	12
	Enrich	31	-4.8	13.3	-19	22	12
	Enrich	41	-1.7	12.9	-28	22	12
	Boron	0	-0.6	10.5	-19	13	12
	Boron	600	-9.4	10.9	-28	16	12

Table 5.6.10 Comparison between Monte Carlo and MPACT-P_2 with ENDF/B-7.0

Comparison	Δk, pcm				$\Delta\rho$, pcm			
	Ave.	SD	Max	Min	Ave.	SD	Max	Min
MCNP-MPACT 4.2m5	29	86	216	-196	17	55	143	-135
KENO-MPACT 4.2m5	18	62	162	-203	**10**	**40**	**107**	**-137**
MCNP-SAMPX 5.0m0	42	79	213	-162	26	51	139	-110
KENO-SAMPX 5.0m0	31	57	155	-169	**19**	**36**	**103**	**-111**

5.7 BWR PIN AND ASSEMBLY BENCHMARK PROBLEMS

5.7.1 Characteristics of Problems

The specifications for the Peach Bottom lattices analyzed in this section come from BWR Turbine Trip Benchmark [Sol01]. Benchmark problems include 7 lattice type as shown in Figure 5.7.1. Each lattice type is simulated over seven state conditions as provided in Table 5.7.1. Types 4a and 4b are using 100-mil and 120-mil channel boxes, respectively.

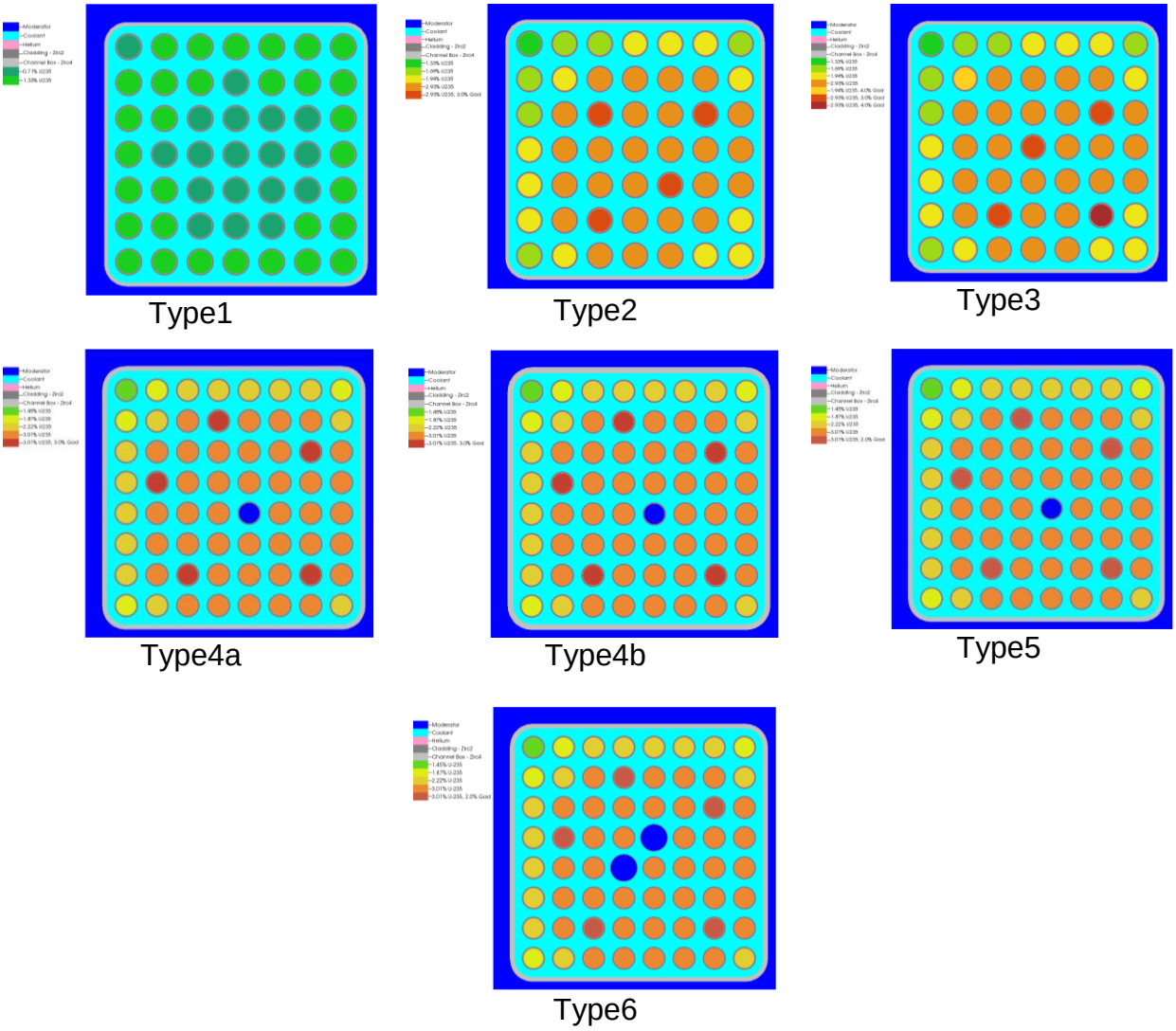

Figure 5.7.1 Peach Bottom lattice models for KENO and MPACT

Table 5.7.1 Peach Bottom lattice simulated conditions

Power	Void %	Moderator Density (g/cc)	Coolant Density (g/cc)	Non-Fuel Material Temperature (K)	Fuel Temperature (K)
Cold Zero Power	0	0.996513	0.996513	293	293
Hot Zero Power	0	0.736690	0.736690	600	600
Hot Full Power	0	0.736690	0.736690	600	900
Hot Full Power	20	0.736690	0.596857	600	900
Hot Full Power	40	0.736690	0.457024	600	900
Hot Full Power	60	0.736690	0.317191	600	900
Hot Full Power	80	0.736690	0.177358	600	900

5.7.2 Benchmark Results

Benchmark calculations have been performed only by using the ENDF/B-7.0 SAMPX 51 and 252-g libraries. Figure 5.7.1~5.7.7 provide benchmark calculation results which can be summarized as follows:

- Cold zero power results by the SAMPX 51-g library are poor in both multiplication factors and power distributions; this might be related to previous evaluations that have identified the need for additional flat-source mesh cells required in the coolant for cold calculations.
- The SAMPX 252-g results are good for most of cases except for Type 1 at cold zero power and Type 6 at hot full power with 80% void. Type 6 case may need more investigation to figure out the significant error in power distribution.
- Hot zero and full power results by the SAMPX 51-g library are poor in both multiplication factors and power distributions, which indicates that the 51-g library is not good enough to be used in BWR simulation.

Table 5.7.2 Benchmark result for Cold Zero Power

Type	KENO		SAMPX 51-g			SAMPX 252-g		
	k-eff	Unc. (pcm)	Δk pcm	Max Diff	RMS	Δk pcm	Max Diff	RMS
Type 1	1.02682	2.1	317	1.48%	0.59%	219	1.13%	0.36%
Type 2a	1.15517	2.1	36	2.33%	0.99%	50	1.29%	0.64%
Type 2b	1.11948	2.2	-53	2.45%	1.01%	-14	1.38%	0.66%
Type 3a	1.15874	2.1	92	2.43%	1.02%	92	1.36%	0.66%
Type 3d	1.11338	2.3	-99	2.31%	1.03%	-55	1.26%	0.66%
Type 3e	1.06720	2.2	-222	2.73%	1.09%	-144	1.64%	0.72%
Type 4 (100-mil)	1.12751	2.3	-118	2.39%	0.87%	-57	1.56%	0.55%
Type 4 (120-mil)	1.12877	2.3	-156	2.25%	0.86%	-93	1.44%	0.55%
Type 5	1.13445	2.1	-88	2.27%	0.87%	-53	1.42%	0.55%
Type 6	1.13103	2.3	-119	2.27%	0.87%	-76	1.43%	0.55%
Average		2.2	153	2.26%	0.88%	94	1.43%	0.56%
Std. Dev.		0.1	41	0.38%	0.16%	20	0.16%	0.11%

Table 5.7.3 Benchmark result for Hot Zero Power

Type	KENO		SAMPX 51-g			SAMPX 252-g		
	k-eff	Unc. (pcm)	Δk pcm	Max Diff	RMS	Δk pcm	Max Diff	RMS
Type 1	1.05393	2.0	-104	0.58%	0.22%	21	0.54%	0.20%
Type 2a	1.14621	2.2	-285	1.02%	0.52%	-141	0.94%	0.47%
Type 2b	1.10536	2.2	-320	1.02%	0.53%	-174	0.94%	0.48%
Type 3a	1.15548	2.2	-384	1.00%	0.49%	-236	0.93%	0.45%
Type 3d	1.09254	2.3	-314	1.09%	0.54%	-171	0.99%	0.49%
Type 3e	1.04024	2.3	-332	1.14%	0.57%	-188	1.05%	0.53%
Type 4 (100-mil)	1.10087	2.2	-231	0.91%	0.44%	-135	0.79%	0.38%
Type 4 (120-mil)	1.09890	2.3	-236	0.88%	0.43%	-142	0.77%	0.38%
Type 5	1.11378	2.2	-202	0.95%	0.44%	-131	0.82%	0.38%
Type 6	1.11257	2.2	-241	0.88%	0.42%	-177	0.76%	0.36%
Average		2.2	238	0.91%	0.43%	138	0.81%	0.39%
Std. Dev.		0.1	60	0.17%	0.11%	38	0.16%	0.10%

Table 5.7.4 Benchmark result for Hot Full Power 0% void

Type	KENO		SAMPX 51-g			SAMPX 252-g		
	k-eff	Unc. (pcm)	Δk pcm	Max Diff	RMS	Δk pcm	Max Diff	RMS
Type 1	1.04770	1.9	-115	0.61%	0.23%	6	0.56%	0.21%
Type 2a	1.13966	2.1	-292	1.02%	0.52%	-150	0.94%	0.47%
Type 2b	1.09904	2.3	-328	1.03%	0.53%	-184	0.95%	0.49%
Type 3a	1.14785	2.2	-284	1.00%	0.50%	-138	0.93%	0.46%
Type 3d	1.08624	2.3	-322	1.09%	0.54%	-181	1.01%	0.49%
Type 3e	1.03423	2.2	-343	1.16%	0.57%	-201	1.07%	0.52%
Type 4 (100-mil)	1.09440	2.2	-236	0.95%	0.44%	-143	0.83%	0.38%
Type 4 (120-mil)	1.09233	2.3	-240	0.92%	0.43%	-148	0.81%	0.37%
Type 5	1.10736	2.3	-212	0.93%	0.44%	-144	0.79%	0.37%
Type 6	1.10629	2.3	-241	0.88%	0.42%	-178	0.76%	0.36%
Average		2.2	245	0.93%	0.43%	143	0.82%	0.39%
Std. Dev.		0.1	28	0.17%	0.11%	13	0.16%	0.10%

Table 5.7.5 Benchmark result for Hot Full Power 20% void

Type	KENO		SAMPX 51-g			SAMPX 252-g		
	k-eff	Unc. (pcm)	Δk pcm	Max Diff	RMS	Δk pcm	Max Diff	RMS
Type 1	1.05010	1.9	-158	0.55%	0.20%	-28	0.48%	0.18%
Type 2a	1.13053	2.2	-285	0.95%	0.45%	-135	0.86%	0.40%
Type 2b	1.09092	2.2	-308	0.93%	0.46%	-155	0.85%	0.42%
Type 3a	1.13990	2.1	-293	0.87%	0.43%	-135	0.80%	0.39%
Type 3d	1.07569	2.2	-297	0.96%	0.46%	-147	0.88%	0.42%
Type 3e	1.02476	2.3	-301	1.03%	0.50%	-149	0.94%	0.45%
Type 4 (100-mil)	1.08318	2.4	-177	1.02%	0.50%	-76	0.89%	0.44%
Type 4 (120-mil)	1.08020	2.4	-181	1.01%	0.49%	-80	0.89%	0.43%
Type 5	1.09685	2.3	-162	1.01%	0.50%	-80	0.88%	0.44%
Type 6	1.09694	2.2	-157	1.82%	0.72%	-85	1.76%	0.67%
Average		2.2	206	1.05%	0.48%	93	0.96%	0.43%
Std. Dev.		0.2	57	0.38%	0.15%	26	0.39%	0.14%

Table 5.7.6 Benchmark result for Hot Full Power 40% void

Type	KENO		SAMPX 51-g			SAMPX 252-g		
	k-eff	Unc. (pcm)	Δk pcm	Max Diff	RMS	Δk pcm	Max Diff	RMS
Type 1	1.04770	1.9	-197	0.54%	0.19%	-52	0.47%	0.16%
Type 2a	1.11652	2.4	-267	0.84%	0.36%	-103	0.75%	0.32%
Type 2b	1.07838	2.3	-284	0.77%	0.37%	-114	0.69%	0.33%
Type 3a	1.12705	2.1	-287	0.79%	0.35%	-112	0.72%	0.31%
Type 3d	1.06061	2.3	-271	0.79%	0.37%	-103	0.70%	0.33%
Type 3e	1.01157	2.3	-271	0.83%	0.39%	-100	0.74%	0.35%
Type 4 (100-mil)	1.06774	2.3	-116	1.37%	0.62%	2	1.30%	0.57%
Type 4 (120-mil)	1.06349	2.2	-116	1.36%	0.62%	2	1.29%	0.57%
Type 5	1.08212	2.3	-96	1.37%	0.62%	-2	1.30%	0.56%
Type 6	1.08313	2.3	-33	3.77%	1.20%	52	3.71%	1.16%
Average		2.2	159	1.43%	0.57%	46	1.36%	0.53%
Std. Dev.		0.1	93	1.09%	0.32%	47	1.09%	0.32%

Table 5.7.7 Benchmark result for Hot Full Power 60% void

Type	KENO		SAMPX 51-g			SAMPX 252-g		
	k-eff	Unc. (pcm)	Δk pcm	Max Diff	RMS	Δk pcm	Max Diff	RMS
Type 1	1.03884	1.9	-242	0.42%	0.17%	-73	0.35%	0.13%
Type 2a	1.09664	2.1	-262	0.63%	0.27%	-66	0.54%	0.24%
Type 2b	1.06038	2.2	-270	0.70%	0.28%	-69	0.61%	0.25%
Type 3a	1.10818	2.1	-283	0.63%	0.27%	-80	0.55%	0.24%
Type 3d	1.04016	2.4	-256	0.64%	0.28%	-60	0.56%	0.25%
Type 3e	0.99388	2.4	-255	0.67%	0.30%	-55	0.60%	0.27%
Type 4 (100-mil)	1.04730	2.2	-66	2.00%	0.79%	84	1.93%	0.74%
Type 4 (120-mil)	1.04121	2.1	-58	2.00%	0.80%	92	1.93%	0.76%
Type 5	1.06239	2.2	-43	1.93%	0.77%	83	1.87%	0.73%
Type 6	1.06405	2.2	110	5.94%	1.73%	221	5.88%	1.69%
Average		2.2	149	1.95%	0.69%	97	1.88%	0.65%
Std. Dev.		0.1	98	1.89%	0.53%	53	1.90%	0.53%

Table 5.7.8 Benchmark result for Hot Full Power 80% Void

Type	KENO		SAMPX 51-g			SAMPX 252-g		
	k-eff	Unc. (pcm)	Δk pcm	Max Diff	RMS	Δk pcm	Max Diff	RMS
Type 1	1.02167	1.9	-310	0.39%	0.15%	-87	0.29%	0.11%
Type 2a	1.06996	2.1	-291	0.41%	0.18%	-28	0.37%	0.16%
Type 2b	1.03614	2.2	-298	0.43%	0.19%	-30	0.40%	0.18%
Type 3a	1.08241	2.1	-308	0.44%	0.17%	-39	0.39%	0.16%
Type 3d	1.01394	2.3	-279	0.42%	0.19%	-18	0.38%	0.18%
Type 3e	0.97135	2.3	-277	0.44%	0.20%	-12	0.41%	0.18%
Type 4 (100-mil)	1.02151	2.2	-63	2.60%	0.97%	163	2.55%	0.94%
Type 4 (120-mil)	1.01275	2.1	-47	2.70%	1.00%	178	2.66%	0.97%
Type 5	1.03727	2.3	-40	2.54%	0.95%	161	2.49%	0.92%
Type 6	1.03908	2.1	233	8.25%	2.26%	411	8.21%	2.23%
Average		2.2	181	2.48%	0.82%	149	2.43%	0.79%
Std. Dev.		0.1	116	2.77%	0.75%	126	2.78%	0.75%

5.8 NON-UNIFORM FUEL TEMPERATURE BENCHMARK PROBLEMS

5.8.1 Characteristics of Problems

Seoul National University (SNU) has developed a benchmark suite for the intra-pellet nonuniform temperature distribution cases [Kim16b]. Table 5.8.1 and Figure 5.8.1 provide the geometrical specifications, including five equi-volume subzones in the fuel pellet, gap, cladding, and moderator. Table 5.8.2 provides the compositional specification, including nuclides and atomic number densities.

Non-uniform temperature profiles as a function of power and average fuel temperatures are shown in Table 5.8.3 and Figure 5.8.2. Benchmark calculations are performed by using both non-uniform and uniform temperature profiles.

Table 5.8.1 Geometrical data

Region	Dimensions		
Fuel	Outer Radius (cm)		0.4127
	Sub-pellet annular ring radius (cm)	1	0.1846
		2	0.2610
		3	0.3197
		4	0.3692
		5	0.4127
Gap			
Clad	Inner Radius (cm)		0.4203
	Outer Radius (cm)		0.4862
Coolant	Cell Pitch (cm)		1.2870

Table 5.8.2 Composition data

Composition	Nuclides		Atomic Number Density (atoms/barn-cm)
3.0 % UO_2	^{235}U	92235	7.13479E-04
	^{238}U	92238	2.27778E-02
	^{16}O	8016	4.69825E-02
Gap	^{16}O	8016	1.00000E-08
Clad	^{90}Zr	40090	2.22157E-02
	^{91}Zr	40091	4.79136E-03
	^{92}Zr	40092	7.24405E-03
	^{94}Zr	40094	7.18475E-03
	^{96}Zr	40096	1.13334E-03
Coolant	^{1}H	1001	4.65690E-02
	^{16}O	8016	2.32840E-02

Table 5.8.3 Non-uniform temperature profiles as a function power

Region		Temperature (K)						
		Power Level (%)						
		50	75	100	125	150	175	200
Pellet	1	787.4	897.7	1017.9	1148.2	1288.2	1437.7	1596.3
	2	754.7	843.7	939.3	1041.7	1150.6	1266.0	1387.5
	3	723.1	792.2	865.1	942.0	1022.7	1107.3	1195.6
	4	683.0	728.3	774.9	823.2	873.0	924.3	977.1
	5	669.2	708.3	748.4	789.4	831.4	874.3	918.2
	Avg.	723.5	794.0	869.1	948.9	1033.2	1121.9	1214.9
Gap		606.1	610.2	614.0	617.7	621.2	624.7	628.1
Clad		606.1	610.2	614.0	617.7	621.2	624.7	628.1
Coolant		586.7	586.7	586.7	586.7	586.7	586.7	586.7

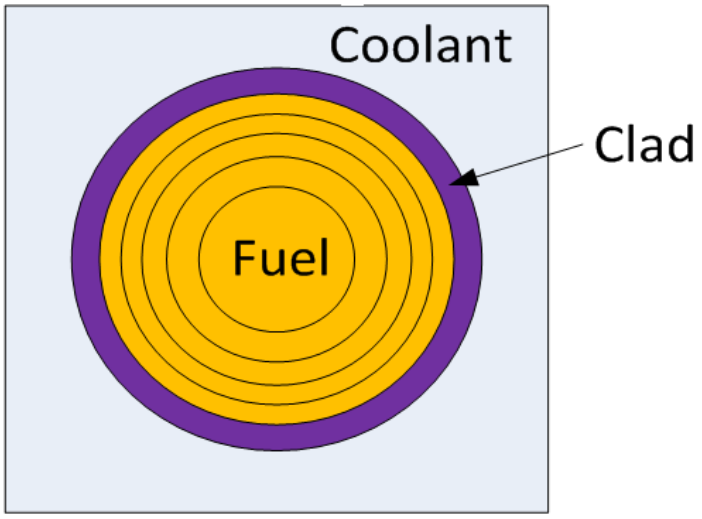

Figure 5.8.1 Geometrical configuration

5.8.2 Benchmark Results

Benchmark calculations were performed using the continuous-energy Monte Carlo codes McCARD and CE-KENO using the ENDF/B-7.0 continuous-energy cross section library and the VERA-CS MPACT using the ENDF/B-7.0 MPACT and SAMPX 51-g libraries. The ACE format continuous-energy cross sections for McCARD were processed for all temperatures by NJOY [Mac94]. SCALE-6.2 with CE-KENO includes a new capability to interpolate continuous-energy cross sections for any specified temperature based on the reference temperatures for base cross sections. However, if the specified temperature differs from the reference temperature within 4 K, no interpolation will be made.

Figure 5.8.2 provides a comparison of reactivities between nonuniform and uniform temperature profile results obtained by McCARD. This comparison indicates that the slopes of nonuniform and uniform temperature profiles, which determine the fuel temperature reactivity coefficient, are different. In other words, the fuel temperature coefficient of the nonuniform temperature is less negative than that of the uniform temperature. Therefore, when performing whole core calculations with thermal/hydraulic (T/H) feedback, nonuniform temperature profiles need to be considered properly in estimating resonance self-shielded cross sections by performing subgroup calculations.

Figure 5.8.3 provides the benchmark results for the uniform temperature cases. There is very good agreement between KENO and MPACT with the MPACT and SAMPX libraries in the reactivities for all temperatures. While there is about 3% difference in fuel temperature coefficient between KENO and MPACT with the MPACT library, very good agreement can be observed between KENO and MPACT with the SAMPX 51-g library. It should be noted that there is an intrinsic difference in reactivity between McCARD and KENO. McCARD is using ACE format library and is almost identical to the MCNP in methodology.

Figure 5.8.4 provides the benchmark results for the nonuniform temperature cases. There is very good agreement between KENO and MPACT with the MPACT and SAMPX libraries in the reactivities for all temperatures. However, while there is about 5% difference in fuel temperature coefficient between KENO and MPACT with the SAMPX library, very good agreement can be observed between KENO and MPACT with the MPACT 51-g library. It should be noted that there is intrinsic difference in reactivity between McCARD and KENO.

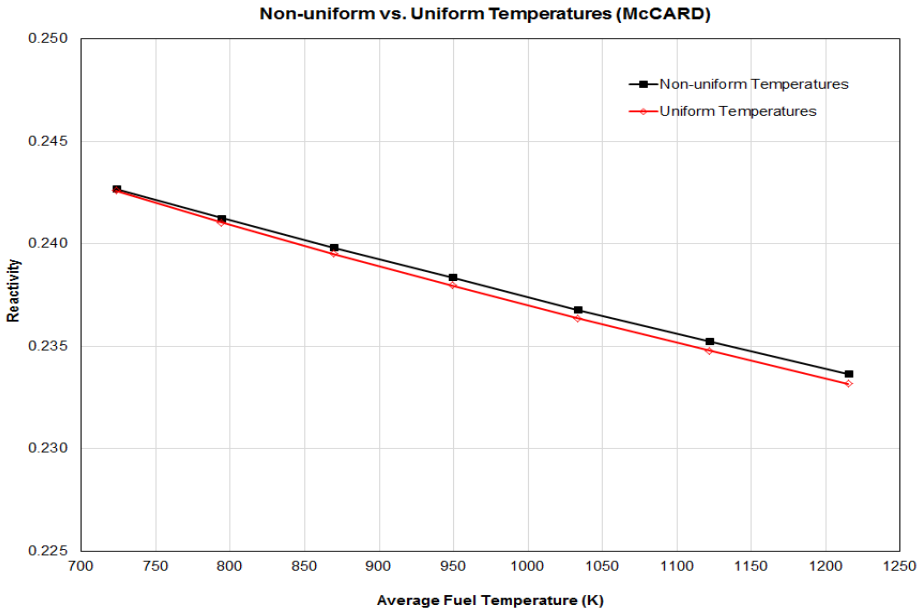

Figure 5.8.2 Comparison of reactivities between nonuniform and uniform temperature distributions.

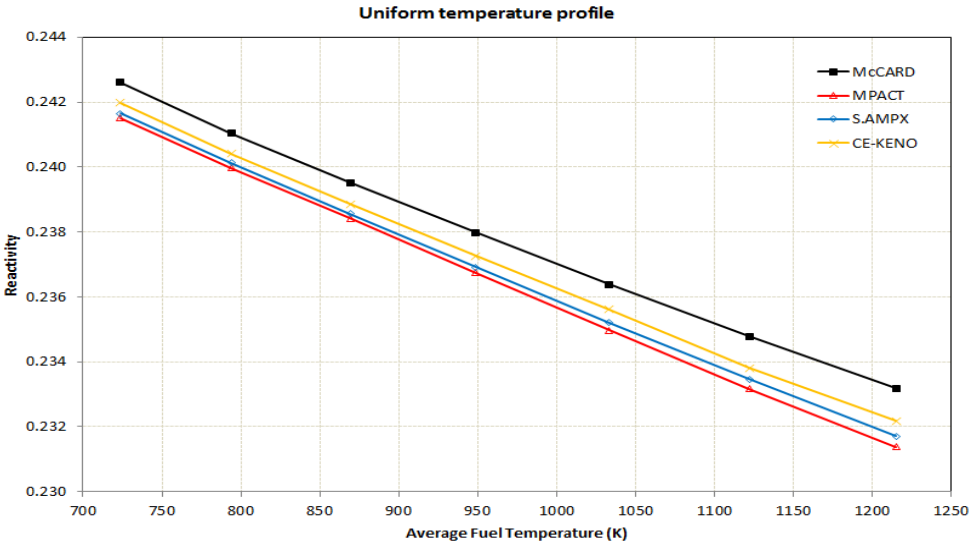

Code	FTC (pcm/K)	[a]-[b,c] (%)	[b]-[a,c](%)
McCARD[a]	-1.934	-	-3.6
CE-KENO[b]	-2.004	3.5	-
SAMPX[c]	-2.032	4.8	1.3
MPACT[c]	-2.068	6.4	3.1

Figure 5.8.3 Comparison of reactivities for the uniform temperature distributions

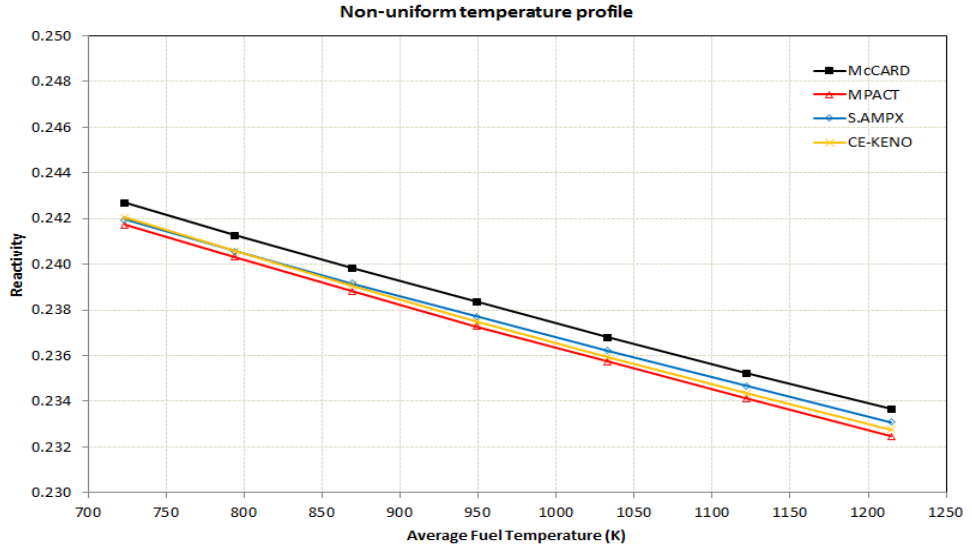

Code	FTC (pcm/K)	[a]-[b,c] (%)	[b]-[a,c](%)
McCARD[a]	-1.847	-	-2.8
CE-KENO[b]	-1.899	2.7	-
S.AMPX[c]	-1.933	-2.0	-4.9
MPACT[c]	-1.788	-2.5	-0.2

Figure 5.8.4 Comparison of reactivities for the nonuniform temperature distributions

5.9 WBN1 POWER PLANT DEPLETION PROBLEMS

5.9.1 Characteristics of Problems [God15]

The WBN1 reactor core is comprised of 193 nuclear fuel assemblies arranged in a cylindrical arrangement (Figure 5.9.1). The fuel assemblies are the Westinghouse 17x17 design comprised of 264 cylindrical fuel rods containing a twelve-foot stack of UO_2 pellets and 25 cylindrical guide and instrument tubes. Approximately 1/3rd of these assemblies are replaced with fresh (or new) fuel during each refueling cycle, while the remaining fuel is shuffled to new core locations to optimize the subsequent fuel cycle length and fuel rod power distributions. The fuel cycles have been approximately 18 months in length, with approximately 40 day refueling outages between cycles. All of these operational characteristics must be considered when performing any realistic reactor analyses.

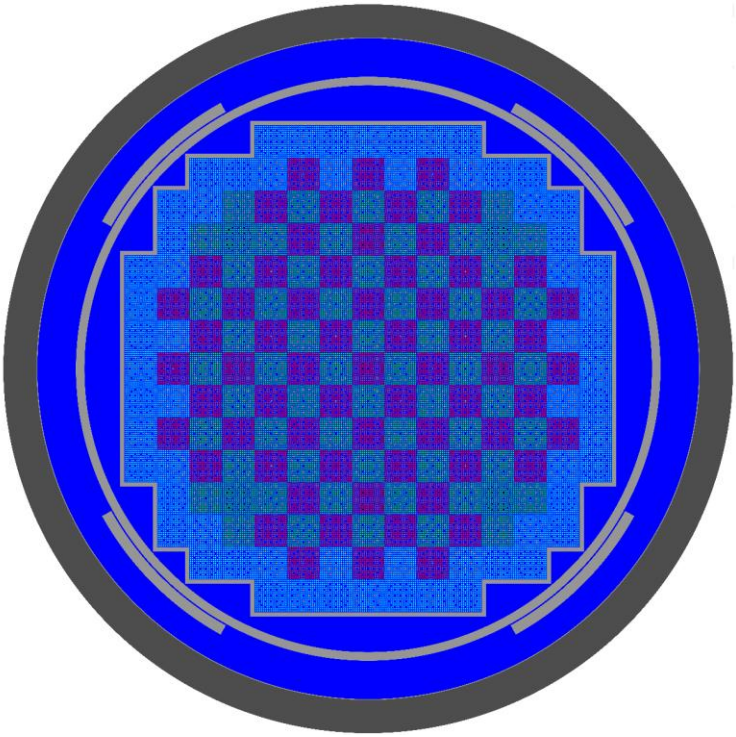

Figure 5.9.1 WBN1 reactor core with 193 fuel assemblies (Cycle 1)

5.9.2 Benchmark Results

Benchmark calculations have been performed for the WBN1 cycles1 through 14 by using the ENDF/B-7.0 v4.2m5 MPACT 51-g library. Figures 5.9.2~5.9.4 provides HZP and HFP critical boron concentrations and 3D flux map RMS errors, respectively. Since there are many factors impacting on the result on the Multiphysics simulation, this is just a demonstration of the power plant simulation.

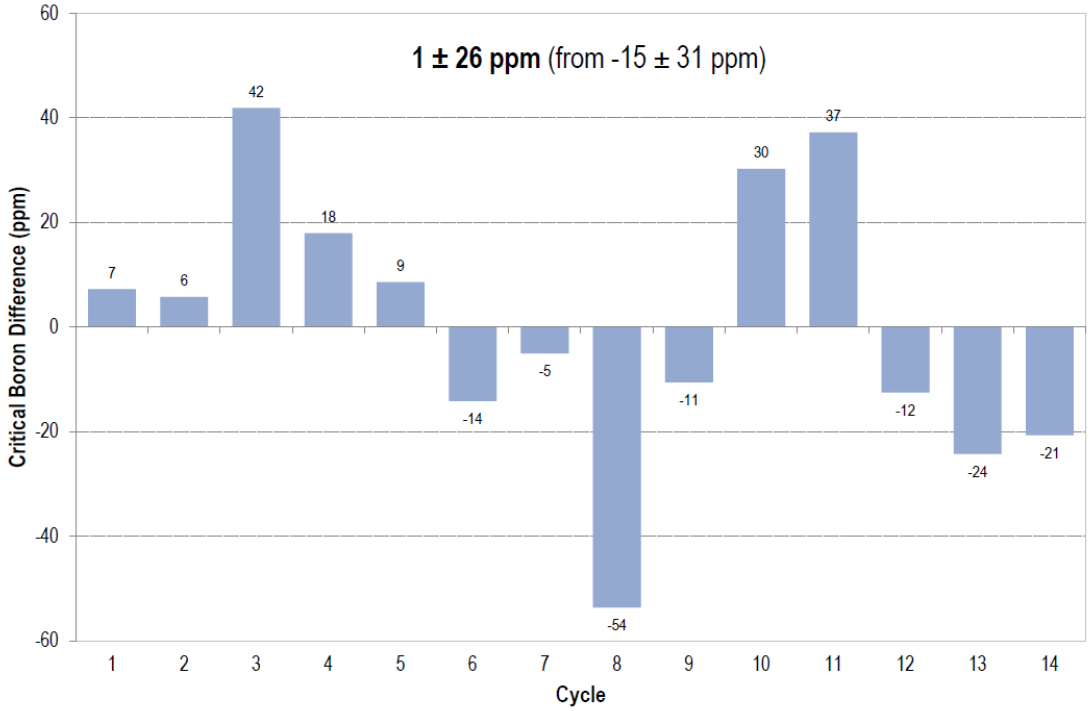

Figure 5.9.2 WBN1 HZP critical boron concentration

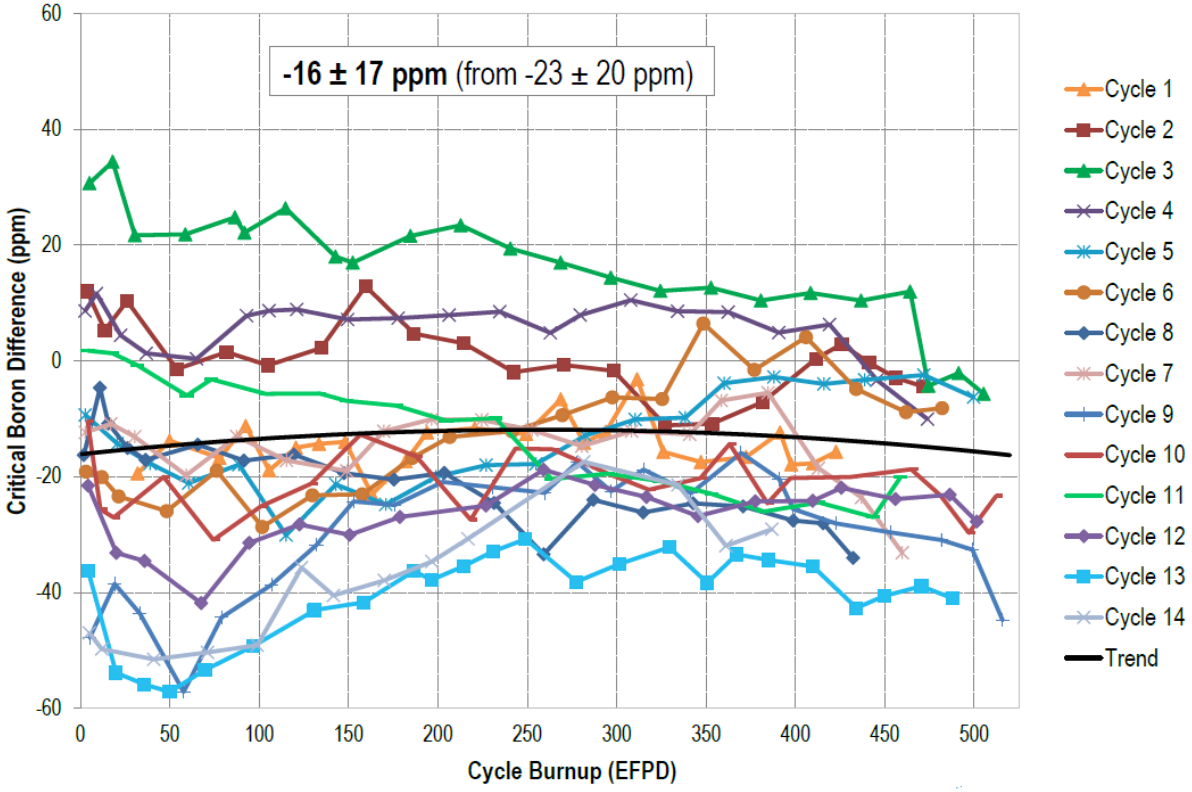

Figure 5.9.3 WBN1 HFP critical boron concentration

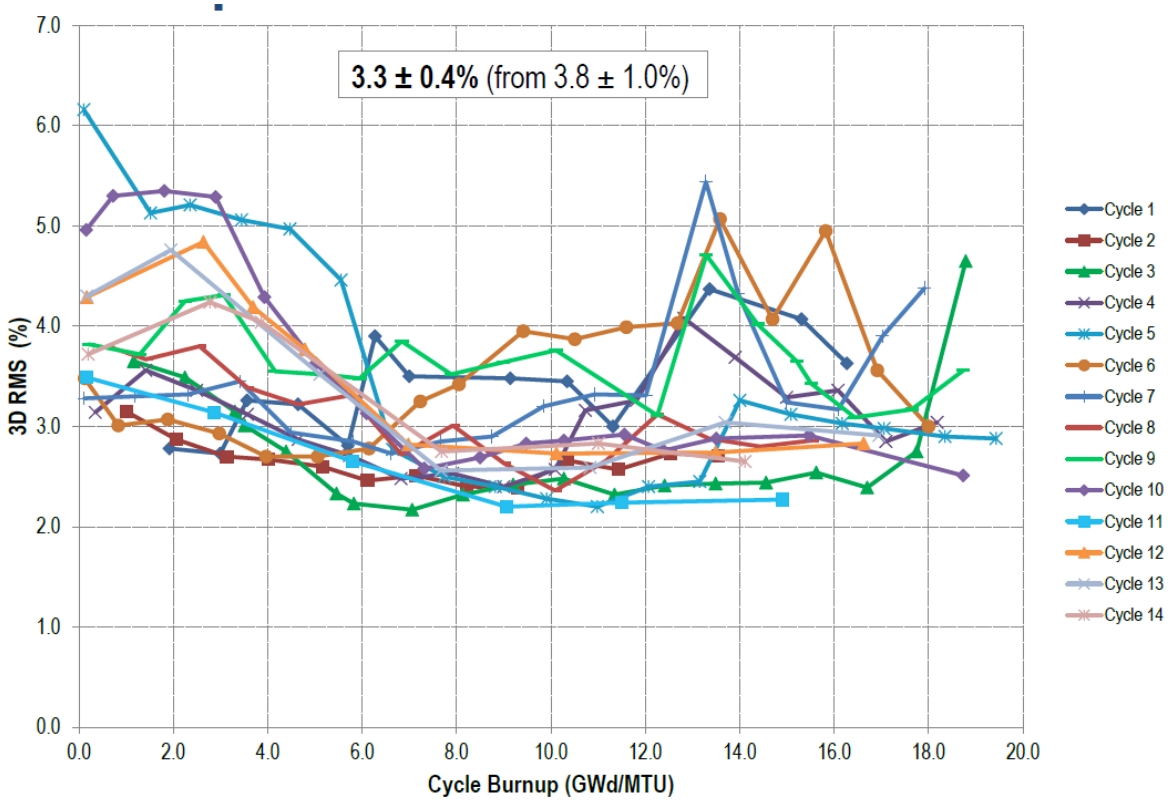

Figure 5.9.4 WBN1 3D flux map RMS errors

6. PERFORMANCE OF CROSS SECTION PROCESSING

One crucial step in the MPACT calculation sequence is the cross section processing, which is identified as a major contribution to the overall computing time [Pal16c]. The self-shielding calculation in MPACT includes the following tasks,

1) the resonance self-shielding calculation to obtain the equivalence cross section in resonance groups,
2) use of equivalence cross section to compute the microscopic cross section in resonance groups, and calculation of region-wise macroscopic cross sections and fission spectra for all energy groups.

Previously, several improvements have been developed to speed up the cross section calculation with the MPACT library [Liu16b]. Figure 6.0.1 shows the total run time as well as MPACT calculation components for running Watts Bar cycle 1 depletion with the first five state points [Pal16c]. Regarding the two tasks of the cross section calculation, '*Self-Shield Calc*' and '*Self-Shield Comm*' correspond to the first, and '*calcMacro*' corresponds to the second. As shown from the figure, the computing time of both tasks are significantly reduced by implementing these improvements.

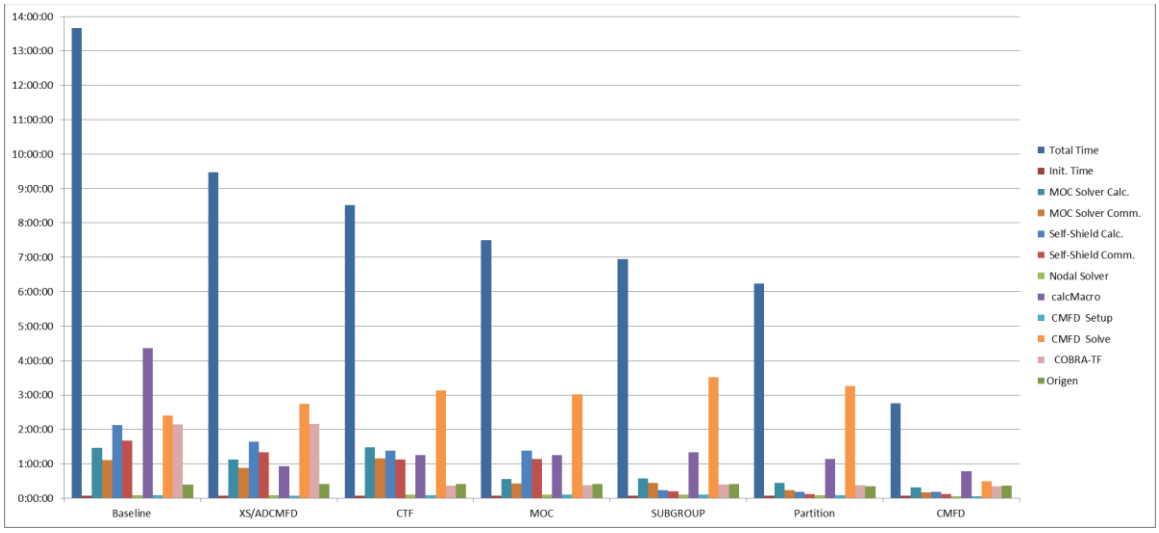

Figure 6.0.1 Progression of speedup for cycle depletion

However, since we are working on the transition from MPACT library to SAMPX library, it is useful to re-estimate the computing resources between the MPACT library and SAMPX libraries.

As SAMPX library includes more isotopes, more resonance data (all groups and all isotopes), and additional scattering data (thermal, elastic, and non-elastic), the memory to read in the library is increased. However, the additional memory should not be sensitive to the size of the problem, because the macroscopic 1D and 2D data stored in each material region has no isotope dependency. To verify this, a pin cell and a lattice

case with fresh fuel and depleted fuel (~150 fuel isotopes) are run with two 51-group libraries. Table 6.0.1 shows that the additional library storage of SAMPX library is about 85 MB (per processor since every processor holds a copy of the cross section data), and the additional memory is not increasing with the problem size or the number of isotopes.

Table 6.0.1 Memory usage (MB) of MPACT and SAMPX libraries

Library	Pin cell		Lattice 17×17		Core 3D
	Fresh	Depleted	Fresh	Depleted	Fresh
MPACT	23.1	23.2	328.8	338.8	1265.1
SAMPX	108.8	108.8	415.6	422.1	1395.7
SAMPX-MPACT	85.7	85.6	86.8	83.6	130.6

Next, the additional computing time of SAMPX library is investigated by running a 2D fuel assembly with depleted fuel composition. To emphasize, most of the performance improvements developed for MPACT library have been implemented in SAMPX library, except for the subgroup non-uniform temperature correction, because SAMPX library does not contain the base cross section shielded by a typical LWR spectrum. Table 6.0.2 shows the computing times of macroscopic cross section and fission spectrum, where the former is further split into 1D cross section and 2D cross section (scattering matrix).

Table 6.0.2 Computing time (s) of MPACT and SAMPX libraries

Item	MPACT library	SAMPX library
1-D XS	4.69	202
2-D XS	5.92	10.5
calcMacroXS(1D+2D)	10.6	214
calcMacroChi	0.453	0.466

The computing time of SAMPX library is large in computing the 1-D cross sections. To investigate this, we further split the calculation time into isotopes with and without subgroup data. For the isotopes with subgroup data, we also have different treatments for absorption/nu-fission and other reaction channels. The detailed comparison is shown in Table 6.0.3.

Table 6.0.3 1D cross section computing time for MPACT and SAMPX libraries

Item	MPACT library	SAMPX library
Res. Subgroup (absorption + nu-fission)	1.83 s	28.8 s
Res. Subgroup (other reaction channels)	1.75	34.5
No-subgroup data	1.11	137

Even though the computing time of cross section processing with the SAMPX library is much more expensive than that of cross section processing with the MPACT library, an overall increase for a 3D quarter core problems is only 10% because of relatively small fraction of cross section processing.

Table 6.0.4 Computing time for 3D quarter core

Item	MPACT library	SAMPX library	Difference
3D quarter core (5A-3D)	1265 s	1396 s	131 s

As compared with the MPACT MG library, all three components see an increased time of SAMPX library. To specify, the differences in library and treatment are compared for the three components.

1. Res. Subgroup (absorption and nu-fission)

The depleted fuel has ~150 isotopes. 16 of them have subgroup data in the MPACT library, but 35 of them have subgroup data in the SAMPX library. 22 groups are resonant in MPACT library but all 51 groups are resonant in the AMPX library. In addition, the calculation of the absorption and ν-fission cross sections do not use *Segev* interpolation in MPACT library, but SAMPX library does not contain a base cross section for subgroup temperature correction, so the expensive *Segev* interpolation is still used in treating the non-uniform temperature. By factoring all those differences, it explains 28.8s versus 1.83s.

2. Res. Subgroup (other reaction channels)

In addition to the absorption and nu-fission cross sections, we only need to shield the total scattering cross section in the MPACT library to renormalize the scattering matrix. However, the SAMPX library shields the following reaction channels, 1) total cross section 2) transport cross section 3) elastic scattering 4) within group scattering. All of these calculations require *Segev* interpolation. If one factors the number of channels, number of resonance groups and number of resonance isotopes, this explains 34.5s versus 1.75s.

3. No-subgroup data

In the MPACT library, an isotope without subgroup data computes the base cross section by temperature interpolation only. In the SAMPX library, we are allowed to shield all the isotopes because of the additional cross section data. Similarly, we shield the cross section of the 6 reaction channels (the four mentioned in 2 plus absorption and nu-fission) over 115 isotopes without subgroup data. So this explains 137s versus 1.11s.

To summarize, the increased computing time is primarily due to the resonance integral interpolation (*Segev*) for additional reaction channels, isotopes and energy groups.

To reduce the computing time of using SAMPX library, the following tasks can be considered.

1. Switch to a simple treatment for non-uniform temperature (e.g., a pre-determined background cross section to avoid *Segev* interpolation).
2. Review *Segev* interpolation for further improvements.
3. Check if shielding all the isotopes is necessary by using reaction rate analysis tool.
4. Investigate sensitivity of the transport correction factor on background cross section, so that the correction factor may be determined from an infinite-diluted total and transport cross sections.

7. CONCLUSION

The ENDF/B-7.0 and 7.1 v4.2m5 MPACT 51-g libraries have been successfully developed through verification and validation which meet VERA-CS SQA requirements and satisfy accuracy requirements. Currently the default cross section library for MPACT is the v4.2m5 ENDF/B-7.1 MPACT 51-g library. In order to overcome some of drawbacks of the MPACT MG library, a new simplified AMPX MG library format has been developed based on the AMPX MG library. The v5.0m0 ENDF/B-7.0 and 7.1 SAMPX 51 and 252-g libraries have been developed and the simplified AMPX capability has been implemented in the VERA-CS MPACT. Benchmark results show that the simplified AMPX libraries are successful and promising for high-fidelity multi-physics whole core simulation. Tables 7.0.1 and 7.0.2 provide the information for the ENDF/B-7.0 and 7.1 v4.2m5 MPACT and v5.0m0 SAMPX 51 and 252-g libraries.

Table 7.0.1 v4.2m5 MPACT 51 and 252-g libraries

Description	File name
ENDF/B-7.0 MPACT 51-g library	mpact51g_70_v4.2m5_12062016_sph.fmt
	2016.12.06 11:11
	df001bd3888cff606fdb07a82f442412
ENDF/B-7.0 MPACT 252-g library	mpact252g_70_v4.2m1_09072016_imsl.fmt
	2016.09.08 00:24
	594541a81e3b48cc27ff576c97f32e89
ENDF/B-7.1 MPACT 51-g library	mpact51g_71_v4.2m5_12062016_sph.fmt
	2016.12.06 11:12
	6a7ae1450530d64abb88a072d4a32d36
ENDF/B-7.1 MPACT 252-g library	mpact252g_71_v4.2m1_09072016_imsl.fmt
	2016.09.08 00:28
	ce5ed00bc3ad164964a43b814df52596

Table 7.0.2 v5.0m0 SAMPX 51 and 252-g libraries

Description	File name
ENDF/B-7.0 SAMPX 51-g library	ampxm2s_51g_70_sph01_020602017.fmt
	5.0 mod0 2017.02.06 13:39
	b130a0238e81992f37d84ac64af7ac7e
ENDF/B-7.0 SAMPX 252-g library	ampxm2s_252g_70_sph01_02062017.fmt
	5.0 mod0 2017.02.06 13:43
	9185407dfe5b16796c2555341746a721
ENDF/B-7.1 SAMPX 51-g library	ampxm2s_51g_71_sph01_02062017.fmt
	5.0 mod0 2017.02.06 13:48
	f37b25bf552cd5cc468aade58185ed28
ENDF/B-7.1 SAMPX 252-g library	ampxm2s_252g_71_sph01_02062017.fmt
	5.0 mod0 2017.02.06 13:52
	3aa6e906e503299a95eef16f84eda61f

REFERENCES

[CAS15] "Consortium for Advanced Simulation of Light Water Reactors (CASL)." URL http://www.casl.gov/ (2015).

[Cho02] J. Y. Cho, H. G. Joo, Kang Seog Kim, S. Q. Zee, "Cell Based CMFD Formulation for Acceleration of Whole-core Method of Characteristics Calculation," Journal of the Korean Nuclear Society, 34, No.3, 250-258 (2002)

[Gen17] Cole Gentry, Andrew T. Godfrey, F. Franceschini, " AP1000® Benchmarking of VERA Neutronics Toolset," M&C 2017. (Submitted)

[God14] Andrew T. Godfrey, "VERA Core Physics Benchmark Progression Problem Specifications," CASL-U-2012-0131-004, Rev. 4 (8/29/2014).

[God15] Andrew T. Godfrey et al., "VERA Benchmarking Results for Watts Bar Nuclear Plant Unit 1 Cycles 1-12," CASL-U-2015-0206-000, Rev. 0 (2015).

[Gol62] R. Goldstein and E. R. Cohen, "Theory of Resonance Absorption of Neutrons," *Nucl. Sci. Eng*., **13**, 132 (1962).

[Her13] Bryan R. Herman, Benoit Forget, Kord Smith, "Improved Diffusion Coefficients Generated from Monte Carlo Codes," M&C 2013, Sun Valley, Idaho, May 5–9, 2013.

[Jam99] M. F. James, "Energy Release in Fission of Th-232, U-233, U-234, U-236, Np-237, Pu-238, Pu-240 and Pu-242," J. Nucl. Energy, 23, 1999.

[Joo09] H. G. Joo and et al., "Subgroup Weight Generation Based on Shielded Pin-Cell Cross Section Conservation," *Ann. Nucl. Energ.*, 36, 859 (2009).

[Jun13] Y. S. Jung, C. B. Shim, C. H. Lim, H. G. Joo, "Practical numerical reactor employing direct whole core neutron transport and subchannel thermal/hydraulic solvers," *Ann. Nucl. Energ.*, **62**, 357–374 (2013).

[Kha71] A. Khairallah and J. Recolin, "Calcul de l'autoprotection résonnante dans les cellules complexes par la méthode des sous-groupes," *Proc. Seminar IAEA-SM-154 on Numerical Reactor Calculation*s, pp. 305–317, I.A.E.A., Vienna (1972).

[Kim03] Kang Seog Kim et al., "Monte Carlo Resonance Treatment for the Deterministic Transport Lattice Codes," *Journal of the Korean Nuclear Society*, **35**, No.6, 581–595 (2003).

[Kim12] Kang Seog Kim, Mark L. Williams, "The Method of Characteristics For 2-D Multigroup and Pointwise Transport Calculation in SCALE/CENTRM," PHYSOR 2012, Knoxville, Tennessee, USA, April 15-20, 2012 (2012).

[Kim15] Kang Seog Kim, "Procedure to Generate the MPACT Multigroup Library," CASL-U-2015-1013-000, ORNL/TM-2016/52 (2015).

[Kim16a] Kang Seog Kim, "Specification for the VERA Depletion Benchmark Suite," CASL-U-2015-1014-000, Rev. 0, ORNL/TM-2016/53 (2016).

[Kim16b] Kang Seog Kim et al., "Subgroup Benchmark Calculations for the Intra-Pellet Non-Uniform Temperature Cases," CASL-U-2016-1069-000, Rev. 0, ORNL/TM-2016/153 (2016).

[Kim16c] Kang Seog Kim, Mark L. Williams, "Assessment of the MPACT Resonance Data Generation Procedure," CASL-U-2016-1164-000, ORNL/SR-2016/360 (2016).

[Kim16d] Kang Seog Kim, "Generation of the V4.2m1 AMPX and MPACT 51 and 252-

group Libraries with ENDF/B-VII.0 and ENDF/B-VII.1," CASL-U-2016-1177-000, ORNL/TM-2016/555 (2016).

[Kim16e] Kang Seog Kim, Mark L. Williams, Dorothea Wiarda, "Investigation of Neutron Leakage Conservation Method to Generate ^{1}H Transport Correction Factors," CASL-U-2016-1163-000, ORNL/TM-2016/266 (2016).

[Kim16f] Kang Seog Kim, "SUBGR: A Program to Generate Subgroup Data for the Subgroup Resonance Self-Shielding Calculation," CASL-U-2016-1070-000 (2016).

[Lee11] C. H. Lee and W. S. Yang, "MC^2-3: Multigroup Cross Section Generation Code for Fast Reactor Analysis," ANL-NE-11-41, Argonne National Laboratory (2011).

[Lee09] D. J. Lee, K. Smith, and J. Rhodes, "The Impact of ^{238}U Resonance Elastic Scattering Approximations on Thermal Reactor Doppler Reactivity," *Ann. Nucl. Energy*, 36, 274–280 (2009).

[Les87] F. Leszczynski, "Neutron Resonance Treatment with Details in Space and Energy for Pin Cells and Rod Clusters," *Ann. Nucl. Energy*, 14, 589–601 (1987).

[Liu16a] Yuxuan Liu, "Reaction Rate Analysis for MPACT Cross Section Library Verification," CASL-U-2016-1255-000, Rev. 0 (10/21/2016).

[Liu16b] Y. Liu, et. al., "Runtime Improvements to the Cross Section Calculation in MPACT," CASL Technical Report CASL-X-2016-1105-000, May (2016).

[Mac94] R. E. MacFarlane, D. W. Muir, "The NJOY Nuclear Data Processing System Version 91," LA-12740-M Manual (1994).

[Mpa13] MPACT: User's Manual Version 1.0.0, November 8, 2013.

[Pal17a] Scott Palmtag, "MPACT Library Verification by Comparison of Pincell Calculations to Monte Carlo Results," CASL-U-2016-0281-002, Rev. 2 (2017).

[Pal16b] Scott Palmtag, "MPACT Library Verification by Comparison of Assembly Calculations to Monte Carlo Results," CASL-U-2016-1052-001, Rev. 0 (2017).

[Pal16c] S. Palmtag, "Demonstrate VERA Core Simulator Performance Improvements," CASL Technical Report CASL-X-2016-0XXX-000, August (2016).

[Ryu14] Min Ryu et al., "Incorporation of Anisotropic Scattering in nTRACER," *Transaction of the Korean Nuclear Society Autumn Meeting*, Pyeongchang, Korea, October 30–31, 2014.

[Sca16] "SCALE: A Modular Code System for Performing Standardized Computer Analyses for Licensing Evaluation," ORNL-TM/2005/39, Version 6.2, Oak Ridge National Laboratory, Oak Ridge, Tennessee (2016). (Available from Radiation Safety Information Computational Center at Oak Ridge National Laboratory as CCC-834.)

[Sol01] J. Solis, K. N. Ivanov, B. Sarikaya, A. M. Olsen, and K. W. Hunt, "Boiling Water Reactor Turbine Trip Benchmark Volume I: Final Specifications," NEA/NSC/DOC (2001).

[Sta98] R. J. J. Stamm'ler et al., "The HELIOS Methods," Studsvik Scandpower (1998).

[Tur16] J. Turner et al., “The Virtual Environment for Reactor Applications (VERA): Design and architecture,” *Journal of Computational Physics*, **326**, 544 (2016).

[Wia14] D. Wiarda, S. Goluoglu, M.E. Dunn, N.M. Green and L. M. Petrie, “AMPX-6: A Modular Code System for Processing ENDF/B Evaluations,” in preparation (2014).

[Wil06] Mark L. Williams, M. Asgari, D. F. Hollenbach, CENTRM: A One-Dimensional Neutron Transport Code For Computing Pointwise Energy Spectra, ORNL/TM-2005/39, Version 5.1, Vol. II, Book 4, Sect. F18 (2006).

[Wil12] Mark L. Williams, Kang-Seog Kim, “The Embedded Self-Shielding Method,” *PHYSOR 2012*, Knoxville, Tennessee, USA, April 15–20, 2012 (2012).

Appendix A.1 Sample Input of IRFFACTOR

```
=csas1x  parm=centrm
hetrocells to compute f-factors of U238;
 ft88f001
read composition
'
' ***CELL-1 Composition
'
u-235 7  0  9.39467E-04  293  end
u-238 7  0  2.22624E-02  293  end
o-16  7  0  4.64223E-02  293  end
al-27 8  0  6.02611E-02  293  end
h-1   9  0  1.17827E-04  293  end
o-16  9  0  5.89135E-05  293  end
'
' ***CELL-2 Composition
'
u-235 10  0  9.39467E-04  293  end
u-238 10  0  2.22624E-02  293  end
o-16  10  0  4.64223E-02  293  end
al-27 11  0  6.02611E-02  293  end
h-1   12  0  9.42618E-03  293  end
o-16  12  0  4.71308E-03  293  end
'
' ***CELL-3 Composition
'
u-235 13  0  9.39467E-04  293  end
u-238 13  0  2.22624E-02  293  end
o-16  13  0  4.64223E-02  293  end
al-27 14  0  6.02611E-02  293  end
h-1   15  0  2.35655E-02  293  end
o-16  15  0  1.17827E-02  293  end
'
' ***CELL-4 Composition
'
u-235 16  0  9.39467E-04   293  end
u-238 16  0  2.22624E-02   293  end
o-16  16  0  4.64223E-02   293  end
al-27 17  0  6.02611E-02   293  end
h-1   18  0  3.53482E-02   293  end
o-16  18  0  1.76741E-02   293  end
'
' ***CELL-5 Composition
'
u-235 19  0  9.39467E-04   293  end
u-238 19  0  2.22624E-02   293  end
o-16  19  0  4.64223E-02   293  end
al-27 20  0  6.02611E-02   293  end
h-1   21  0  4.71309E-02   293  end
o-16  21  0  2.35654E-02   293  end
'
' ***CELL-6 Composition
'
u-235 22  0  9.39467E-04   293  end
u-238 22  0  2.22624E-02   293  end
o-16  22  0  4.64223E-02   293  end
al-27 23  0  6.02611E-02   293  end
h-1   24  0  4.71309E-02   293  end
o-16  24  0  2.35654E-02   293  end
'
' ***CELL-7 Composition
'
u-235 25  0  9.39467E-04   293  end
u-238 25  0  2.22624E-02   293  end
o-16  25  0  4.64223E-02   293  end
al-27 26  0  6.02611E-02   293  end
h-1   27  0  4.71309E-02   293  end
o-16  27  0  2.35654E-02   293  end
```

```
'
' ***CELL-8 Composition
'
u-235 28  0  4.69734E-04   293  end
u-238 28  0  1.11312E-02   293  end
o-16  28  0  2.32112E-02   293  end
al-27 29  0  6.02611E-02   293  end
h-1   30  0  4.71309E-02   293  end
o-16  30  0  2.35654E-02   293  end
'
' ***CELL-9 Composition
'
u-235 31  0  2.34867E-04   293  end
u-238 31  0  5.56560E-03   293  end
o-16  31  0  1.16056E-02   293  end
al-27 32  0  6.02611E-02   293  end
h-1   33  0  4.71309E-02   293  end
o-16  33  0  2.35654E-02   293  end
'
' ***CELL-10 Composition
'
u-235 34  0  1.17433E-04   293  end
u-238 34  0  2.78280E-03   293  end
o-16  34  0  5.80279E-03   293  end
al-27 35  0  6.02611E-02   293  end
h-1   36  0  4.71309E-02   293  end
o-16  36  0  2.35654E-02   293  end
'
' ***CELL-11 Composition
'
u-235 37  0  5.87167E-05   293  end
u-238 37  0  1.39140E-03   293  end
o-16  37  0  2.90139E-03   293  end
al-27 38  0  6.02611E-02   293  end
h-1   39  0  4.71309E-02   293  end
o-16  39  0  2.35654E-02   293  end
'
' ***CELL-12 Composition
'
u-235 40  0  2.93583E-05   293  end
u-238 40  0  6.95700E-04   293  end
o-16  40  0  1.45070E-03   293  end
al-27 41  0  6.02611E-02   293  end
h-1   42  0  4.71309E-02   293  end
o-16  42  0  2.35654E-02   293  end
'
' ***CELL-13 Composition
'
u-235 43  0  9.39467E-06   293  end
u-238 43  0  2.22624E-04   293  end
o-16  43  0  4.64223E-04   293  end
al-27 44  0  6.02611E-02   293  end
h-1   45  0  4.71309E-02   293  end
o-16  45  0  2.35654E-02   293  end
'
' ***CELL-14 Composition
'
u-235 49  0  9.39467E-06   293  end
u-238 49  0  2.22624E-05   293  end
o-16  49  0  4.64223E-04   293  end
al-27 50  0  6.02611E-02   293  end
h-1   51  0  4.71309E-02   293  end
o-16  51  0  2.35654E-02   293  end
'
' ***CELL-15 Composition
'
u-235 55  0  9.39467E-06   293  end
u-238 55  0  2.22624E-07   293  end
o-16  55  0  4.64223E-04   293  end
al-27 56  0  6.02611E-02   293  end
h-1   57  0  4.71309E-02   293  end
```

```
o-16  57  0  2.35654E-02   293  end
'
' ***CELL-16 Composition
'
u-235 58  0  9.39467E-06   293  end
u-238 58  0  2.22624E-09   293  end
o-16  58  0  4.64223E-04   293  end
al-27 59  0  6.02611E-02   293  end
h-1   60  0  4.71309E-02   293  end
o-16  60  0  2.35654E-02   293  end
'-------------------------------------------------------
end composition

read celldata
'
' ***CELL-1 Geometry
 latticecell  squarepitch  pitch=1.2620 9 fuelr=0.4025 7
              cladr=0.4759 8   end
 centrmdata  demin=.0001  demax=9.E3 iup=15 npxs=6 end centrmdata
'
' ***CELL-2 Geometry
 latticecell  squarepitch  pitch=1.2620 12 fuelr=0.4025 10
              cladr=0.4759 11   end
 centrmdata  demin=.0001  demax=9.E3 iup=15 npxs=6 end centrmdata
'
' ***CELL-3 Geometry
 latticecell  squarepitch  pitch=1.2620 15 fuelr=0.4025 13
              cladr=0.4759 14   end
 centrmdata  demin=.0001  demax=9.E3 iup=15 npxs=6 end centrmdata
'
' ***CELL-4 Geometry
 latticecell  squarepitch  pitch=1.2620 18  fuelr=0.4025 16
              cladr=0.4759 17   end
 centrmdata  demin=.0001  demax=9.E3 iup=15 npxs=6 end centrmdata
'
' ***CELL-5 Geometry
 latticecell  squarepitch  pitch=1.2620 21  fuelr=0.4025 19
              cladr=0.4759 20   end
 centrmdata  demin=.0001  demax=9.E3 iup=15 npxs=6 end centrmdata
'
' ***CELL-6 Geometry
 latticecell  squarepitch  pitch=1.5728 24  fuelr=0.4025 22
              cladr=0.4759 23   end
 centrmdata  demin=.0001  demax=9.E3 iup=15 npxs=6 end centrmdata
'
' ***CELL-7 Geometry
 latticecell  squarepitch  pitch=2.2621 27  fuelr=0.4025 25
              cladr=0.4759 26   end
 centrmdata  demin=.0001  demax=9.E3 iup=15 npxs=6 end centrmdata
'
' ***CELL-8 Geometry
 latticecell  squarepitch  pitch=2.2621 30  fuelr=0.4025 28
              cladr=0.4759 29   end
 centrmdata  demin=.0001  demax=9.E3 iup=15 npxs=6 end centrmdata
'
' ***CELL-9 Geometry
 latticecell  squarepitch  pitch=2.2621 33  fuelr=0.4025 31
              cladr=0.4759 32   end
 centrmdata  demin=.0001  demax=9.E3 iup=15 npxs=6 end centrmdata
'
' ***CELL-10 Geometry
 latticecell  squarepitch  pitch=2.2621 36 fuelr=0.4025 34
              cladr=0.4759 35   end
 centrmdata  demin=.0001  demax=9.E3 iup=15 npxs=6 end centrmdata
'
' ***CELL-11 Geometry
 latticecell  squarepitch  pitch=2.2621 39  fuelr=0.4025 37
              cladr=0.4759 38   end
 centrmdata  demin=.0001  demax=9.E3 iup=15 npxs=6 end centrmdata
'
' ***CELL-12 Geometry
```

```
 latticecell  squarepitch  pitch=2.2621 42  fuelr=0.4025 40
             cladr=0.4759 41   end
 centrmdata  demin=.0001  demax=9.E3 iup=15 npxs=6 end centrmdata
'
' ***CELL-13 Geometry
 latticecell  squarepitch  pitch=2.2621 45  fuelr=0.4025 43
             cladr=0.4759 44   end
 centrmdata  demin=.0001  demax=9.E3 iup=15 npxs=6 end centrmdata
'
' ***CELL-14 Geometry
 latticecell  squarepitch  pitch=2.2621 51  fuelr=0.4025 49
             cladr=0.4759 50   end
 centrmdata  demin=.0001  demax=9.E3 iup=15 npxs=6 end centrmdata
'
' ***CELL-15 Geometry
 latticecell  squarepitch  pitch=2.2621 57  fuelr=0.4025 55
             cladr=0.4759 56   end
 centrmdata  demin=.0001  demax=9.E3 iup=15 npxs=6 end centrmdata
'
' ***CELL-16 Geometry
 latticecell  squarepitch  pitch=2.2621 60  fuelr=0.4025 58
             cladr=0.4759 59   end
 centrmdata  demin=.0001  demax=9.E3 iup=15 npxs=6 end centrmdata
'-------------------------------------------------------
end celldata

end
```

Appendix A.2 Transient Data from ENDF/B-7.0 and ENDF/B-7.1

[ENDF/B-7.0]

```
   21    6
         90232  2.417105E+00
 1.240000E-02  3.340000E-02  1.210000E-01  3.210000E-01  1.210000E+00  3.290000E+00
 8.237550E-04  2.839532E-03  3.391569E-03  9.961879E-03  3.760367E-03  1.827437E-03
         91231  2.429466E+00
 1.240000E-02  3.340000E-02  1.210000E-01  3.210000E-01  1.210000E+00  3.290000E+00
 3.772028E-04  1.018876E-03  7.348728E-04  1.774840E-03  4.798565E-04  1.831329E-04
         91233  2.429815E+00
 1.240000E-02  3.340000E-02  1.210000E-01  3.210000E-01  1.210000E+00  3.290000E+00
 7.746643E-04  2.092295E-03  1.509164E-03  3.645136E-03  9.855432E-04  3.761569E-04
         92233  2.500074E+00
 1.247938E-02  3.227449E-02  1.046448E-01  2.941518E-01  1.242443E+00  1.022323E+01
 2.567975E-04  7.701037E-04  5.537597E-04  1.142208E-03  2.146458E-04  2.239787E-05
         92234  2.633240E+00
 1.248240E-02  3.129530E-02  1.074630E-01  3.032230E-01  1.288730E+00  1.044220E+01
 2.754770E-04  1.165225E-03  8.999964E-04  2.034102E-03  4.624642E-04  6.164186E-05
         92235  2.438879E+00
 1.249056E-02  3.182406E-02  1.093753E-01  3.169898E-01  1.353983E+00  8.636377E+00
 2.183402E-04  1.136937E-03  1.102438E-03  3.142815E-03  9.126013E-04  3.225451E-04
         92236  2.585205E+00
 1.248999E-02  3.068560E-02  1.091980E-01  3.224705E-01  1.378583E+00  1.021014E+01
 2.294104E-04  1.726554E-03  1.473179E-03  3.893188E-03  1.382420E-03  2.693897E-04
         92237  2.556079E+00
 1.249577E-02  3.037978E-02  1.068975E-01  3.240317E-01  1.334253E+00  9.544175E+00
 2.081865E-04  2.419830E-03  2.019126E-03  6.103966E-03  2.421639E-03  5.043196E-04
         92238  2.788314E+00
 1.249423E-02  3.025520E-02  1.159376E-01  3.414764E-01  1.318630E+00  9.979027E+00
 1.631869E-04  1.811873E-03  2.016816E-03  7.130047E-03  3.684767E-03  9.734561E-04
         93237  2.943373E+00
 1.248610E-02  3.077587E-02  1.065464E-01  3.139911E-01  1.334211E+00  1.050869E+01
 1.169523E-04  7.177156E-04  6.106869E-04  1.677948E-03  4.688961E-04  8.045746E-05
         94238  2.992942E+00
 1.332500E-02  3.117100E-02  1.161500E-01  2.888400E-01  8.561400E-01  2.713800E+00
 5.261947E-05  3.337788E-04  2.202819E-04  4.974348E-04  2.221220E-04  7.038188E-05
         94239  2.867711E+00
 1.248110E-02  2.994667E-02  1.071553E-01  3.176193E-01  1.352380E+00  1.069116E+01
 7.441243E-05  6.029267E-04  4.208394E-04  8.788662E-04  2.338068E-04  3.832867E-05
         94240  3.081800E+00
 1.332900E-02  3.051000E-02  1.151600E-01  2.974000E-01  8.476600E-01  2.879600E+00
 9.336029E-05  7.385726E-04  4.404519E-04  9.638943E-04  5.243305E-04  1.597601E-04
         94241  2.946479E+00
 1.359900E-02  2.996600E-02  1.167300E-01  3.069100E-01  8.701000E-01  3.002800E+00
 9.923741E-05  1.233243E-03  7.840723E-04  1.920227E-03  1.086294E-03  3.750161E-04
         94242  3.146448E+00
 1.360300E-02  3.023800E-02  1.154300E-01  3.041900E-01  8.272100E-01  3.137200E+00
 1.229591E-04  1.449077E-03  7.864419E-04  2.042159E-03  1.412084E-03  4.483058E-04
         95241  3.236158E+00
 1.333800E-02  3.079800E-02  1.130500E-01  2.867700E-01  8.653600E-01  2.643000E+00
 4.687282E-05  3.351367E-04  2.062589E-04  4.438472E-04  2.274633E-04  5.988720E-05
         95243  3.564782E+00
 1.349900E-02  2.975900E-02  1.137700E-01  2.985900E-01  8.820200E-01  2.811100E+00
 5.213651E-05  6.568510E-04  3.428585E-04  7.020686E-04  3.694160E-04  1.071179E-04
         96242  3.753388E+00
 1.295600E-02  3.124500E-02  1.129100E-01  2.783400E-01  8.710400E-01  2.196900E+00
 2.760101E-05  1.027275E-04  5.117072E-05  1.024804E-04  6.385763E-05  1.359061E-05
         96245  3.597515E+00
 1.340000E-02  3.070000E-02  1.130000E-01  3.001000E-01  8.340000E-01  2.768600E+00
 3.942668E-05  3.180151E-04  2.974124E-04  6.592391E-04  3.654310E-04  9.948328E-05
         98249  3.888388E+00
 1.351700E-02  2.945000E-02  1.053200E-01  2.929800E-01  8.474900E-01  2.469800E+00
 1.709062E-05  2.721421E-04  9.365231E-05  1.804290E-04  1.120952E-04  1.896568E-05
         98251  4.140665E+00
 1.569700E-02  2.883000E-02  1.076900E-01  3.245800E-01  8.837100E-01  2.631400E+00
 9.953225E-06  6.522987E-04  3.156976E-04  4.898075E-04  3.069656E-04  4.397731E-05
```

[ENDF/B-7.1]

```
 21    6
     90232  2.411777E+00
1.240000E-02  3.340000E-02  1.210000E-01  3.210000E-01  1.210000E+00  3.290000E+00
8.255745E-04  2.845804E-03  3.399061E-03  9.983884E-03  3.768673E-03  1.831473E-03
       91231  2.429466E+00
1.240000E-02  3.340000E-02  1.210000E-01  3.210000E-01  1.210000E+00  3.290000E+00
3.772028E-04  1.018876E-03  7.348728E-04  1.774840E-03  4.798565E-04  1.831329E-04
       91233  2.429815E+00
1.240000E-02  3.340000E-02  1.210000E-01  3.210000E-01  1.210000E+00  3.290000E+00
7.746643E-04  2.092295E-03  1.509164E-03  3.645136E-03  9.855432E-04  3.761569E-04
       92233  2.500071E+00
1.291100E-02  3.473800E-02  1.192800E-01  2.861700E-01  7.877000E-01  2.441700E+00
2.543527E-04  6.785117E-04  5.272808E-04  1.040570E-03  3.381606E-04  1.210402E-04
       92234  2.633240E+00
1.308200E-02  3.368400E-02  1.209500E-01  2.951700E-01  8.136300E-01  2.572100E+00
2.692696E-04  9.621251E-04  8.833544E-04  1.899366E-03  6.487422E-04  2.360508E-04
       92235  2.438879E+00
1.333600E-02  3.273900E-02  1.207800E-01  3.027800E-01  8.494900E-01  2.853000E+00
2.390653E-04  1.234844E-03  1.178981E-03  2.644606E-03  1.084020E-03  4.539337E-04
       92236  2.585157E+00
1.338000E-02  3.215500E-02  1.201500E-01  3.112900E-01  8.793600E-01  2.840500E+00
2.705910E-04  1.545577E-03  1.452846E-03  3.447380E-03  1.593054E-03  6.648573E-04
       92237  2.473125E+00
1.376200E-02  3.159100E-02  1.210700E-01  3.162200E-01  9.073100E-01  3.036800E+00
2.521976E-04  2.088010E-03  2.042045E-03  5.462226E-03  2.961695E-03  1.329655E-03
       92238  2.788314E+00
1.363000E-02  3.133400E-02  1.233400E-01  3.237300E-01  9.059700E-01  3.048700E+00
2.199428E-04  1.779951E-03  2.067630E-03  6.077609E-03  4.008024E-03  1.626984E-03
       93237  2.943373E+00
1.325200E-02  3.160300E-02  1.167900E-01  3.006500E-01  8.666900E-01  2.760000E+00
1.468441E-04  7.939564E-04  5.722121E-04  1.334282E-03  6.091536E-04  2.162096E-04
       94238  3.016309E+00
1.330000E-02  3.120000E-02  1.162000E-01  2.888000E-01  8.561000E-01  2.713800E+00
5.883199E-05  3.731866E-04  2.462895E-04  5.561645E-04  2.483469E-04  7.869152E-05
       94239  2.867711E+00
1.327100E-02  3.088100E-02  1.133700E-01  2.925000E-01  8.574900E-01  2.729700E+00
8.165795E-05  5.317942E-04  4.024443E-04  7.347421E-04  3.827096E-04  1.158321E-04
       94240  3.115728E+00
1.332900E-02  3.051000E-02  1.151600E-01  2.974000E-01  8.476600E-01  2.879600E+00
9.234370E-05  7.305303E-04  4.356558E-04  9.533985E-04  5.186211E-04  1.580205E-04
       94241  2.946479E+00
1.359900E-02  2.996600E-02  1.167300E-01  3.069100E-01  8.701000E-01  3.002800E+00
9.923741E-05  1.233243E-03  7.840723E-04  1.920227E-03  1.086294E-03  3.750161E-04
       94242  3.186877E+00
1.360000E-02  3.020000E-02  1.154000E-01  3.042000E-01  8.272000E-01  3.137200E+00
9.428473E-05  1.111148E-03  6.030415E-04  1.565922E-03  1.082782E-03  3.437596E-04
       95241  3.234345E+00
1.333800E-02  3.079800E-02  1.130500E-01  2.867700E-01  8.653600E-01  2.643000E+00
4.689909E-05  3.353245E-04  2.063745E-04  4.440959E-04  2.275907E-04  5.992077E-05
       95243  3.565905E+00
1.349900E-02  2.975900E-02  1.137700E-01  2.985900E-01  8.820200E-01  2.811100E+00
5.212010E-05  6.566443E-04  3.427506E-04  7.018477E-04  3.692998E-04  1.070842E-04
       96242  3.604296E+00
1.300000E-02  3.120000E-02  1.129000E-01  2.783000E-01  8.710000E-01  2.196900E+00
4.474185E-05  1.669628E-04  8.320904E-05  1.661650E-04  1.034226E-04  2.202095E-05
       96245  3.597681E+00
1.340000E-02  3.070000E-02  1.130000E-01  3.001000E-01  8.340000E-01  2.768600E+00
3.993004E-05  3.220746E-04  3.012094E-04  6.676537E-04  3.700950E-04  1.007533E-04
       98249  4.064592E+00
1.350000E-02  2.940000E-02  1.053000E-01  2.930000E-01  8.475000E-01  2.469800E+00
1.695527E-05  2.699868E-04  9.291064E-05  1.790002E-04  1.112075E-04  1.881548E-05
       98251  4.106293E+00
1.570000E-02  2.880000E-02  1.077000E-01  3.246000E-01  8.837000E-01  2.631400E+00
7.863301E-06  5.153326E-04  2.494091E-04  3.869603E-04  2.425106E-04  3.474318E-05
```

Appendix A.3 Recoverable Energy per Fission

Nuclide	Recoverable energy (w-s)			Recoverable energy (MeV)		
	ENDF/B-7.0	ENDF/B-7.1	SERPENT-7.0	ENDF/B-7.0	ENDF/B-7.1	SERPENT-7.0
90230	3.24352E-11	3.08011E-11	3.188496E-11	202.44	192.24	199.01
90232	3.22079E-11	3.22079E-11	3.152922E-11	201.02	201.02	196.79
91231	3.22345E-11	3.13618E-11	3.345809E-11	201.19	195.74	208.83
91233	3.27020E-11	3.18390E-11	3.345809E-11	204.11	198.72	208.83
92232	3.22345E-11	3.12001E-11	3.161771E-11	201.19	194.73	197.34
92233	3.20712E-11	3.20712E-11	3.195916E-11	200.17	200.17	199.47
92234	3.26107E-11	3.26107E-11	3.209299E-11	203.54	203.54	200.31
92235	3.24142E-11	3.24017E-11	3.236792E-11	202.31	202.23	202.02
92236	3.29604E-11	3.29604E-11	3.253631E-11	205.72	205.72	203.07
92237	3.30896E-11	3.17375E-11	3.011228E-11	206.53	198.09	187.94
92238	3.39762E-11	3.39368E-11	3.312885E-11	212.06	211.82	206.77
92240	3.33592E-11	3.33592E-11	3.312350E-11	208.21	208.21	206.74
93237	3.36975E-11	3.36975E-11	3.285082E-11	210.32	210.32	205.04
93238	3.34842E-11	3.35984E-11	3.345791E-11	208.99	209.70	208.83
93239	3.40989E-11	3.26536E-11	3.178517E-11	212.83	203.81	198.39
94236	3.26352E-11	3.34433E-11	3.262163E-11	203.69	208.73	203.61
94237	3.30131E-11	3.38885E-11	3.277219E-11	206.05	211.51	204.55
94238	3.36489E-11	3.41258E-11	3.301977E-11	210.02	212.99	206.09
94239	3.36876E-11	3.36970E-11	3.326465E-11	210.26	210.32	207.62
94240	3.42944E-11	3.42944E-11	3.336942E-11	214.05	214.05	208.27
94241	3.42699E-11	3.42699E-11	3.378934E-11	213.89	213.89	210.89
94242	3.47382E-11	3.49302E-11	3.372240E-11	216.82	218.02	210.48
94244	3.41266E-11	3.35567E-11	3.393486E-11	213.00	209.44	211.80
95241	3.48153E-11	3.48153E-11	3.378599E-11	217.30	217.30	210.87
95242	3.45085E-11	3.51714E-11	3.345809E-11	215.38	219.52	208.83
95243	3.56147E-11	3.56147E-11	3.406366E-11	222.29	222.29	212.61
95342	3.56147E-11	3.56147E-11	3.345809E-11	222.29	222.29	208.83
96241	3.40465E-11	3.51880E-11	3.385121E-11	212.50	219.62	211.28
96242	3.42433E-11	3.43892E-11	3.388467E-11	213.73	214.64	211.49
96243	3.41026E-11	3.43147E-11	3.345809E-11	212.85	214.17	208.83
96244	3.42189E-11	3.51043E-11	3.345809E-11	213.58	219.10	208.83
96245	3.43622E-11	3.45060E-11	3.345809E-11	214.47	215.37	208.83
96246	3.47142E-11	3.54721E-11	3.345809E-11	216.67	221.40	208.83
96247	3.48348E-11	3.51698E-11	3.345809E-11	217.42	219.51	208.83
96248	3.50703E-11	3.55936E-11	3.492020E-11	218.89	222.16	217.95
97249	3.50703E-11	3.60559E-11				
98249	3.50703E-11	3.55494E-11				
98250	3.50703E-11	3.68134E-11				
98251	3.50703E-11	3.58147E-11				
98252	3.50703E-11	3.68984E-11				

Appendix B.1 Nuclides of the ENDF/B-7.0 and 7.1 MPACT 51 and 252-g Libraries

1	40091	9.090563E+01	ZR-91	101	40092	9.190501E+01	ZR-92	201	36585	8.491254E+01	KR-85
2	40096	9.590830E+01	ZR-96	102	40094	9.390630E+01	ZR-94	202	36586	8.591062E+01	KR-86
3	42595	9.490589E+01	MO-95	103	41093	9.290319E+01	NB-93	203	38589	8.890776E+01	SR-89
4	43599	9.890767E+01	TC-99	104	42000	9.593756E+01	MO-NAT	204	38590	8.990776E+01	SR-90
5	45103	1.029050E+02	RH-103	105	44601	1.009058E+02	RU-101	205	39589	8.890585E+01	Y-89
6	46608	1.079039E+02	PD-108	106	45603	1.029040E+02	RH-103	206	39590	8.990715E+01	Y-90
7	47107	1.069054E+02	AG-107	107	45605	1.049112E+02	RH-105	207	39591	9.090734E+01	Y-91
8	47109	1.089046E+02	AG-109	108	46605	1.049052E+02	PD-105	208	40591	9.090563E+01	ZR-91
9	49113	1.129039E+02	IN-113	109	46607	1.069054E+02	PD-107	209	40593	9.290642E+01	ZR-93
10	49115	1.149041E+02	IN-115	110	47609	1.089046E+02	AG-109	210	40595	9.490801E+01	ZR-95
11	54631	1.309056E+02	XE-131	111	48000	1.124111E+02	CD-NAT	211	40596	9.590830E+01	ZR-96
12	55633	1.329057E+02	CS-133	112	48110	1.099031E+02	CD-110	212	41595	9.490680E+01	NB-95
13	62152	1.519201E+02	SM-152	113	48111	1.109037E+02	CD-111	213	42095	9.490589E+01	MO-95
14	63151	1.509164E+02	EU-151	114	48112	1.119033E+02	CD-112	214	42596	9.590467E+01	MO-96
15	63152	1.519221E+02	EU-152	115	48113	1.128999E+02	CD-113	215	42597	9.690597E+01	MO-97
16	63153	1.529217E+02	EU-153	116	48114	1.139035E+02	CD-114	216	42598	9.790536E+01	MO-98
17	63154	1.539223E+02	EU-154	117	49000	1.148185E+02	IN-NAT	217	42599	9.890767E+01	MO-99
18	63155	1.549209E+02	EU-155	118	49615	1.149041E+02	IN-115	218	42600	9.990726E+01	MO-100
19	64155	1.549229E+02	GD-155	119	50000	1.187101E+02	SN-NAT	219	44600	9.990413E+01	RU-100
20	64156	1.559225E+02	GD-156	120	50112	1.119043E+02	SN-112	220	44602	1.019054E+02	RU-102
21	64157	1.569241E+02	GD-157	121	50114	1.139025E+02	SN-114	221	44603	1.029040E+02	RU-103
22	64158	1.579237E+02	GD-158	122	50115	1.149031E+02	SN-115	222	44604	1.039026E+02	RU-104
23	66160	1.599248E+02	DY-160	123	50116	1.159017E+02	SN-116	223	44605	1.049112E+02	RU-105
24	66161	1.609264E+02	DY-161	124	50117	1.169033E+02	SN-117	224	44606	1.059068E+02	RU-106
25	66162	1.619270E+02	DY-162	125	50118	1.179018E+02	SN-118	225	46604	1.039040E+02	PD-104
26	66163	1.629286E+02	DY-163	126	50119	1.189034E+02	SN-119	226	46606	1.059035E+02	PD-106
27	66164	1.639292E+02	DY-164	127	50120	1.199020E+02	SN-120	227	47710	1.099061E+02	AG-110M
28	68166	1.659304E+02	ER-166	128	50122	1.219032E+02	SN-122	228	47611	1.109057E+02	AG-111
29	68167	1.669320E+02	ER-167	129	50124	1.239054E+02	SN-124	229	48610	1.099031E+02	CD-110
30	72176	1.759414E+02	HF-176	130	51000	1.217632E+02	SB-NAT	230	48611	1.109037E+02	CD-111
31	72177	1.769430E+02	HF-177	131	51121	1.209087E+02	SB-121	231	48613	1.128999E+02	CD-113
32	72178	1.779436E+02	HF-178	132	51123	1.229058E+02	SB-123	232	50125	1.249080E+02	SN-125
33	72179	1.789462E+02	HF-179	133	54634	1.339104E+02	XE-134	233	51621	1.209087E+02	SB-121
34	72180	1.799468E+02	HF-180	134	60643	1.429097E+02	ND-143	234	51625	1.249050E+02	SB-125
35	74182	1.819531E+02	W-182	135	60645	1.449129E+02	ND-145	235	51627	1.269069E+02	SB-127
36	74183	1.829517E+02	W-183	136	61647	1.469151E+02	PM-147	236	52727	1.269052E+02	TE-127M
37	74184	1.839502E+02	W-184	137	61748	1.479207E+02	PM-148M	237	52729	1.289074E+02	TE-129M
38	74186	1.859575E+02	W-186	138	62153	1.529217E+02	SM-153	238	52632	1.319082E+02	TE-132
39	90232	2.320383E+02	TH-232	139	62647	1.469151E+02	SM-147	239	53627	1.269045E+02	I-127
40	92233	2.330396E+02	U-233	140	62649	1.489173E+02	SM-149	240	53629	1.289054E+02	I-129
41	92235	2.350439E+02	U-235	141	62650	1.499169E+02	SM-150	241	53631	1.309056E+02	I-131
42	92236	2.360456E+02	U-236	142	62651	1.509195E+02	SM-151	242	53635	1.349089E+02	I-135
43	92238	2.380508E+02	U-238	143	62652	1.519201E+02	SM-152	243	54628	1.279027E+02	XE-128
44	94238	2.380495E+02	PU-238	144	63156	1.559255E+02	EU-156	244	54630	1.299039E+02	XE-130
45	94239	2.390522E+02	PU-239	145	63157	1.569251E+02	EU-157	245	54632	1.319031E+02	XE-132
46	94240	2.400542E+02	PU-240	146	63653	1.529217E+02	EU-153	246	54633	1.329057E+02	XE-133
47	94241	2.410487E+02	PU-241	147	63654	1.539223E+02	EU-154	247	54635	1.349069E+02	XE-135
48	94242	2.420584E+02	PU-242	148	63655	1.549209E+02	EU-155	248	54636	1.359075E+02	XE-136
49	95241	2.410568E+02	AM-241	149	64152	1.519201E+02	GD-152	249	55634	1.339073E+02	CS-134
50	1001	1.007830E+00	H-1	150	64154	1.539213E+02	GD-154	250	55635	1.349059E+02	CS-135
51	1002	2.014100E+00	H-2	151	64160	1.599269E+02	GD-160	251	55636	1.359065E+02	CS-136
52	1006	1.007830E+00	H-1CH2	152	64655	1.549229E+02	GD-155	252	55637	1.369071E+02	CS-137
53	1040	1.007830E+00	H-1ZRH	153	64656	1.559225E+02	GD-156	253	56634	1.339043E+02	BA-134
54	2004	4.002600E+00	HE-4	154	64657	1.569241E+02	GD-157	254	56637	1.369061E+02	BA-137
55	3006	6.015070E+00	LI-6	155	64658	1.579237E+02	GD-158	255	56640	1.399099E+02	BA-140
56	3007	7.016000E+00	LI-7	156	68162	1.619291E+02	ER-162	256	57639	1.389033E+02	LA-139
57	4009	9.012200E+00	BE-9	157	68164	1.639292E+02	ER-164	257	57640	1.399099E+02	LA-140
58	5000	1.081101E+01	B-NAT	158	68168	1.679296E+02	ER-168	258	58640	1.399049E+02	CE-140
59	5010	1.001294E+01	B-10	159	68170	1.699358E+02	ER-170	259	58641	1.409105E+02	CE-141
60	5011	1.100928E+01	B-11	160	71176	1.759414E+02	LU-176	260	58642	1.419091E+02	CE-142
61	6000	1.200110E+01	C-NAT	161	72174	1.739402E+02	HF-174	261	58643	1.429127E+02	CE-143
62	6001	1.200110E+01	C-GRAPH	162	73181	1.809545E+02	TA-181	262	58644	1.439143E+02	CE-144
63	7014	1.400307E+01	N-14	163	73182	1.819501E+02	TA-182	263	59641	1.409075E+02	PR-141
64	8001	1.599730E+01	O-UO2	164	74000	1.838464E+02	W-NAT	264	59643	1.429107E+02	PR-143
65	8016	1.599491E+01	O-16	165	79197	1.969660E+02	AU-197	265	60642	1.419081E+02	ND-142
66	9019	1.899820E+01	F-19	166	82206	2.059744E+02	PB-206	266	60644	1.439103E+02	ND-144
67	11023	2.298949E+01	NA-23	167	82207	2.069759E+02	PB-207	267	60646	1.459135E+02	ND-146
68	12000	2.430505E+01	MG-NAT	168	82208	2.079766E+02	PB-208	268	60647	1.469161E+02	ND-147
69	13027	2.698154E+01	AL-27	169	83209	2.089803E+02	BI-209	269	60648	1.479167E+02	ND-148
70	14000	2.808590E+01	SI-NAT	170	90230	2.300361E+02	TH-230	270	60650	1.499209E+02	ND-150
71	15031	3.097408E+01	P-31	171	91231	2.310357E+02	PA-231	271	61648	1.479167E+02	PM-148
72	16000	3.206429E+01	S-NAT	172	91233	2.330399E+02	PA-233	272	61649	1.489183E+02	PM-149
73	17000	3.545273E+01	CL-NAT	173	92232	2.320371E+02	U-232	273	61651	1.509215E+02	PM-151
74	19000	3.909858E+01	K-NAT	174	92234	2.340409E+02	U-234	274	62648	1.479147E+02	SM-148
75	20000	4.007803E+01	CA-NAT	175	92237	2.370488E+02	U-237	275	62653	1.529217E+02	SM-153
76	22000	4.789328E+01	TI-NAT	176	93237	2.370482E+02	NP-237	276	62654	1.539223E+02	SM-154
77	23000	5.094162E+01	V-NAT	177	93238	2.380510E+02	NP-238	277	63651	1.509164E+02	EU-151
78	24000	5.199589E+01	CR-NAT	178	93239	2.390526E+02	NP-239	278	63656	1.559255E+02	EU-156

79	24050	4.994606E+01	CR-50	179	94236	2.360458E+02	PU-236	279	63657	1.569251E+02	EU-157
80	24052	5.194019E+01	CR-52	180	95242	2.420594E+02	AM-242	280	64654	1.539213E+02	GD-154
81	24053	5.294079E+01	CR-53	181	95342	2.420594E+02	AM-242M	281	64660	1.599269E+02	GD-160
82	24054	5.393937E+01	CR-54	182	95243	2.430614E+02	AM-243	282	65159	1.589253E+02	TB-159
83	25055	5.493805E+01	MN-55	183	96242	2.420584E+02	CM-242	283	65160	1.599269E+02	TB-160
84	26000	5.584473E+01	FE-NAT	184	96243	2.430610E+02	CM-243	284	65161	1.609276E+02	TB-161
85	26054	5.393937E+01	FE-54	185	96244	2.440626E+02	CM-244	285	65659	1.589253E+02	TB-159
86	26056	5.593451E+01	FE-56	186	96245	2.450652E+02	CM-245	286	65660	1.599269E+02	TB-160
87	26057	5.693510E+01	FE-57	187	96246	2.460668E+02	CM-246	287	65661	1.609276E+02	TB-161
88	26058	5.793368E+01	FE-58	188	96247	2.470705E+02	CM-247	288	66660	1.599248E+02	DY-160
89	27059	5.893317E+01	CO-59	189	96248	2.480721E+02	CM-248	289	66661	1.609264E+02	DY-161
90	28000	5.869361E+01	NI-NAT	190	97249	2.490797E+02	BK-249	290	66662	1.619270E+02	DY-162
91	28058	5.793570E+01	NI-58	191	98249	2.490797E+02	CF-249	291	66663	1.629286E+02	DY-163
92	28060	5.993084E+01	NI-60	192	98250	2.500763E+02	CF-250	292	66664	1.639292E+02	DY-164
93	28061	6.093143E+01	NI-61	193	98251	2.510799E+02	CF-251	293	67165	1.649298E+02	HO-165
94	28062	6.192799E+01	NI-62	194	98252	2.520815E+02	CF-252	294	67665	1.649298E+02	HO-165
95	28064	6.392818E+01	NI-64	195	1003	3.015500E+00	T-3	295	77191	1.909605E+02	IR-191
96	29063	6.292960E+01	CU-63	196	2003	3.014930E+00	HE-3	296	77193	1.929626E+02	IR-193
97	29065	6.492776E+01	CU-65	197	35581	8.091631E+01	BR-81	297	91232	2.320383E+02	PA-232
98	40000	9.122365E+01	ZR-NAT	198	36582	8.191348E+01	KR-82	298	91234	2.340433E+02	PA-234
99	40001	9.122365E+01	ZR-ZRH2	199	36583	8.291428E+01	KR-83				
100	40090	8.990473E+01	ZR-90	200	36584	8.391154E+01	KR-84				

Appendix B.2 Structure of the MPACT MG library

[Structure]

```
%VERSION:
    [iversion, adte]
%DIM:
    [nog, nofg, norg, nchi, nelt, nelr, nres, nyld, nsubg, nflxhel]
%GRP:
    [enbhel(ig)]ig=1,nog
%CHI:
    [chix(ig)]ig=1,nog
%DIR:
    do i=1,nelt
        [ix, nid, amass, ityp, ifpy, ichi, inmn, ntemp, nrtemp, np1temp, npot, aid]
    enddo
%NUC:  [i, nid, amass, ityp, ifpy, ichi, inmn, ntemp, nrtemp, np1temp, npot, aid]
    ["TP1+"]
    [temp(it)] it=1, ntemp
    ["XSD+"]
    do ig=1,nog
          do it=1,ntemp
              [ig, it, siga, {sigf, signf, sigtr, sigs,  ib,ie, sm(jg)jg= ib, ie}]
          enddo
    enddo
    [" SP1+"]
          do ig=1,nog
              do it=1,np1temp
                  [ig, it, sigsp1(ig,it), ib, ie, smp1(jg,it)jg= ib, ie]
              enddo
          enddo
    ["POT+"]
     {[lamsigp(ig)] ig=igresb,igrese
     [sigsres(ig)] ig=igresb,igrese
     [nu(ig)] ig=igresb,igrese
    [" TP2+"]
        [rtemp(it)] it=1,nrtemp
    [" XS0+"]
        [sigpot(ip)] ip=1,npot
    [" RIA+"]
        do ig=igresb,igrese
            do it=1,ldiso(i)%nrtemp
                [ig, it, ria(ip,it,ig)ip=1, npot]
            enddo
        enddo
    ["RIS+"]
     do ig=igresb,igrese
            do it=1,ldiso(i)%nrtemp
                [ig, it, ris(ip,it,ig)ip=1, npot]
            enddo
    enddo
    ["RNF+"]
        do ig=igresb,igrese
            do it=1,ldiso(i)%nrtemp
                [ig, it, rinf(ip,it,ig)ip=1, npot]
            enddo
```

```
 enddo
["SA7+"]
 do ig=igresb,igrese
        [ig, sgsa(ix,ig)ix=1,nsubg]
 enddo
 do ig=igresb,igrese
        do it=1,ldiso(i)%nrtemp
             [ig, it, sgwa(ix,it,ig)ix=1,nsubg]
        enddo
 enddo
["SF7+"]
 do ig=igresb,igrese
        [ig, sgsnf(ix,ig)ix=1,nsubg]
 enddo
 do ig=igresb,igrese
        do it=1,ldiso(i)%nrtemp
             [ig, it, sgwnf(ix,it,ig)ix=1,nsubg]
        enddo
 enddo
["SA4+"]
 do ig=igresb,igrese
         [ig, sgsafsp(ix,ig)ix=1,nflx]
 enddo
 do ig=igresb,igrese+1
        do it=1,ldiso(i)%nrtemp
             [ig, it, sgwafsp(ix,it,ig)ix=1,nflx]
        enddo
 enddo
["CHI+"]
 [chi(ig)] ig=1,nog
["CHI-"]
 [chid(ig)] ig=1,nog
[" FIS+"]
 [kappa, kappa0]
 [beta(ib)] ib=0,6
 [dcybeta(ib)] ib=1,6
 [yield(iy)] iy=1,nyld
[" DCY+"]
 [ldiso(i)%dcy]
[" TP3+"]
    [ldiso(i)%p1temp(it)] it=1,np1temp
[" SP2+"]
      do ig=1,nog
          do it=1,np1temp
              [ig, it, sigsp1(ig,it), ib, ie, smp2(jg,it)jg= ib, ie]
          enddo
      enddo
[" SP3+"]
      do ig=1,nog
          do it=1,np1temp
              [ig, it, sigsp1(ig,it), ib, ie, smp3(jg,it)jg= ib, ie]
          enddo
      enddo
[" N2N+"]
    [ldiso(i)%sign2n(ig)]ig=1,nog
[" N3N+"]
    [ldiso(i)%sign3n(ig)]ig=1,nog
```

```
**Repeat %NUC: for nelt nuclides.
%END:
```

Variables	Type	Description
nog	I	The number of energy groups
nofg	I	The number of fast energy groups
norg	I	The number of resonance energy groups
nchi	I	The number of energy groups w/ fission spectra
nelt	I	The total number of nuclides
nelr	I	The number of nuclides w/ full xs sets
nyld	I	The number of fission product nuclides
nres	I	The number of resonant nuclides
nsubg	I	The number of subgroup levels
nflx	I	The number of coarse subgroup levels
igresb	I	Starting group for resonance (=nofg+1)
igrese	I	Ending group for resonance (=nofg+norg)
u(ig)	R	Lethargy energy group boundaries (ig=1,nog)
enb(ig)	R	Energy group boundaries (ig=1,nog)
chix(ig)	R	Common fission spectrum (ig=1,nog)
sm(p?)(i,j)%	T	[scatmat] P0~p3 scattering matrix
%ib	I	Stating energy group (in)
%ie	I	Ending energy group (in)
%ioutsb	I	Stating energy group (out)
%ioutse	I	Ending energy group (out)
%from(k)	R	Scattering matrix (k=%ib,%ie)
ldiso(i)%	T	[libdata] Nuclidewise multigroup data (i=1,nelt)
%nid	I	Nuclide id.
%ityp	I	Indicator for data type 0 non depletable >0 depletable (w/ decay constant) 2 ri-a (fissionable w/ kappa, beta, fpy) 3 ri-a & ri-nf (same as above)
%ichi	I	Indicator for fission spectrum (0/>0 : no/yes)
%ifpy	I	Indicator & ordering no. for f.p.y.
%inmn	I	Indicator for (n,2n) & (n,3n) xs (0/1/2/3 : no/(n,2n)/(n,3n)/both)
%ntemp	I	The number of temperatures for xs
%nrtemp	I	The number of temperatures for ri
%npot	I	The number of sig-0's for ri
%np1temp	I	The number of temperatures for p1~p3
%aid	A8	Alphanumeric nuclide id.
%aw	R	Atomic mass
%kappa	R	Energy release per fission (w/sec) only w/o neutrino energy
%kappa0	R	Energy release per fission (w/sec) w/o decay and neutron kinetic energy
%crit_nd	R	Critical pnd
%dcy	R	Decay constant (/sec)
%chi(j)	R	Fission spectrum (j=1,nog)
%chid(j)	R	Delayed neutron spectrum (j=1,nog)
%beta(j)	R	Delayed neutron yields (j=1,6)
%dcybeta(j)	R	Delayed neutron decay constant (j=1,6)
%rtemp(j)	R	Square root temperatures for ri (j=1,%nrtemp)
%sigpot(j)	R	Square root sig-0's for ri (j=1,%npot)
%temp(j)	R	Temperatures for xs (j=1,%ntemp)

%p1temp(j)	R	Temperatures for p1~p3 (j=1,%np1temp)
%lamsigp(j)	R	Lambda*potential xs (j=igresb,igrese)
%sigsres(j)	R	Scattering xs (j=igresb,igrese)
%nu(j)	R	The number of neutrons released (j=igresb,igrese)
%yield(j,k)	R	Fission product yields (j=1, ;k=1,)
%siga(j,k)	R	Absorption xs (j=1,nog; k=1,%ntemp)
%sigf(j,k)	R	Fission xs (j=1,nog; k=1,%ntemp)
%signf(j,k)	R	Nu*fission xs (j=1,nog; k=1,%ntemp)
%sigtr(j,k)	R	Transport xs (j=1,nog; k=1,%ntemp)
%sigs(j,k)	R	Scattering xs (j=1,nog; k=1,%ntemp)
%sigstr(j,k)	R	Transport correct scattering xs (j=1,nog; k=1,%ntemp)
%sigsp1(j,k)	R	P1 scattering xs (j=1,nog; k=1,%np1temp)
%sigsp2(j,k)	R	P2 scattering xs (j=1,nog; k=1,%np1temp)
%sigsp3(j,k)	R	P3 scattering xs (j=1,nog; k=1,%np1temp)
%sign2n(j)	R	(n,2n) xs (j=1,nog)
%sign3n(j)	R	(n,3n) xs (j=1,nog)
%sm(j,k)%	T	[scatmat] P0 corrected scattering matrix (j=1,nog; k=1,%np1temp)
%smp1(j,k)%	T	[scatmat] P1 scattering matrix (j=1,nog; k=1,%np1temp)
%smp2(j,k)%	T	[scatmat] P2 scattering matrix (j=1,nog; k=1,%np1temp)
%smp3(j,k)%	T	[scatmat] P3 scattering matrix (j=1,nog; k=1,%np1temp)
%ria(j,k,l)	R	Absorption ri (j=1,%npot; k=1,%nrtemp; l=igresb,igrese)
%rinf(j,k,l)	R	Nu*fission ri (j=1,%npot; k=1,%nrtemp; l=igresb,igrese)
%ris(j,k,l)	R	Scattering ri (j=1,%npot; k=1,%nrtemp; l=igresb,igrese)
%sgsa(j,k)	R	Subgroup levels of absorption ri (j=1,nsubg; k=igresb,igrese)
%sgsnf(j,k)	R	Subgroup levels of nu*fission ri (j=1,nsubg; k=igresb,igrese)
%sgsafsp(j,k)	R	Subgroup levels of absorption ri (j=1,nflx; k=igresb,igrese+1)
%sgwa(j,k,l)	R	Subgroup weights of absorption ri (j=1,nsubg; k=1,%nrtemp; k=igresb,igrese)
%sgwnf(j,k,l)	R	Subgroup weights of nu*fission ri (j=1,nsubg; k=1,%nrtemp; k=igresb,igrese)
%sgwafsp(j,k,l)	R	Subgroup weights of absorption ri (j=1,nflx; k=1,%nrtemp; k=igresb,igrese+1)

Appendix B.3 Data format for the simplified AMPX library

```
!     --------------------------------
!     +  variables : simplified ampx +
!     --------------------------------
!     ------------------------------------------------------------------------------
!     Variable               Format  Description
!     ------------------------------------------------------------------------------
!     libtext                 a400   Library description
!     nonuc                   i      The number of nuclides
!     nong                    i      The number of neutron energy group
!     nong1                   i      The number of fast energy groups
!     nong2                   i      The number of resonant energy groups for subgroup
!     nong3                   i      The first thermal energy group
!     nogg                    i      The number of gamma energy group
!     nosubg                  i      The number of sub-groups
!     nosubg0                 i      The number of condensed sub-groups
!     n2gbdry                 i      Cutoff energy group for thermal scattering data
!     mapnucl(i)              r      Nuclide id mapping (i=1,100000)
!     engrp(ig)               r      Neutron energy group boundaries (ig=1,nong+1)
!     ungrp(ig)               r      Neutron lethargy group boundaries (ig=1,nong+1)
!     eggrp(ig)               r      Gamma energy group boundaries (ig=1,nogg+1)
!     uggrp(ig)               r      Gamma lethargy group boundaries (ig=1,nogg+1)
!     ampxslib(i)%            t      Ampxtype: type for xs library (i=1,nonuc)
!            %anuclid         a10    Alphanumeric nuclide id.
!            %nuclid          i      Numeric nuclide id.
!            %nsig0           i      The number of background xs
!            %ntemp1          i      The number of temperatures for 1-D & 2-D
!                                     0  : none
!                                     >0 : number
!            %ntemp2          i      The number of temperatures for s(a,b)
!                                     0  : none
!                                     >0 : number
!            %ireso           i      Indicator for resonance nuclide
!                                     0  : no
!                                     1  : rough treatment
!                                     2  : explicit treatment
!            %igsab           i      Initial energy group for s(a,b)
!            %isub            l      Indicator for subgroup data
!                                     0/1/2  : no/ab/ab+nf
!            %itrc            l      Indicator for transport correction
!                                     0  : none
!                                     1  : inscatter approximation (ampx)
!                                     2  : outscatter approximation (p1)
!                                     3  : leakage conservation (casmo)
!            %lsab            l      Indicator for s(a,b) thermal scattering data
!                                     T/F  : yes/no
!            %lburn           l      Depletable or not
!                                     T/F  : yes/no
!            %lfiss           l      Fissionable or not
!                                     T/F  : yes/no
!                                            yes : fissionable (kappa+beta+spectrum)
!            %lspn            l      Indicator for pn scattering
!                                     T/F  : yes/no
!                                            yes : p1~p3
!            %ln2n            l      Indicator for (n,2n) xs
!                                     T/F  : yes/no
!            %ln3n            l      Indicator for (n,3n) xs
!                                     T/F  : yes/no
!            %lwithin         l      Indicator for within-group correction
!                                     T/F  : yes/no
!            %ldlyd           l      Indicator for delayed neutron data
!                                     T/F  : yes/no
!            %lepiup          l      Indicator for epithermal upscattering
!                                     T/F  : yes/no
!            %amass           r      Atomic mass
!            %kappa           r      Energy release per fission (ENDF/B based)
!            %kappa0          r      Energy release per capture
!            %kappa1          r      Energy release per fission+capture
```

```
!            %sigpot           r      Potential xs
!            %temp1(i)         r      Temperatures for xs (i=1,%ntemp1)
!            %temp2(i)         r      Temperatures for thermal scattering matrix
!                                      (i=1,%ntemp2)
!            %sig0(i)          r      Background xs (i=1,%nsig0)
!            %sigtot(i,j,k)    r      Total xs (i=1,nsig0; j=1,%ntemp1; k=1,nong)
!            %sigtr(i,j,k)     r      Transport xs (i=1,nsig0; j=1,%ntemp1; k=1,nong)
!            %sigab(i,j,k)     r      Absorption xs
!                                      (i=1,nsig0; j=1,%ntemp1; k=1,nong)
!            %sigfi(i,j,k)     r      Fission xs (i=1,nsig0; j=1,%ntemp1; k=1,nong)
!            %sigel(i,j,k)     r      Elastic scattering xs
!                                      (i=1,nsig0; j=1,%ntemp1; k=1,nong)
!            %sigwel(i,j,k)    r      Within-group elastic scattering xs
!                                      (i=1,nsig0; j=1,%ntemp1; k=1,nong)
!            %xlambda(i)       r      Lambda(IR parameter) (i=1,nong)
!            %xnu(i)           r      The number of released neutrons (i=1,nong)
!            %chix(i)          r      Fission spectrum (i=1,nong)
!            %signe(i)         r      Nonelastic scattering xs (i=1,nong)
!            %sign2n(i)        r      (n,2n) xs (i=1,nong)
!            %sign3n(i)        r      (n,3n) xs (i=1,nong)
!            %delaydc(i)       r      Decay constant for Delayed neutron (i=1,6)
!            %beta(i)          r      Delayed neutron yields (i=1,6)
!            %xnud(i)          r      The number of released delayed neutrons (i=1,nong)
!            %chixd(i)         r      Delayed fission spectrum (i=1,nong)
!            %subgxsab(i,j)    r      Absorption subgroup xs sets
!                                      (i=1,nsubg; j=nong1+1,nong1+nong2)
!            %subgxsnf(i,j)    r      Nu*fission subgroup xs sets
!                                      (i=1,nsubg; j=nong1+1,nong1+nong2)
!            %subgwab(i,j,k)   r      Absorption subgroup weight sets
!                                      (i=1,nsubg; j=1,%ntemp1; k=nong1+1,nong1+nong2)
!            %subgwnf(i,j,k)   r      Nu*fission subgroup weight sets
!                                      (i=1,nsubg; j=1,%ntemp1; k=nong1+1,nong1+nong2)
!            %subgxsab0(i,j)   r      Absorption nflx-subgroup xs sets
!                                      (i=1,nsubg0; j=nong1+1,nong1+nong2)
!            %subgwab0(i,j,k)  r      Absorption nflx-subgroup weight xs sets
!                                      (i=1,nsubg0; j=1,%ntemp1; k=nong1+1,nong1+nong2)
!            %els(i,j)         t      Elastic pn scattering matrix (i=1,nong; j=0,3)
!            %nels(i,j)        t      Nonelastic pn scattering matrix
!                                      (i=1,nong; j=0,3)
!            %sab(i,j,k)       t      Pn thermal scattering matrix
!                                      (i=1,ntemp2; j=%igsab,nong; k=0,3)
!     sm?(i,j)%                t 1     type for scattering matrix
!                                      (i=1,%ntemp1; j=1,nog)
!             %ib              i      Starting energy group
!             %ie              i      Ending energy group
!             %tot             r      total sum
!             %sigss(k)        r      Scattering components (k=%ib,%ie)
!     ------------------------------------------------------------------------------
```

Appendix B.4 Nuclides of the ENDF/B-7.0 and 7.1 SAMPX MG Library

[ENDF/B-7.0]

1	1801	1.007825E+00	h1	108	39090	8.990715E+01	y90	215	56136	1.359045E+02	ba136
2	1802	2.014102E+00	h2	109	39091	9.090735E+01	y91	216	56137	1.369061E+02	ba137
3	1003	3.015501E+00	h3	110	40090	8.990473E+01	zr90	217	56138	1.379047E+02	ba138
4	2003	3.014932E+00	he3	111	40091	9.090563E+01	zr91	218	56140	1.399099E+02	ba140
5	2004	4.002604E+00	he4	112	40092	9.190501E+01	zr92	219	57138	1.379067E+02	la138
6	3006	6.015072E+00	li6	113	40093	9.290652E+01	zr93	220	57139	1.389033E+02	la139
7	3007	7.016003E+00	li7	114	40094	9.390630E+01	zr94	221	57140	1.399099E+02	la140
8	4007	7.014760E+00	be7	115	40095	9.490800E+01	zr95	222	58136	1.359075E+02	ce136
9	4009	9.012199E+00	be9	116	40096	9.590830E+01	zr96	223	58138	1.379057E+02	ce138
10	5010	1.001294E+01	b10	117	41093	9.290319E+01	nb93	224	58139	1.389063E+02	ce139
11	5011	1.100928E+01	b11	118	41094	9.390732E+01	nb94	225	58140	1.399049E+02	ce140
12	6000	1.200110E+01	c	119	41095	9.490680E+01	nb95	226	58141	1.409105E+02	ce141
13	7014	1.400307E+01	n14	120	42092	9.190683E+01	mo92	227	58142	1.419091E+02	ce142
14	7015	1.499986E+01	n15	121	42094	9.390509E+01	mo94	228	58143	1.429127E+02	ce143
15	8016	1.599491E+01	o16	122	42095	9.490589E+01	mo95	229	58144	1.439143E+02	ce144
16	8017	1.699913E+01	o17	123	42096	9.590468E+01	mo96	230	59141	1.409075E+02	pr141
17	9019	1.899820E+01	f19	124	42097	9.690598E+01	mo97	231	59142	1.419101E+02	pr142
18	11023	2.298949E+01	na23	125	42098	9.790536E+01	mo98	232	59143	1.429107E+02	pr143
19	12024	2.398504E+01	mg24	126	42099	9.890767E+01	mo99	233	60142	1.419081E+02	nd142
20	12025	2.498584E+01	mg25	127	42100	9.990726E+01	mo100	234	60143	1.429097E+02	nd143
21	12026	2.598260E+01	mg26	128	43099	9.890626E+01	tc99	235	60144	1.439103E+02	nd144
22	13027	2.698153E+01	al27	129	44096	9.590760E+01	ru96	236	60145	1.449129E+02	nd145
23	14028	2.797734E+01	si28	130	44098	9.790526E+01	ru98	237	60146	1.459135E+02	nd146
24	14029	2.897693E+01	si29	131	44099	9.890585E+01	ru99	238	60147	1.469161E+02	nd147
25	14030	2.997349E+01	si30	132	44100	9.990423E+01	ru100	239	60148	1.479167E+02	nd148
26	15031	3.097408E+01	p31	133	44101	1.009058E+02	ru101	240	60150	1.499209E+02	nd150
27	16032	3.197196E+01	s32	134	44102	1.019054E+02	ru102	241	61147	1.469151E+02	pm147
28	16033	3.297104E+01	s33	135	44103	1.029040E+02	ru103	242	61148	1.479167E+02	pm148
29	16034	3.396800E+01	s34	136	44104	1.039026E+02	ru104	243	61601	1.479207E+02	pm148m1
30	16036	3.596698E+01	s36	137	44105	1.049112E+02	ru105	244	61149	1.489183E+02	pm149
31	17035	3.496885E+01	cl35	138	44106	1.059068E+02	ru106	245	61151	1.509215E+02	pm151
32	17037	3.696591E+01	cl37	139	45103	1.029050E+02	rh103	246	62144	1.439123E+02	sm144
33	18036	3.596748E+01	ar36	140	45105	1.049012E+02	rh105	247	62147	1.469151E+02	sm147
34	18038	3.796272E+01	ar38	141	46102	1.019056E+02	pd102	248	62148	1.479147E+02	sm148
35	18040	3.996240E+01	ar40	142	46104	1.039040E+02	pd104	249	62149	1.489173E+02	sm149
36	19039	3.896402E+01	k39	143	46105	1.049052E+02	pd105	250	62150	1.499169E+02	sm150
37	19040	3.996401E+01	k40	144	46106	1.059035E+02	pd106	251	62151	1.509195E+02	sm151
38	19041	4.096199E+01	k41	145	46107	1.069054E+02	pd107	252	62152	1.519201E+02	sm152
39	20040	3.996260E+01	ca40	146	46108	1.079038E+02	pd108	253	62153	1.529217E+02	sm153
40	20042	4.195863E+01	ca42	147	46110	1.099051E+02	pd110	254	62154	1.539223E+02	sm154
41	20043	4.295877E+01	ca43	148	47601	1.099062E+02	ag110m1	255	63151	1.509164E+02	eu151
42	20044	4.395548E+01	ca44	149	47111	1.109057E+02	ag111	256	63152	1.519221E+02	eu152
43	20046	4.595370E+01	ca46	150	48106	1.059058E+02	cd106	257	63153	1.529217E+02	eu153
44	20048	4.795254E+01	ca48	151	48108	1.079039E+02	cd108	258	63154	1.539223E+02	eu154
45	21045	4.495408E+01	sc45	152	48110	1.099031E+02	cd110	259	63155	1.549209E+02	eu155
46	22046	4.595266E+01	ti46	153	48111	1.109037E+02	cd111	260	63156	1.559255E+02	eu156
47	22047	4.695174E+01	ti47	154	48112	1.119033E+02	cd112	261	63157	1.569251E+02	eu157
48	22048	4.796807E+01	ti48	155	48114	1.139035E+02	cd114	262	64152	1.519201E+02	gd152
49	22049	4.894789E+01	ti49	156	48601	1.149051E+02	cd115m1	263	64153	1.529217E+02	gd153
50	22050	4.994475E+01	ti50	157	48116	1.159047E+02	cd116	264	64154	1.539213E+02	gd154
51	23000	5.094162E+01	v	158	50112	1.119053E+02	sn112	265	64160	1.599268E+02	gd160
52	24050	4.994606E+01	cr50	159	50113	1.129049E+02	sn113	266	65159	1.589252E+02	tb159
53	24052	5.194019E+01	cr52	160	50114	1.139035E+02	sn114	267	65160	1.599268E+02	tb160
54	24053	5.294079E+01	cr53	161	50115	1.149031E+02	sn115	268	66156	1.559245E+02	dy156
55	24054	5.393937E+01	cr54	162	50116	1.159017E+02	sn116	269	66158	1.579247E+02	dy158
56	25055	5.493805E+01	mn55	163	50117	1.169033E+02	sn117	270	66160	1.599248E+02	dy160
57	26054	5.393937E+01	fe54	164	50118	1.179018E+02	sn118	271	66161	1.609265E+02	dy161
58	26056	5.593451E+01	fe56	165	50119	1.189035E+02	sn119	272	66162	1.619270E+02	dy162
59	26057	5.693510E+01	fe57	166	50120	1.199020E+02	sn120	273	66163	1.629286E+02	dy163
60	26058	5.793368E+01	fe58	167	50122	1.219032E+02	sn122	274	66164	1.639292E+02	dy164
61	27058	5.793580E+01	co58	168	50123	1.229058E+02	sn123	275	67165	1.649298E+02	ho165
62	27601	5.793580E+01	co58m1	169	50124	1.239054E+02	sn124	276	67601	1.659324E+02	ho166m1
63	27059	5.893317E+01	co59	170	50125	1.249080E+02	sn125	277	68162	1.619290E+02	er162
64	28058	5.793570E+01	ni58	171	50126	1.259076E+02	sn126	278	68164	1.639292E+02	er164
65	28059	5.893438E+01	ni59	172	51121	1.209087E+02	sb121	279	68166	1.659304E+02	er166
66	28060	5.993084E+01	ni60	173	51123	1.229058E+02	sb123	280	68168	1.679296E+02	er168
67	28061	6.093143E+01	ni61	174	51124	1.239064E+02	sb124	281	68170	1.699358E+02	er170
68	28062	6.192799E+01	ni62	175	51125	1.249050E+02	sb125	282	71175	1.749408E+02	lu175
69	28064	6.392818E+01	ni64	176	51126	1.259076E+02	sb126	283	71176	1.759414E+02	lu176
70	29063	6.292960E+01	cu63	177	52120	1.199040E+02	te120	284	72174	1.739402E+02	hf174
71	29065	6.492776E+01	cu65	178	52122	1.219032E+02	te122	285	72176	1.759414E+02	hf176
72	30000	6.539578E+01	zn	179	52123	1.229038E+02	te123	286	72177	1.769430E+02	hf177
73	31069	6.892571E+01	ga69	180	52124	1.239034E+02	te124	287	72178	1.779436E+02	hf178
74	31071	7.092428E+01	ga71	181	52125	1.249040E+02	te125	288	72179	1.789462E+02	hf179
75	32070	6.992429E+01	ge70	182	52126	1.259026E+02	te126	289	72180	1.799468E+02	hf180
76	32072	7.192205E+01	ge72	183	52601	1.269052E+02	te127m1	290	73181	1.809545E+02	ta181
77	32073	7.292345E+01	ge73	184	52128	1.279038E+02	te128	291	73182	1.819500E+02	ta182
78	32074	7.392123E+01	ge74	185	52611	1.289074E+02	te129m1	292	74182	1.819531E+02	w182
79	32076	7.592141E+01	ge76	186	52130	1.299060E+02	te130	293	74183	1.829517E+02	w183
80	33074	7.392395E+01	as74	187	52132	1.319082E+02	te132	294	74184	1.839502E+02	w184
81	33075	7.492162E+01	as75	188	53127	1.269045E+02	i127	295	74186	1.859575E+02	w186
82	34074	7.392253E+01	se74	189	53129	1.289054E+02	i129	296	75185	1.849528E+02	re185
83	34076	7.591918E+01	se76	190	53130	1.299070E+02	i130	297	75187	1.869561E+02	re187
84	34077	7.691988E+01	se77	191	53131	1.309055E+02	i131	298	77191	1.909605E+02	ir191
85	34078	7.791725E+01	se78	192	53135	1.349089E+02	i135	299	77193	1.929626E+02	ir193
86	34079	7.891845E+01	se79	193	54123	1.229058E+02	xe123	300	79197	1.969660E+02	au197
87	34080	7.991653E+01	se80	194	54124	1.239044E+02	xe124	301	80196	1.959654E+02	hg196
88	34082	8.191670E+01	se82	195	54126	1.259036E+02	xe126	302	80198	1.979666E+02	hg198
89	35079	7.891825E+01	br79	196	54128	1.279028E+02	xe128	303	80199	1.989682E+02	hg199
322	90229	2.290315E+02	th229								
323	90230	2.300361E+02	th230								
324	90233	2.330419E+02	th233								
325	90234	2.340436E+02	th234								
326	91231	2.310357E+02	pa231								
327	91232	2.320383E+02	pa232								
328	91233	2.330399E+02	pa233								
329	92232	2.320371E+02	u232								
330	92234	2.340409E+02	u234								
331	92237	2.370488E+02	u237								
332	92239	2.390543E+02	u239								
333	92240	2.400566E+02	u240								
334	92241	2.410603E+02	u241								
335	93235	2.350441E+02	np235								
336	93236	2.360468E+02	np236								
337	93237	2.370482E+02	np237								
338	93238	2.380510E+02	np238								
339	93239	2.390526E+02	np239								
340	94236	2.360458E+02	pu236								
341	94237	2.370484E+02	pu237								
342	94243	2.430620E+02	pu243								
343	94244	2.440647E+02	pu244								
344	94246	2.460699E+02	pu246								
345	95242	2.420595E+02	am242								
346	95601	2.420595E+02	am242m1								
347	95243	2.430614E+02	am243								
348	95244	2.440647E+02	am244								
349	95611	2.440647E+02	am244m1								
350	96241	2.410578E+02	cm241								
351	96242	2.420584E+02	cm242								
352	96243	2.430610E+02	cm243								
353	96244	2.440626E+02	cm244								
354	96245	2.450652E+02	cm245								
355	96246	2.460668E+02	cm246								
356	96247	2.470705E+02	cm247								
357	96248	2.480721E+02	cm248								
358	96249	2.490757E+02	cm249								
359	96250	2.500783E+02	cm250								
360	97249	2.490797E+02	bk249								
361	97250	2.500783E+02	bk250								
362	98249	2.490797E+02	cf249								
363	98250	2.500763E+02	cf250								
364	98251	2.510799E+02	cf251								
365	98252	2.520815E+02	cf252								
366	98253	2.530841E+02	cf253								
367	98254	2.540878E+02	cf254								
368	99253	2.530841E+02	es253								
369	99254	2.540878E+02	es254								
370	99255	2.550904E+02	es255								
371	100255	2.550904E+02	fm255								
372	13701	2.698153E+01	al27								
373	26601	5.393937E+01	fe56								
374	26611	5.593451E+01	fe56								
375	26621	5.693510E+01	fe56								
376	26631	5.793368E+01	fe56								
377	4309	9.012199E+00	be_metal								
378	4509	9.012199E+00	be_beo								
379	8516	1.599491E+01	be_beo								
380	1002	2.014102E+00	d_d2o								
381	1901	1.007825E+00	h_ch2								
382	1001	1.007825E+00	h_h2o								
383	1701	1.007825E+00	h_zrh								
384	4607	9.012199E+00	o_beo								
385	6607	1.200110E+01	o_beo								
386	8607	1.599491E+01	o_uo2								
387	92702	2.350439E+02	u_uo2								
388	6608	1.200110E+01	u_uo2								
389	40790	8.990473E+01	zr_zrh								
390	40791	9.090563E+01	zr_zrh								
391	40792	9.190501E+01	zr_zrh								
392	40793	9.290652E+01	zr_zrh								
393	40794	9.390630E+01	zr_zrh								
394	40795	9.490800E+01	zr_zrh								
395	40796	9.590830E+01	zr_zrh								
396	1601	1.007825E+00	benzine								
397	6500	1.200110E+01	benzine								
398	6312	1.200110E+01	graphite								
399	1101	1.007825E+00	l_ch4								
400	400102	2.014102E+00	ortho_d								
401	1401	1.007825E+00	ortho_h								
402	1502	2.014102E+00	para_d								
403	1501	1.007825E+00	para_h								
404	1201	1.007825E+00	s_ch4								
405	47107	1.069054E+02	ag107								
406	47109	1.089045E+02	ag109								
407	48113	1.128999E+02	cd113								
408	49113	1.129039E+02	in113								
409	49115	1.149041E+02	in115								
410	64155	1.549229E+02	gd155								

90	35081	8.091631E+01	br81	197	54129	1.289054E+02	xe129	304	80200	1.999678E+02	hg200	411	64156	1.559225E+02	gd156
91	36078	7.792038E+01	kr78	198	54130	1.299039E+02	xe130	305	80201	2.009704E+02	hg201	412	64157	1.569241E+02	gd157
92	36080	7.991642E+01	kr80	199	54131	1.309055E+02	xe131	306	80202	2.019710E+02	hg202	413	64158	1.579236E+02	gd158
93	36082	8.191348E+01	kr82	200	54132	1.319031E+02	xe132	307	80204	2.039732E+02	hg204	414	68167	1.669320E+02	er167
94	36083	8.291428E+01	kr83	201	54133	1.329057E+02	xe133	308	82204	2.039730E+02	pb204	415	90232	2.320383E+02	th232
95	36084	8.391154E+01	kr84	202	54134	1.339104E+02	xe134	309	82206	2.059744E+02	pb206	416	92233	2.330396E+02	u233
96	36085	8.491254E+01	kr85	203	54135	1.349069E+02	xe135	310	82207	2.069759E+02	pb207	417	92235	2.350439E+02	u235
97	36086	8.591061E+01	kr86	204	54136	1.359075E+02	xe136	311	82208	2.079766E+02	pb208	418	92236	2.360456E+02	u236
98	37085	8.491184E+01	rb85	205	55133	1.329057E+02	cs133	312	83209	2.089803E+02	bi209	419	92238	2.380508E+02	u238
99	37086	8.591113E+01	rb86	206	55134	1.339073E+02	cs134	313	88223	2.230188E+02	ra223	420	94238	2.380495E+02	pu238
100	37087	8.690919E+01	rb87	207	55135	1.349059E+02	cs135	314	88224	2.240204E+02	ra224	421	94239	2.390522E+02	pu239
101	38084	8.391346E+01	sr84	208	55136	1.359065E+02	cs136	315	88225	2.250241E+02	ra225	422	94240	2.400542E+02	pu240
102	38086	8.590931E+01	sr86	209	55137	1.369071E+02	cs137	316	88226	2.260257E+02	ra226	423	94241	2.410487E+02	pu241
103	38087	8.690889E+01	sr87	210	56130	1.299060E+02	ba130	317	89225	2.250231E+02	ac225	424	94242	2.420584E+02	pu242
104	38088	8.790515E+01	sr88	211	56132	1.319051E+02	ba132	318	89226	2.260257E+02	ac226	425	95241	2.410568E+02	am241
105	38089	8.890776E+01	sr89	212	56133	1.329057E+02	ba133	319	89227	2.270273E+02	ac227				
106	38090	8.990765E+01	sr90	213	56134	1.339043E+02	ba134	320	90227	2.270273E+02	th227				
107	39089	8.890585E+01	y89	214	56135	1.349059E+02	ba135	321	90228	2.280289E+02	th228				

[ENDF/B-7.1]

1	1801	1.007825E+00	h1	117	40091	9.090563E+01	zr91	233	58142	1.419091E+02	ce142	349	92237	2.370488E+02	u237
2	1802	2.014102E+00	h2	118	40092	9.190501E+01	zr92	234	58143	1.429127E+02	ce143	350	92239	2.390543E+02	u239
3	1003	3.015501E+00	h3	119	40093	9.290652E+01	zr93	235	58144	1.439143E+02	ce144	351	92240	2.400566E+02	u240
4	2003	3.014932E+00	he3	120	40094	9.390630E+01	zr94	236	59141	1.409075E+02	pr141	352	92241	2.410603E+02	u241
5	2004	4.002604E+00	he4	121	40095	9.490800E+01	zr95	237	59142	1.419101E+02	pr142	353	93234	2.340425E+02	np234
6	3006	6.015072E+00	li6	122	40096	9.590830E+01	zr96	238	59143	1.429107E+02	pr143	354	93235	2.350441E+02	np235
7	3007	7.016003E+00	li7	123	41093	9.290319E+01	nb93	239	60142	1.419081E+02	nd142	355	93236	2.360468E+02	np236
8	4007	7.014760E+00	be7	124	41094	9.390732E+01	nb94	240	60143	1.429097E+02	nd143	356	93237	2.370482E+02	np237
9	4009	9.012199E+00	be9	125	41095	9.490680E+01	nb95	241	60144	1.439103E+02	nd144	357	93238	2.380510E+02	np238
10	5010	1.001294E+01	b10	126	42092	9.190683E+01	mo92	242	60145	1.449129E+02	nd145	358	93239	2.390526E+02	np239
11	5011	1.100928E+01	b11	127	42094	9.390509E+01	mo94	243	60146	1.459135E+02	nd146	359	94236	2.360458E+02	pu236
12	6000	1.200110E+01	c	128	42095	9.490589E+01	mo95	244	60147	1.469161E+02	nd147	360	94237	2.370484E+02	pu237
13	7014	1.400307E+01	n14	129	42096	9.590468E+01	mo96	245	60148	1.479167E+02	nd148	361	94243	2.430620E+02	pu243
14	7015	1.499986E+01	n15	130	42097	9.690598E+01	mo97	246	60150	1.499209E+02	nd150	362	94244	2.440647E+02	pu244
15	8016	1.599491E+01	o16	131	42098	9.790536E+01	mo98	247	61147	1.469151E+02	pm147	363	94246	2.460699E+02	pu246
16	8017	1.699913E+01	o17	132	42099	9.890767E+01	mo99	248	61148	1.479167E+02	pm148	364	95240	2.400552E+02	am240
17	9019	1.899820E+01	f19	133	42100	9.990726E+01	mo100	249	61601	1.479207E+02	pm148m1	365	95242	2.420595E+02	am242
18	11023	2.298949E+01	na23	134	43099	9.890626E+01	tc99	250	61149	1.489183E+02	pm149	366	95601	2.420595E+02	am242m1
19	12024	2.398504E+01	mg24	135	44096	9.590760E+01	ru96	251	61151	1.509215E+02	pm151	367	95243	2.430614E+02	am243
20	12025	2.498584E+01	mg25	136	44098	9.790526E+01	ru98	252	62144	1.439123E+02	sm144	368	95244	2.440647E+02	am244
21	12026	2.598260E+01	mg26	137	44099	9.890585E+01	ru99	253	62147	1.469151E+02	sm147	369	95611	2.440647E+02	am244m1
22	13027	2.698153E+01	al27	138	44100	9.990423E+01	ru100	254	62148	1.479147E+02	sm148	370	96240	2.400552E+02	cm240
23	14028	2.797734E+01	si28	139	44101	1.009058E+02	ru101	255	62149	1.489173E+02	sm149	371	96241	2.410578E+02	cm241
24	14029	2.897693E+01	si29	140	44102	1.019054E+02	ru102	256	62150	1.499169E+02	sm150	372	96242	2.420584E+02	cm242
25	14030	2.997349E+01	si30	141	44103	1.029040E+02	ru103	257	62151	1.509195E+02	sm151	373	96243	2.430610E+02	cm243
26	15031	3.097408E+01	p31	142	44104	1.039026E+02	ru104	258	62152	1.519201E+02	sm152	374	96244	2.440626E+02	cm244
27	16032	3.197196E+01	s32	143	44105	1.049112E+02	ru105	259	62153	1.529217E+02	sm153	375	96245	2.450652E+02	cm245
28	16033	3.297104E+01	s33	144	44106	1.059068E+02	ru106	260	62154	1.539223E+02	sm154	376	96246	2.460668E+02	cm246
29	16034	3.396800E+01	s34	145	45103	1.029050E+02	rh103	261	63151	1.509164E+02	eu151	377	96247	2.470705E+02	cm247
30	16036	3.596698E+01	s36	146	45105	1.049012E+02	rh105	262	63152	1.519221E+02	eu152	378	96248	2.480721E+02	cm248
31	17035	3.496885E+01	cl35	147	46102	1.019056E+02	pd102	263	63153	1.529217E+02	eu153	379	96249	2.490757E+02	cm249
32	17037	3.696591E+01	cl37	148	46104	1.039040E+02	pd104	264	63154	1.539223E+02	eu154	380	96250	2.500783E+02	cm250
33	18036	3.596748E+01	ar36	149	46105	1.049052E+02	pd105	265	63155	1.549209E+02	eu155	381	97245	2.450663E+02	bk245
34	18038	3.796272E+01	ar38	150	46106	1.059035E+02	pd106	266	63156	1.559255E+02	eu156	382	97246	2.460689E+02	bk246
35	18040	3.996240E+01	ar40	151	46107	1.069054E+02	pd107	267	63157	1.569251E+02	eu157	383	97247	2.470705E+02	bk247
36	19039	3.896402E+01	k39	152	46108	1.079038E+02	pd108	268	64152	1.519201E+02	gd152	384	97248	2.480731E+02	bk248
37	19040	3.996401E+01	k40	153	46110	1.099051E+02	pd110	269	64153	1.529217E+02	gd153	385	97249	2.490747E+02	bk249
38	19041	4.096199E+01	k41	154	47601	1.099062E+02	ag110m1	270	64154	1.539213E+02	gd154	386	97250	2.500783E+02	bk250
39	20040	3.996260E+01	ca40	155	47111	1.109057E+02	ag111	271	64160	1.599268E+02	gd160	387	98246	2.460689E+02	cf246
40	20042	4.195863E+01	ca42	156	48106	1.059058E+02	cd106	272	65159	1.589252E+02	tb159	388	98248	2.480721E+02	cf248
41	20043	4.295877E+01	ca43	157	48108	1.079039E+02	cd108	273	65160	1.599268E+02	tb160	389	98249	2.490747E+02	cf249
42	20044	4.395548E+01	ca44	158	48110	1.099031E+02	cd110	274	66156	1.559245E+02	dy156	390	98250	2.500763E+02	cf250
43	20046	4.595370E+01	ca46	159	48111	1.109037E+02	cd111	275	66158	1.579247E+02	dy158	391	98251	2.510799E+02	cf251
44	20048	4.795254E+01	ca48	160	48112	1.119033E+02	cd112	276	66160	1.599248E+02	dy160	392	98252	2.520815E+02	cf252
45	21045	4.495408E+01	sc45	161	48114	1.139035E+02	cd114	277	66161	1.609265E+02	dy161	393	98253	2.530851E+02	cf253
46	22046	4.595266E+01	ti46	162	48601	1.149051E+02	cd115m1	278	66162	1.619270E+02	dy162	394	98254	2.540878E+02	cf254
47	22047	4.695174E+01	ti47	163	48116	1.159047E+02	cd116	279	66163	1.629286E+02	dy163	395	99251	2.510799E+02	es251
48	22048	4.794800E+01	ti48	164	50112	1.119053E+02	sn112	280	66164	1.639292E+02	dy164	396	99252	2.520825E+02	es252
49	22049	4.894789E+01	ti49	165	50113	1.129049E+02	sn113	281	67165	1.649298E+02	ho165	397	99253	2.530851E+02	es253
50	22050	4.994475E+01	ti50	166	50114	1.139035E+02	sn114	282	67601	1.659324E+02	ho166m1	398	99254	2.540878E+02	es254
51	23050	4.994717E+01	v50	167	50115	1.149031E+02	sn115	283	68162	1.619290E+02	er162	399	99601	2.540878E+02	es254m1
52	23051	5.094394E+01	v51	168	50116	1.159017E+02	sn116	284	68164	1.639292E+02	er164	400	99255	2.550904E+02	es255
53	24050	4.994606E+01	cr50	169	50117	1.169033E+02	sn117	285	68166	1.659304E+02	er166	401	100255	2.550904E+02	fm255
54	24052	5.194019E+01	cr52	170	50118	1.179018E+02	sn118	286	68168	1.679296E+02	er168	402	13701	2.698153E+01	al27
55	24053	5.294079E+01	cr53	171	50119	1.189035E+02	sn119	287	68170	1.699358E+02	er170	403	26601	5.393937E+01	fe56
56	24054	5.393937E+01	cr54	172	50120	1.199020E+02	sn120	288	69168	1.679346E+02	tm168	404	26611	5.593451E+01	fe56
57	25055	5.493805E+01	mn55	173	50122	1.219032E+02	sn122	289	69169	1.689342E+02	tm169	405	26621	5.693510E+01	fe56
58	26054	5.393937E+01	fe54	174	50123	1.229058E+02	sn123	290	69170	1.699358E+02	tm170	406	26631	5.793368E+01	fe56
59	26056	5.593451E+01	fe56	175	50124	1.239054E+02	sn124	291	71175	1.749408E+02	lu175	407	4309	9.012199E+00	be_metal
60	26057	5.693510E+01	fe57	176	50125	1.249080E+02	sn125	292	71176	1.759414E+02	lu176	408	4509	9.012199E+00	be_beo
61	26058	5.793368E+01	fe58	177	50126	1.259076E+02	sn126	293	72174	1.739402E+02	hf174	409	8516	1.599491E+01	be_beo
62	27058	5.793580E+01	co58	178	51121	1.209087E+02	sb121	294	72176	1.759404E+02	hf176	410	1002	2.014102E+00	d_d2o
63	27601	5.793580E+01	co58m1	179	51123	1.229058E+02	sb123	295	72177	1.769400E+02	hf177	411	1901	1.007825E+00	h_ch2
64	27059	5.893317E+01	co59	180	51124	1.239064E+02	sb124	296	72178	1.779396E+02	hf178	412	1001	1.007825E+00	h_h2o
65	28058	5.793570E+01	ni58	181	51125	1.249050E+02	sb125	297	72179	1.789503E+02	hf179	413	1701	1.007825E+00	h_zrh
66	28059	5.893438E+01	ni59	182	51126	1.259076E+02	sb126	298	72180	1.799499E+02	hf180	414	8605	1.599491E+01	o_beo
67	28060	5.993084E+01	ni60	183	52120	1.199040E+02	te120	299	73180	1.799474E+02	ta180	415	8607	1.599491E+01	o_uo2
68	28061	6.093143E+01	ni61	184	52122	1.219032E+02	te122	300	73181	1.809480E+02	ta181	416	92601	2.300341E+02	o_uo2
69	28062	6.192799E+01	ni62	185	52123	1.229038E+02	te123	301	73182	1.819500E+02	ta182	417	92611	2.310367E+02	o_uo2
70	28064	6.392818E+01	ni64	186	52124	1.239034E+02	te124	302	74180	1.799468E+02	w180	418	92701	1.599491E+01	sio2

71	29063	6.292960E+01	cu63	187	52125	1.249040E+02	te125	303	74182	1.819480E+02	w182
72	29065	6.492776E+01	cu65	188	52126	1.259026E+02	te126	304	74183	1.829506E+02	w183
73	30064	6.392919E+01	zn64	189	52601	1.269052E+02	te127m1	305	74184	1.839512E+02	w184
74	30065	6.492928E+01	zn65	190	52128	1.279038E+02	te128	306	74186	1.859544E+02	w186
75	30066	6.592604E+01	zn66	191	52611	1.289074E+02	te129m1	307	75185	1.849529E+02	re185
76	30067	6.692714E+01	zn67	192	52130	1.299060E+02	te130	308	75187	1.869557E+02	re187
77	30068	6.792481E+01	zn68	193	52132	1.319082E+02	te132	309	77191	1.909605E+02	ir191
78	30070	6.992529E+01	zn70	194	53127	1.269045E+02	i127	310	77193	1.929626E+02	ir193
79	31069	6.892571E+01	ga69	195	53129	1.289054E+02	i129	311	79197	1.969660E+02	au197
80	31071	7.092428E+01	ga71	196	53130	1.299070E+02	i130	312	80196	1.959654E+02	hg196
81	32070	6.992429E+01	ge70	197	53131	1.309055E+02	i131	313	80198	1.979666E+02	hg198
82	32072	7.192205E+01	ge72	198	53135	1.349089E+02	i135	314	80199	1.989682E+02	hg199
83	32073	7.292345E+01	ge73	199	54123	1.229084E+02	xe123	315	80200	1.999678E+02	hg200
84	32074	7.392123E+01	ge74	200	54124	1.239059E+02	xe124	316	80201	2.009704E+02	hg201
85	32076	7.592141E+01	ge76	201	54126	1.259036E+02	xe126	317	80202	2.019710E+02	hg202
86	33074	7.392395E+01	as74	202	54128	1.279028E+02	xe128	318	80204	2.039732E+02	hg204
87	33075	7.492162E+01	as75	203	54129	1.289054E+02	xe129	319	81203	2.029726E+02	tl203
88	34074	7.392253E+01	se74	204	54130	1.299039E+02	xe130	320	81205	2.049749E+02	tl205
89	34076	7.591918E+01	se76	205	54131	1.309055E+02	xe131	321	82204	2.039730E+02	pb204
90	34077	7.691988E+01	se77	206	54132	1.319031E+02	xe132	322	82206	2.059744E+02	pb206
91	34078	7.791725E+01	se78	207	54133	1.329057E+02	xe133	323	82207	2.069759E+02	pb207
92	34079	7.891845E+01	se79	208	54134	1.339104E+02	xe134	324	82208	2.079766E+02	pb208
93	34080	7.991653E+01	se80	209	54135	1.349069E+02	xe135	325	83209	2.089803E+02	bi209
94	34082	8.191670E+01	se82	210	54136	1.359075E+02	xe136	326	88223	2.230188E+02	ra223
95	35079	7.891825E+01	br79	211	55133	1.329057E+02	cs133	327	88224	2.240204E+02	ra224
96	35081	8.091631E+01	br81	212	55134	1.339073E+02	cs134	328	88225	2.250241E+02	ra225
97	36078	7.792037E+01	kr78	213	55135	1.349059E+02	cs135	329	88226	2.260257E+02	ra226
98	36080	7.991642E+01	kr80	214	55136	1.359065E+02	cs136	330	89225	2.250231E+02	ac225
99	36082	8.191348E+01	kr82	215	55137	1.369071E+02	cs137	331	89226	2.260257E+02	ac226
100	36083	8.291428E+01	kr83	216	56130	1.299060E+02	ba130	332	89227	2.270273E+02	ac227
101	36084	8.391154E+01	kr84	217	56132	1.319051E+02	ba132	333	90227	2.270273E+02	th227
102	36085	8.491254E+01	kr85	218	56133	1.329057E+02	ba133	334	90228	2.280289E+02	th228
103	36086	8.591061E+01	kr86	219	56134	1.339043E+02	ba134	335	90229	2.290315E+02	th229
104	37085	8.491184E+01	rb85	220	56135	1.349059E+02	ba135	336	90230	2.300331E+02	th230
105	37086	8.591113E+01	rb86	221	56136	1.359045E+02	ba136	337	90231	2.310367E+02	th231
106	37087	8.690919E+01	rb87	222	56137	1.369061E+02	ba137	338	90233	2.330419E+02	th233
107	38084	8.391346E+01	sr84	223	56138	1.379047E+02	ba138	339	90234	2.340436E+02	th234
108	38086	8.590931E+01	sr86	224	56140	1.399099E+02	ba140	340	91229	2.290325E+02	pa229
109	38087	8.690889E+01	sr87	225	57138	1.379067E+02	la138	341	91230	2.300341E+02	pa230
110	38088	8.790515E+01	sr88	226	57139	1.389033E+02	la139	342	91231	2.310357E+02	pa231
111	38089	8.890776E+01	sr89	227	57140	1.399099E+02	la140	343	91232	2.320383E+02	pa232
112	38090	8.990765E+01	sr90	228	58136	1.359075E+02	ce136	344	91233	2.330399E+02	pa233
113	39089	8.890585E+01	y89	229	58138	1.379057E+02	ce138	345	92230	2.300341E+02	u230
114	39090	8.990715E+01	y90	230	58139	1.389063E+02	ce139	346	92231	2.310367E+02	u231
115	39091	9.090735E+01	y91	231	58140	1.399049E+02	ce140	347	92232	2.320373E+02	u232
116	40090	8.990473E+01	zr90	232	58141	1.409105E+02	ce141	348	92234	2.340409E+02	u234

419	40790	8.990473E+01	zr_zrh				
420	40791	9.090563E+01	zr_zrh				
421	40792	9.190501E+01	zr_zrh				
422	40793	9.290652E+01	zr_zrh				
423	40794	9.390630E+01	zr_zrh				
424	40795	9.490800E+01	zr_zrh				
425	40796	9.590830E+01	zr_zrh				
426	1601	1.007825E+00	benzine				
427	6500	1.200110E+01	benzine				
428	6312	1.200110E+01	graphite				
429	1101	1.007825E+00	l_ch4				
430	400102	2.014102E+00	ortho_d				
431	1401	1.007825E+00	ortho_h				
432	1502	2.014102E+00	para_d				
433	1501	1.007825E+00	para_h				
434	1201	1.007825E+00	s_ch4				
435	47107	1.069054E+02	ag107				
436	47109	1.089045E+02	ag109				
437	48113	1.128999E+02	cd113				
438	49113	1.129039E+02	in113				
439	49115	1.149041E+02	in115				
440	64155	1.549229E+02	gd155				
441	64156	1.559225E+02	gd156				
442	64157	1.569241E+02	gd157				
443	64158	1.579236E+02	gd158				
444	68167	1.669320E+02	er167				
445	90232	2.320383E+02	th232				
446	92233	2.330396E+02	u233				
447	92235	2.350439E+02	u235				
448	92236	2.360456E+02	u236				
449	92238	2.380508E+02	u238				
450	94238	2.380496E+02	pu238				
451	94239	2.390522E+02	pu239				
452	94240	2.400538E+02	pu240				
453	94241	2.410487E+02	pu241				
454	94242	2.420584E+02	pu242				
455	95241	2.410568E+02	am241				

Appendix C.1 Specification of the Geometry and Composition for the VERA Progression and Depletion Problems

Table C.1.1 Geometry and material data

Material	Parameter	Value	Remark
Core	Pressure (bar)	155.13	2250 psia
	Power Density (w/gU)	40.00	
	Fuel assembly power (MW)/cm	0.050324728	Variable
	Assembly Pitch (cm)	21.5000	
	Pin Pitch (cm)	1.2600	
Fuel	Pellet Radius (cm)	0.4096	
	Material	UO_2	Various ^{235}U w/o
	Density (g/cm^3)	10.2570	
Gadolinia Rod	Pellet Radius (cm)	0.4096	
	Material	UO_2+Gd_2O_3	1.8w/o ^{235}U, 5% Gd_2O_3
	Density (g/cm^3)	10.1110	
Clad	Inner Radius (cm)	0.4180	
	Outer Radius (cm)	0.4750	
	Material	Zircaloy-4	
	Density (g/cm^3)	6.5600	
Guide Tube	Inner Radius (cm)	0.5610	
	Outer Radius (cm)	0.6020	
	Material	Zircaloy-4	
	Density (g/cm^3)	6.5600	
Instrumentation Tube	Inner Radius (cm)	0.5590	
	Outer Radius (cm)	0.6050	
	Material	Zircaloy-4	
	Density (g/cm^3)	6.5600	
Thimble inside Instrumentation Tube	Inner Radius of thimble (cm)	0.2580	
	Outer Radius of thimble (cm)	0.3820	
	Material	SS304	
	Internal material	^4He	
	Material between thimble and IT	Moderator	
Control Rod (AgInCd & B_4C)	AgInCd Radius (cm)	0.3820	
	AgInCd Density (g/cm^3)	10.2000	
	B_4C Radius (cm)	0.3730	
	B_4C Density (g/cm^3)	1.7600	
	Clad Inner Radius (cm)	0.3860	
	Clad Outer Radius (cm)	0.4840	
	SS304 Clad Density (g/cm^3)	7.8000	
IFBA	Coating Thickness (μm)	10.0000	
	Material	ZrB_2	
	^{10}B enrichment (w/o)	50.0	
	Density (g/cm^3)	3.8500	
WABA	Material	B_4C+Al_2O_3	
	Density (g/cm^3)	3.6500	
	Inner Clad Inner Radius (cm)	0.2860	

	Inner Clad Outer Radius (cm)	0.3390	
	Inner/Outer Clad Material	Zircaloy-4	
	Poison Inner Radius (cm)	0.3530	
	Poison Outer Radius (cm)	0.4040	
	Outer Clad Inner Radius (cm)	0.4180	
	Outer Clad Outer Radius (cm)	0.4840	
Pyrex	Material	B_2O_3+SiO_2	12.5 w/o B_2O_3
	Density (g/cm^3)	2.2500	
	Inner Clad Inner Radius (cm)	0.2140	
	Inner Clad Outer Radius (cm)	0.2310	
	Inner/Outer Clad Material	SS-304	
	Poison Inner Radius (cm)	0.2410	
	Poison Outer Radius (cm)	0.4270	
	Outer Clad Inner Radius (cm)	0.4370	
	Outer Clad Outer Radius (cm)	0.4840	

Table C.1.2 Density and atomic number density for each material

Material	Density(g/cm^3)	Isotope ID	PND (/barn-cm)	Isotope ID	PND (/barn-cm)
Fuel (2.1%)	10.257	92234	4.02487E-06	92238	2.23868E-02
		92235	4.86484E-04	8016	4.57590E-02
		92236	2.23756E-06		
Fuel (3.1%)	10.257	92234	6.11864E-06	92238	2.21546E-02
		92235	7.18132E-04	8016	4.57642E-02
		92236	3.29861E-06		
Fuel (3.6%)	10.257	92234	7.21203E-06	92238	2.20384E-02
		92235	8.33952E-04	8016	4.57669E-02
		92236	3.82913E-06		
Fuel (4.6%)	10.257	92234	9.39876E-06	92238	2.18062E-02
		92235	1.06559E-03	8016	4.57721E-02
		92236	4.89014E-06		
Gap	1.79E-04	2004	2.68714E-05		
Cladding (Zirc-4)	6.56	40090	2.18865E-02	26054	8.68307E-06
		40091	4.77292E-03	26056	1.36306E-04
		40092	7.29551E-03	26057	3.14789E-06
		40094	7.39335E-03	26058	4.18926E-07
		40096	1.19110E-03	24050	3.30121E-06
		50112	4.68066E-06	24052	6.36606E-05
		50114	3.18478E-06	24053	7.21860E-06
		50115	1.64064E-06	24054	1.79686E-06
		50116	7.01616E-05	72174	3.54138E-09
		50117	3.70592E-05	72176	1.16423E-07
		50118	1.16872E-04	72177	4.11686E-07
		50119	4.14504E-05	72178	6.03806E-07
		50120	1.57212E-04	72179	3.01460E-07
		50122	2.23417E-05	72180	7.76449E-07
		50124	2.79392E-05		

Moderator 565 K 1300 ppm	0.743	8016	2.48112E-02	5010	1.07070E-05
		1001	4.96224E-02	5011	4.30971E-05
Moderator 600 K 1300 ppm	0.700	8016	2.33753E-02	5010	1.00874E-05
		1001	4.67505E-02	5011	4.06030E-05
IFBA	3.85	5010	2.16410E-02	40092	3.54348E-03
		5011	1.96824E-02	40094	3.59100E-03
		40090	1.06304E-02	40096	5.78528E-04
		40091	2.31824E-03		
Pyrex	2.25	5010	9.63266E-04	14028	1.81980E-02
		5011	3.90172E-03	14029	9.24474E-04
		8016	4.67761E-02	14030	6.10133E-04
Gadolinia 5% Gd_2O_3 95% UO_2 1.8% ^{235}U Fuel	10.111	92234	3.18096E-06	64155	2.48606E-04
		92235	3.90500E-04	64156	3.43849E-04
		92236	1.79300E-06	64157	2.62884E-04
		92238	2.10299E-02	64158	4.17255E-04
		64152	3.35960E-06	64160	3.67198E-04
		64154	3.66190E-05	8016	4.53705E-02
SS304	7.8	6000	3.20895E-04	26054	3.44776E-03
		14028	1.58197E-03	26056	5.41225E-02
		14029	8.03653E-05	26057	1.24992E-03
		14030	5.30394E-05	26058	1.66342E-04
		15031	6.99938E-05	28058	5.30854E-03
		24050	7.64915E-04	28060	2.04484E-03
		24052	1.47506E-02	28061	8.88879E-05
		24053	1.67260E-03	28062	2.83413E-04
		24054	4.16346E-04	28064	7.21770E-05
		25055	1.75387E-03		
AgInCd	10.2	47107	2.36159E-02	48112	6.59276E-04
		47109	2.19403E-02	48113	3.33873E-04
		48106	3.41523E-05	48114	7.84957E-04
		48108	2.43165E-05	48116	2.04641E-04
		48110	3.41250E-04	49113	3.44262E-04
		48111	3.49720E-04	49115	7.68050E-03
B_4C	1.76	5010	1.52689E-02	6000	1.91820E-02
		5011	6.14591E-02		
WABA B_4C-Al_2O_3	3.65	5010	2.98553E-03	8016	5.85563E-02
		5011	1.21192E-02	13027	3.90223E-02
		6000	3.77001E-03		

Appendix C.2 Specification of the Geometry and Composition for the Extended VERA Progression Problems

Table C.2.1 Initial composition and geometry

Zone	radius (cm)	Temp. (K)	Material	#	MPACT ID	Atomic number density
Pellet	0.4096	900	UO_2	1	8016	4.57655E-02
				2	92234	6.12970E-06
				3	92235	7.18155E-04
				4	92236	3.28949E-06
				5	92238	2.21553E-02
Gap	0.4180	600	^{16}O	1	8016	2.64802E-05
Cladding	0.4750	600	^{nat}Zr Cladding	1	40090	2.22810E-02
				2	40091	4.85893E-03
				3	40092	7.42697E-03
				4	40094	7.52657E-03
				5	40096	1.21257E-03
Moderator	1.2600	600	H_2O+B Moderator	1	1001	4.70060E-02
				2	8016	2.35030E-02
				3	5010	4.67672E-06
				4	5011	1.88244E-05

Table C.2.1 Burnt fuel composition

No	ID	Burnup MWD/kgU			
		10	20	40	60
1	8016	4.57657E-02	4.57657E-02	4.57657E-02	4.57657E-02
2	35581	4.58096E-07	8.81151E-07	1.63343E-06	2.28808E-06
3	36582	8.68557E-10	2.87048E-09	9.50339E-09	1.91489E-08
4	36583	1.08983E-06	1.90775E-06	2.96584E-06	3.50062E-06
5	36584	2.22291E-06	4.25889E-06	8.06912E-06	1.17040E-05
6	36585	5.73474E-07	1.02716E-06	1.70603E-06	2.18731E-06
7	36586	4.08484E-06	7.47376E-06	1.30099E-05	1.75261E-05
8	38589	2.48887E-06	2.14319E-06	1.62241E-06	1.33533E-06
9	38590	1.17259E-05	2.11268E-05	3.56656E-05	4.66041E-05
10	39589	7.21242E-06	1.54988E-05	2.87383E-05	3.91299E-05
11	39590	3.01847E-09	5.51152E-09	9.40141E-09	1.23513E-08
12	39591	3.59975E-06	3.22691E-06	2.54411E-06	2.16356E-06
13	40591	8.59408E-06	1.91714E-05	3.66544E-05	5.08192E-05
14	40593	1.37732E-05	2.58865E-05	4.69696E-05	6.53105E-05
15	40595	4.74381E-06	4.67496E-06	4.21407E-06	3.94334E-06
16	40596	1.44196E-05	2.78355E-05	5.27798E-05	7.61003E-05
17	41595	2.41434E-06	2.54355E-06	2.29124E-06	2.13526E-06
18	42595	7.17590E-06	1.98841E-05	4.26237E-05	6.14428E-05
19	42596	7.15654E-08	4.83985E-07	2.62474E-06	6.51817E-06
20	42597	1.38966E-05	2.71567E-05	5.23057E-05	7.61133E-05
21	42598	1.38174E-05	2.74616E-05	5.43877E-05	8.10814E-05
22	42599	2.20495E-07	2.18127E-07	2.16127E-07	2.15963E-07
23	42600	1.51668E-05	3.03118E-05	6.04114E-05	9.02537E-05
24	43599	1.41826E-05	2.73037E-05	4.99676E-05	6.83691E-05
25	44600	5.25932E-07	2.12710E-06	8.50090E-06	1.88529E-05
26	44601	1.26264E-05	2.51482E-05	4.93227E-05	7.19031E-05
27	44602	1.14534E-05	2.41615E-05	5.25346E-05	8.42333E-05
28	44603	2.15982E-06	2.53549E-06	2.96868E-06	3.21617E-06
29	44604	6.70714E-06	1.56421E-05	3.75229E-05	6.26610E-05
30	44605	6.28968E-09	8.19338E-09	1.06368E-08	1.20495E-08

31	44606	2.39991E-06	5.56403E-06	1.14573E-05	1.57796E-05
32	45603	6.38389E-06	1.42864E-05	2.71964E-05	3.59393E-05
33	45605	4.50138E-08	6.04629E-08	7.79456E-08	8.78833E-08
34	46604	6.92009E-07	3.42392E-06	1.48924E-05	3.27304E-05
35	46605	4.24244E-06	1.06159E-05	2.65581E-05	4.44160E-05
36	46606	9.08253E-07	3.59391E-06	1.47494E-05	3.28198E-05
37	46607	1.84999E-06	5.37217E-06	1.52567E-05	2.70430E-05
38	46608	1.10001E-06	3.38781E-06	1.01980E-05	1.87941E-05
39	47609	6.70792E-07	1.95937E-06	5.22585E-06	8.54371E-06
40	47611	1.14647E-08	1.73117E-08	2.56445E-08	3.13748E-08
41	47710	2.93096E-09	1.49615E-08	6.50016E-08	1.34880E-07
42	48610	7.45884E-08	4.57108E-07	2.72095E-06	7.38288E-06
43	48611	1.77743E-07	5.29069E-07	1.60078E-06	3.08892E-06
44	48613	4.67963E-09	6.17657E-09	7.79877E-09	8.98192E-09
45	49615	4.62368E-08	7.68249E-08	1.06073E-07	1.18986E-07
46	51621	6.50160E-08	1.42741E-07	3.15487E-07	4.96627E-07
47	51625	1.31339E-07	2.72978E-07	5.30939E-07	7.37486E-07
48	52632	1.92327E-07	1.94622E-07	1.97258E-07	1.98873E-07
49	52727	8.33525E-09	1.03790E-08	1.16935E-08	1.21690E-08
50	52729	5.07484E-08	5.82705E-08	6.54176E-08	6.89289E-08
51	53627	5.17009E-07	1.17254E-06	2.58431E-06	3.97552E-06
52	53629	1.50229E-06	3.30913E-06	7.26347E-06	1.13532E-05
53	53631	3.34477E-07	3.43979E-07	3.53817E-07	3.59027E-07
54	53635	2.29101E-08	2.28167E-08	2.28284E-08	2.28930E-08
55	54628	8.79371E-09	4.29465E-08	2.14965E-07	5.49622E-07
56	54630	8.29501E-09	3.36054E-08	1.45789E-07	3.52986E-07
57	54631	6.24388E-06	1.17504E-05	1.95610E-05	2.39580E-05
58	54632	1.13384E-05	2.45322E-05	5.48500E-05	8.90047E-05
59	54633	4.63915E-07	4.61000E-07	4.58696E-07	4.59096E-07
60	54634	1.86065E-05	3.68640E-05	7.27783E-05	1.08192E-04
61	54635	9.29960E-09	9.23651E-09	8.71865E-09	8.42938E-09
62	54636	2.70908E-05	5.45650E-05	1.10529E-04	1.67441E-04
63	55633	1.49341E-05	2.89519E-05	5.28200E-05	7.15709E-05
64	55634	4.96561E-07	1.87537E-06	6.35324E-06	1.18342E-05
65	55635	4.26354E-06	8.66102E-06	1.74290E-05	2.64442E-05
66	55636	7.36640E-09	1.45476E-08	3.04087E-08	4.81622E-08
67	55637	1.47157E-05	2.92005E-05	5.74629E-05	8.48030E-05
68	56634	3.92787E-08	3.06934E-07	2.18944E-06	6.45414E-06
69	56637	7.58965E-09	2.93331E-08	1.12964E-07	2.47734E-07
70	56640	9.89251E-07	9.54730E-07	9.15723E-07	8.96073E-07
71	57639	1.47548E-05	2.88400E-05	5.57660E-05	8.14965E-05
72	57640	1.31264E-07	1.35170E-07	1.31878E-07	1.31404E-07
73	58640	1.32712E-05	2.75951E-05	5.60431E-05	8.40869E-05
74	58641	2.37160E-06	2.29706E-06	2.19131E-06	2.13471E-06
75	58642	1.33975E-05	2.61150E-05	5.02698E-05	7.33511E-05
76	58643	9.70042E-08	9.14337E-08	8.46570E-08	8.12887E-08
77	58644	8.97303E-06	1.29784E-05	1.51724E-05	1.50498E-05
78	59641	1.10329E-05	2.38272E-05	4.79251E-05	7.05013E-05
79	59643	9.56901E-07	8.68075E-07	8.01275E-07	7.66646E-07
80	60642	2.95595E-08	1.41917E-07	6.46000E-07	1.54641E-06
81	60643	1.12605E-05	2.08362E-05	3.35906E-05	4.04017E-05
82	60644	4.12370E-06	1.39671E-05	4.21849E-05	7.56748E-05
83	60645	8.61609E-06	1.60289E-05	2.81075E-05	3.72912E-05
84	60646	7.28465E-06	1.48578E-05	3.13206E-05	4.96547E-05
85	60647	3.11143E-07	3.04084E-07	2.98062E-07	2.97005E-07
86	60648	4.11754E-06	8.17836E-06	1.62107E-05	2.41408E-05
87	60650	1.78074E-06	3.72167E-06	7.90710E-06	1.23326E-05
88	61647	3.69572E-06	5.68332E-06	6.90397E-06	6.88705E-06
89	61648	2.44778E-08	3.98093E-08	5.29989E-08	5.62272E-08
90	61649	4.06212E-08	4.65049E-08	5.28612E-08	5.57944E-08
91	61651	8.46708E-09	9.42060E-09	1.07909E-08	1.17188E-08
92	61748	3.44401E-08	5.63440E-08	7.10972E-08	7.25744E-08
93	62647	3.41043E-07	1.09864E-06	2.64155E-06	3.59619E-06
94	62648	5.02305E-07	1.94024E-06	6.49539E-06	1.21766E-05
95	62649	8.30554E-08	9.36656E-08	9.88405E-08	1.00705E-07
96	62650	2.76415E-06	5.90974E-06	1.20603E-05	1.72962E-05

97	62651	3.16704E-07	4.23170E-07	5.99482E-07	7.50128E-07
98	62652	1.38828E-06	2.68413E-06	4.51704E-06	5.76726E-06
99	62653	1.57767E-08	2.73393E-08	4.70086E-08	6.19501E-08
100	62654	2.81120E-07	6.68471E-07	1.64476E-06	2.78378E-06
101	63651	3.38783E-10	4.82035E-10	6.46099E-10	7.71453E-10
102	63653	7.69984E-07	2.14561E-06	5.35779E-06	8.06197E-06
103	63654	8.87601E-08	3.74058E-07	1.27970E-06	2.16456E-06
104	63655	4.93227E-08	1.30121E-07	3.88846E-07	6.48635E-07
105	63656	3.04195E-08	7.11517E-08	2.10323E-07	3.61658E-07
106	63657	3.06590E-10	4.96908E-10	9.46275E-10	1.39429E-09
107	64654	1.60520E-09	1.34562E-08	9.67494E-08	2.57800E-07
108	64655	3.56976E-10	9.99123E-10	3.19729E-09	5.84878E-09
109	64656	1.99712E-07	7.75738E-07	3.93563E-06	1.04035E-05
110	64657	1.48452E-09	2.63297E-09	5.96015E-09	1.11524E-08
111	64658	8.44984E-08	2.59075E-07	9.38048E-07	2.26162E-06
112	64660	5.54463E-09	1.68434E-08	5.14502E-08	9.75558E-08
113	65659	1.24633E-08	3.75753E-08	1.17380E-07	2.38100E-07
114	65660	2.58257E-10	1.05540E-09	4.21688E-09	9.61451E-09
115	66660	2.03949E-10	1.65232E-09	1.25024E-08	3.95866E-08
116	66661	2.12472E-09	6.19887E-09	1.72873E-08	3.27440E-08
117	66662	1.25171E-09	4.05262E-09	1.32459E-08	2.71724E-08
118	66663	6.06210E-10	2.14527E-09	8.48815E-09	2.02555E-08
119	66664	1.77643E-10	5.12167E-10	1.80595E-09	4.37701E-09
120	67665	1.20818E-10	3.95420E-10	1.57754E-09	4.29608E-09
121	90230	1.15679E-11	2.06446E-11	3.25268E-11	3.80969E-11
122	90232	4.43851E-11	7.60922E-11	1.14201E-10	1.29917E-10
123	91231	8.39424E-13	1.95189E-12	4.34636E-12	6.22852E-12
124	91233			1.31690E-12	1.71350E-12
125	92232	1.60372E-11	2.99848E-11	4.98960E-11	6.01618E-11
126	92233	2.06696E-10	3.36127E-10	4.21996E-10	3.86077E-10
127	92234	5.50164E-06	4.69676E-06	3.37238E-06	2.41292E-06
128	92235	4.95227E-04	3.40486E-04	1.52123E-04	6.33676E-05
129	92236	4.44121E-05	7.12300E-05	9.76726E-05	1.01832E-04
130	92237	1.30225E-07	1.93523E-07	2.73785E-07	3.02997E-07
131	92238	2.19874E-02	2.18046E-02	2.13982E-02	2.09494E-02
132	93237	2.03229E-06	5.43411E-06	1.29090E-05	1.85268E-05
133	93238	5.81351E-09	1.65509E-08	4.38583E-08	6.72374E-08
134	93239	2.01870E-06	2.17648E-06	2.46540E-06	2.65489E-06
135	94236			1.08099E-12	3.65090E-12
136	94238	1.85719E-07	1.01762E-06	5.13214E-06	1.12974E-05
137	94239	8.71896E-05	1.23504E-04	1.47968E-04	1.55330E-04
138	94240	1.40414E-05	3.29036E-05	6.18601E-05	7.80511E-05
139	94241	5.84987E-06	1.89152E-05	3.98335E-05	5.03149E-05
140	94242	4.91128E-07	3.46992E-06	1.61414E-05	3.14953E-05
141	95241	5.28659E-08	3.30394E-07	1.12713E-06	1.63693E-06
142	95242	5.26816E-10	4.49686E-09	1.79924E-08	2.71380E-08
143	95243	2.98229E-08	4.59889E-07	4.19958E-06	1.08513E-05
144	95342	1.44189E-10	9.12910E-10	3.34636E-09	5.10009E-09
145	96242	6.26655E-09	7.46721E-08	4.52778E-07	8.45083E-07
146	96243	3.86950E-11	1.00702E-09	1.29477E-08	3.49758E-08
147	96244	2.27259E-09	7.93293E-08	1.71055E-06	7.32053E-06
148	96245	4.37905E-11	3.10268E-09	1.27249E-07	7.35428E-07
149	96246				1.27966E-07

Appendix C.3 Specification of the Geometry and Composition for the AP1000 Depletion Problems

A detailed depiction of the assembly layouts along with pin-cell geometries are described in Figure C.3.1 and Table C.3.1. All remaining model specifications are summarized in Table C.3.2.

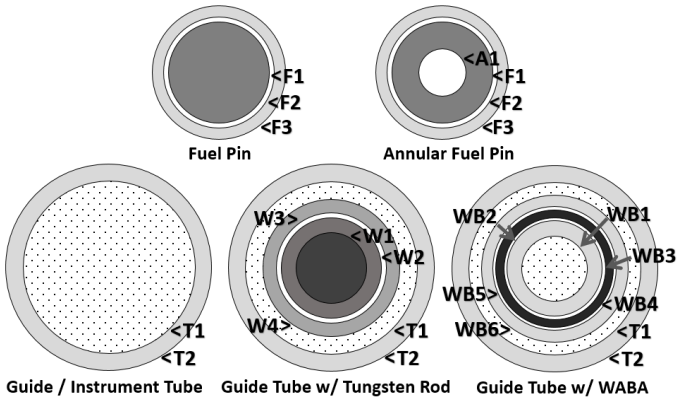

Figure C.3.1 AP1000 2D Lattice Model Pin-Cell Diagrams.

Table C.3.1 Pin-Cell Radii and Material Descriptions

ID	Material	Radii (cm)	ID	Material	Radii (cm)
A1	Helium	0.19685	T1	Coolant	0.56134
F1	Fuel	0.40958	T2	Zirlo	0.61214
F2	Helium	0.41783	WB1	Coolant	0.29000
F3	Zirlo	0.47498	WB2	Zirc 4	0.34000
W1	Tungsten	0.25019	WB3	Helium	0.35000
W2	Inconel	0.39370	WB4	WABA	0.40386
W3	Helium	0.41910	WB5	Helium	0.41783
W4	Stainless Steel	0.48387	WB6	Zirc 4	0.48387

Table C.3.2 Additional Model Specifications

Parameter	Value
Fuel Temp (K)	900
Non-Fuel Temp (K)	600
Coolant Dens. (g/cc)	0.7441292
Coolant Boron (ppm)	1321
IFBA Layer Thickness (cm)	0.000508
Assembly Pitch (cm)	21.5
Pin Pitch	1.26
Model Power (MW)	0.05075
Model Height (cm)	1